Adaptive LQG Based Stabilization and Energy Based GA Tuned PD Swing-up Controller Design for Rotary Inverted Pendulum

Menbere Lulie Yitayih

A Thesis Submitted to
The Department of Electrical Power and Control Engineering
School Electrical Engineering and Computing

Presented in Partial Fulfillment of the Requirement for the Degree of Master of Science in Electrical Power and Control (Control Engineering)

Office of Graduate Studies
Adama Science and Technology University

May 2021

Adama, Ethiopia

Adaptive LQG Based Stabilization and Energy Based GA Tuned PD Swing-up Controller Design for Rotary Inverted Pendulum

Menbere Lulie Yitayih
Advisor: Prof. Seungnam Kim

A Thesis Submitted to
The Department of Electrical Power and Control Engineering
School Electrical Engineering and Computing

Presented in Partial Fulfillment of the Requirement for the Degree of Master of Science in Electrical Power and Control (Control Engineering)

Office of Graduate Studies
Adama Science and Technology University

May 2021
Adama, Ethiopia

DECLARATION

I hereby declare that this Master Thesis entitled "Adaptive LQG Based Stabilization and Energy Based GA tuned PD Swing up controller Design for Rotary Inverted pendulum" is my original work. That is, it has not been submitted for the award of any academic degree, diploma, or certificate in any other university. All sources of materials that are used for this thesis have been duly acknowledged through citation.

Name of Student	Signature	Date

RECOMMENDATION

I certify that I have read and revised the thesis entitled "Adaptive LQG Based Stabilization and Energy Based GA Tuned PD Swing Up Controller Design for Rotary Inverted Pendulum" prepared under our guidance by **Menbere Lulie** submitted in partial fulfillment of the requirements for the degree of Master of Science, Therefore, I recommend the submission of revised version of the thesis to the department following the applicable procedures.

______________________________	______________	______________
Prof Seungnam kim	Signature	Date

APPROVAL SHEET

I, the advisor of the thesis entitled "Adaptive LQG Based Stabilization and Energy Based GA Tuned PD Swing up Controller Design for Rotary Inverted Pendulum" by **Menbere Lulie**, hereby certify that the recommendation and suggestions made by the board of examiners are appropriately incorporated into the final version of the thesis.

Prof Seungnam kim	Signature	Date

We, the undersigned, members of the Board of Examiners of the thesis by **Menbere Lulie**, have read and evaluated the thesis entitled "Adaptive LQG Based Stabilization and Energy Based GA Tuned PD Swing up Controller Design for Rotary Inverted Pendulum" and examined the candidate during open defense. This is, therefore, to certify that the thesis is accepted for partial fulfillment of the requirement of the degree of Master of Science in Electrical Power and Control Engineering (Control).

Chairperson	Signature	Date
Internal Examiner	Signature	Date
External Examiner	Signature	Date

Finally, approval and acceptance of the thesis is contingent upon submission of its final copy to the Office of Postgraduate Studies (OPGS) through the Department Graduate Council (DGC) and School Graduate Committee (SGC).

Department Head	Signature	Date
School Dean	Signature	Date
Office of Postgraduate Studies, Dean	Signature	Date

ACKNOWLEDGMENT

First, my hearty gratitude goes to the almighty God. Then I am highly grateful to my advisor **Prof Seungnam Kim,** as with his encouragement, insight, and guidance the completion of this work would not have been possible. I also give great gratitude to my co-advisor **Prof Gang Gyoo Jin** for his initiation and open-mindedness.

I want to give also great gratitude to **Dr. Tefera Terefe** for his voluntarism and open minded ness for help.

Next, my honorable gratitude goes to my friends, Mr. Danel Abebe, Mr. Minyamir Gelaw, and Mr. Asefa Seifu for their support from the start of selecting the title up to the end of paper editing whenever I asking help from them.

Finally, I want to give great gratitude to, Department Head **Mr. Mesfin Merga** and department Postgraduate Coordinator **Dr. Milkias Brhanu** for their initiation for accomplishing the thesis in proper time.

DEDICATION

To my father Lulie Yitayih, my mother Yezina Lingerih, my brother Yishagerew Lulie, My sister Selamawit Lulie and my friends.

TABLE OF CONTENTS

LIST OF FIGURES

LIST OF TABLES

ACRONYM'S (ABBREVIATION'S)

ALQGSC	Adaptive LQG Stabilizing Controller
DC	Direact Current
EBPDSUC	Energy- Based Proportional Derivative Swing Up Controller
GA	Genetic Algorithm
LQE	Linear Quadratic Estimator
LQG	Linear Quadratic Gaussian
LQR	Linear Quadratic Regulator
MATLAB	Matrix Laboratory
PD	Proportional Derivative
PID	Proportional Integral Derivative
RIP	Rotary Inverted Pendulum
SIMO	Single Input Multi Output
U	Potential Energy
Er	Reference Energy

ABSTRACT

This thesis presents about adaptive Linear Quadratic Gaussian (LQG) stabilizing controller design and an energy-based Genetic Algorithm (GA) tuned Proportional Derivative (PD) swing-up controller for Rotary Inverted Pendulum. Rotary Inverted Pendulum (RIP) is highly nonlinear dynamic and unstable under actuated system, which is composed of the rotating arm and the pendulum with two degrees of freedom. The arm is mounted on the DC motor shaft and rotated to the horizontal plane by the DC motor and the pendulum is swinging on the arm with a revolute joint by receiving the signal from the DC motor. Mathematical modeling, controller design methods, and linearization techniques are applied to this system for the selection of different controllers. The main objective is to balance this pendulum in the upright position on the arm pivot. Adaptive inverse control technique will be applied to each Linear Quadratic Gaussian control signals. An adaptive inverse control method is used for compensation of unknown parameters of a rotary inverted pendulum, while the LQG method is used to cancel non-linearity in the system by linearizing the parameters of the system. LQG controller stabilizes an adaptive signal by avoiding the robustness of the system's nonlinearity. The energy-based GA tuned PD swing-up controller is needed to control RIP from swinging up in some degree. In addition, GA is used for optimizing the parameters of the PD controller. The hybrid of adaptive and LQG with energy based GA tuned PD swing-up controller gives a better performance for the stability of RIP[1]. The output results are analyzed using the controller response and the output of the EBPDSUC and PDSUC controllers are compared. All the processes are done using MATLAB / SIMULINK.

Keywords: *-Adaptive control, Linear Quadratic Controller, GA, PID controller, and Rotary Inverted Pendulum*

CHAPTER 1

INTRODUCTION

1.1. Background of the Study

A Rotary inverted pendulum is a modern control issue as a thesis and projects in control courses due to its simplicity of mathematical model and the complexity of controller design. RIP is composed of the rotating arm controlled by the DC or servo Motor and the pendulum. It is an additional great stage for verification and applies diverse control strategies in control theory [1]. Rotational Inverted Pendulum has significant real-life applications, in the area of aerospace, vehicle control [2], and robotics [3]–[5]. Considering this application, RIP is chosen as the controlled system and parts of control issues are concerned by analysts, such as stabilizing the pendulum around the unstable vertical position[6], [7]swinging the pendulum from its hanging position to its upright vertical position and making movement around its unsteady(unstable) vertical position[8]–[10].

The control goals of RIP in this thesis is to control the pendulum from a downward steady(stable) position to an upward unsteady(unstable) position, i.e., swing-up control, and to keep the motor at a specific precise position while controlling the pendulum [11].

RIP has two degrees of freedom, which are the arm rotational angle and pendulum angle, and has one input state, which is the torque. Since the system has one input torque and two outputs then the system is SIMO underactuated system. Underactuation is a specialized term utilized in mechanical autonomy or robotics and control theory to describe the mechanical system that cannot be commanded to follow arbitrary trajectories in configuration space.

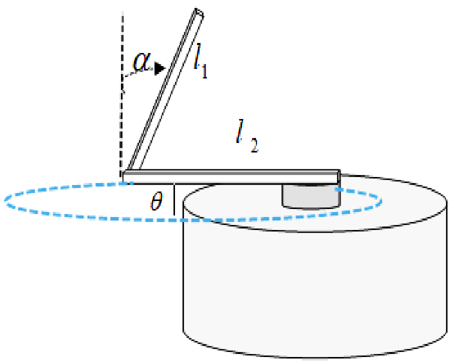

Figure 1. 1.Schematic diagram for RIP

Control of the rotary inverted pendulum is difficult due to certain properties it possesses. A Rotary inverted pendulum is an under-actuated mechanical system due to the lack of direct control over some direction it needs to be controlled. The arm rotates with the DC motor and the pendulum swings or makes an equilibrium position to the downward position[10]. Both the arm and pendulum angle are measured with the potentiometer (angular position sensor) which is attached to the motor.

The mathematical dynamics of the system are described by the state of the system, which consists of the arm rotational angle, the angular velocity of the arm, angular position of a pendulum, and angular velocity of a pendulum. The physical system has state and control constraints [12].

In this study, an adaptive LQG- based stabilizing controller is proposed for the stabilization of a pendulum when it is near to the upright position in its state by accepting a parametrized signal from the adaptive controller added to the LQG signal. To drive the pendulum from a downward stable position to an inverted position a feedforward controller is required. This feedforward controller is called a swing-up controller. The swing-up controller is mainly designed based on the energy of the system. During the design of this controller, energy of the pendulum or overall system is taken into consideration. The approaches to designing swing-up controllers are derived from this energy method and the nature of the dynamic system. To apply this controller first construct a mathematical model for the system using the Lagrange system. The next step will be finding the state-space representation for the purpose of stabilizing controller design [13].

Adaptive Linear Quadratic Gaussian optimal control theory is one of the major accomplishments of the present-day control area. This controller design methodology enables a controller to be synthesized which is optimal to a specified quadratic performance index in which parameters are adapted for the different conditions of the parameters of RIP [14]. An adaptive controller is based on the signals coming with time-varying parameters from the rotational actuator through the arm for control adaptation to handle system uncertainty. In this system, adaptive control action is started when the system parameters start to vary. LQG controller controls the system using the state feedback gain combined with adaptive control signal[15]. An Energy-based GA tuned PD controller is needed for this system to control the swinging condition of the pendulum. This energy-based PD controller has better control performance than a linear PD controller does.GA is used for optimizing gain parameters of PD controller Kp and Kd. In this thesis, GA is selected for optimizing PD since it is simple for programming and implementation.

Generally, two different controllers are used for controlling RIP. Adaptive LQG-based stabilizing controller, which is the combination of Adaptive and LQG controllers, is used to create a new hybrid controller of the two to stabilize RIP. An energy-based GA tuned PD swing up controller is also used for controlling the swinging up of the inverted pendulum. The two controller's i.e adaptive LQG and energy based GA tuned PD linear controllers are important for controlling RIP for this study.

1.2. Statement of the Problem

The problem in this thesis is to balance the pendulum on a rotating arm rotating about the pivot to its upright position by swinging up the pendulum from its downward position under model imperfection and unknown RIP parameters. The effect of non-linearity is handled by linearization technique called Jacobian linearization. While the effect of unknown system parameters is solved by using an adaptive control mechanism. This thesis investigates that an adaptive LQG-based stabilizing controller is a solution for the stability problem of a rotary inverted pendulum about its upright position. While swing-up of the pendulum from its downward to its pendant position is solved by an energy-based GA tuned PD controller.

1.3. Objectives of the Study

1.3.1. Main Objective

Modeling, designing, and analyzing an adaptive LQG-based stabilizing controller and energy-based GA tuned PD swing-up controller for the rotary inverted pendulum are the main objective of this thesis.

1.3.2. Specific Objectives

The specific objective of the studies is -

- Studying the mathematical model of the system and design linearizing input.
- Designing an adaptive LQG-based stabilizing controller.
- Designing energy-based GA tuned PD swing-up controller.
- Analyzing the performance of each controller using MATHLAB/SIMULINK.

1.4. Scope of the Study

The Thesis focuses on studying the mathematical model of a rotary inverted pendulum and its electrical actuator in which the arm is rotating. Then design and test for an adaptive LQG-based stabilizing controller and energy-based GA tuned PD swing-up controller for the rotary inverted pendulum.

1.5. Significance of the Study

At the present day, robots and robotic applications replace different manual systems and work. Since RIP is, the part of a different robot body and underactuated mechanical system that rotates faster for delivery and another purpose. This rotation helps the robot to work through its specific objectives. In this way, this study has great significance in the area of robotics and other mechanical system for flexibility of the different body parts in the present day and of the future. For this system, a mass of up to 3kg on the arm and up to 2.3kg on pendulum can be supported for robotic application.

1.6. Organization of the Thesis

This thesis is organized into eight chapters excluding an appendix. Introduction about the system is described in chapter 1.The next part of this thesis discusses, reviewing related and relevant previous research works in chapter 2. Modeling of the dynamical system of the Rotary inverted pendulum with its electrical actuator in Chapter 3. Linearization and controller design methods in chapter 4, energy-based swing-up controller design in chapter 5, and adaptive LQG controller design in chapter 6. Model verification, validation, and performance test of the controllers using simulation in chapter 7. Conclusion and recommendations will be presented in chapter 8. Finally, codes and models used in the simulation are stated in the appendix.

CHAPTER 2

LITERATURE REVIEW

The objective of control is to control, coordinate and command different systems to the specified system. Control is everywhere; it exists naturally or is created by human beings [16]. Almost all naturally, existing systems surrounding us do not respond proportionally or in the desired way to the stimulus applied to them. Long time ago control engineers try to solve this problem through different approaches. The first approaches were the design of linear controllers based on linear models developed for systems under various assumptions. Later on, advancements in the field of control system lead to the formulation of nonlinear control theories like feedback linearization, sliding mode control, back-stepping, adaptive control, passivity-based control, high gain observers, intelligent controllers based on genetic algorithm, fuzzy logic, neural network, particle swarm optimization and recently contracting system theory[17]

A Rotary inverted pendulum explained in chapter 1 is one of the best systems for checking the performance of different controllers due to the following characteristics.

- Its dynamic nonlinearity
- Instability during rotation and swinging
- It’s under actuation
- Its parameter selection for control action
- It is highly sensitive to external disturbance, etc.

RIP was proposed in 1992 [18], and since then it has been investigated by many researchers[19], [20]. The control objectives of the RIP can be categorized into four[21]: 1)controlling the pendulum from downward steady position to upward unsteady position, i.e., swing-up control[22]; 2) Regulating the pendulum to stay at the unstable position, i.e., stabilization control[23]; 3) Exchanging between swing-up control and stabilization control, i.e., switching control; and 4) Controlling the RIP in such a way that the arm tracks the desired time-varying trajectory while the pendulum remains at the unstable position, i.e., trajectory tracking control. In these setting, distinctive sorts of control, algorithms have been applied for these control destinations.

Despite the importance of RIP and the increasing number of researches that uses it as a benchmark, the different review has been conducted on RIP. Acosta [24] studied RIP as a conventional nonlinear system for the theory and practice of control strategies. He considered two control objectives of RIP namely, swing up and stabilization controls. The autonomous oscillations are also studied. The model of RIP described in Ref[24] is based on Newton-Euler Lagrange. From this publication, even if there is testing of hardware experimentation for controller validation but there is no good homoclinic orbit in the swing up of the pendulum. These different problems are solved by genetic algorithm and energy optimization in this thesis.

The publications are considered in [8] Were up to the year 2009. However, from 2009 to date, many control investigations are used RIP for testing the controllers. In ref [8] feedback, linearization and energy method is applied on the system trajectory tracking of the pendulum. However, this paper do not use any optimization theqniques for exact energy compensation and for getting the linearizing inputs. This is solved in this paper by using genetic algorithm with energy optimization and adaptive inverse technique for driving different inputs.

There is also a need to include trajectory tracking and L_1 adaptive control[25], [26].L1 adaptive controller by itself have its own limitation on avoiding measurement errors. However, in this paper this controller have good performance by forming a hybrid with linear quadratic Gaussian controller. This makes the adaptive LQG controller to have good performance for controlling RIP.

Other research community has considered and proposed different changes to the classical PID approach in RIP system: linear PID with direct control of each system variable[27], Fuzzy Logic focused on a fuzzy controller [28], Optimum state regulator [20], and genetic algorithm-based controller (GA)[29].

Swing up controller can be designed based on the energy of the whole system or only the energy of the pendulum[30]. Additionally this method can be approximated by fuzzy logic [31]or neural network[32]. There are many approaches used in designing energy-based swing up controller. An impulse momentum approach is one of those approaches used in designing energy based method swing up controller[33]. Any energy-based methods can be heuristic to swing up the pendulum in short period of time[34].

Stabilizing controllers for Rotary inverted pendulum can be linear model-based classical direct controllers or nonlinear controllers. LQR controller, PID controller [35], and pole placement controller design methods are categorized under a linear model-based controller design. Nonlinear controller design methods take non-linearity in the dynamic systems into consideration during designing controllers for the dynamic system. There are many controllers designed using this method for the stabilization of inverted pendulum on a cart. The authors of [36] design adaptive sliding mode controller for rotary inverted pendulum using fuzzy logic-based reference model.

In this study, an adaptive LQG-based stabilizing-based controller is proposed for the stabilization of the rotary inverted pendulum to its upright position with system varying uncertainty, and energy-based GA tuned PD swing-up the controller is proposed for controlling the swing up of the pendulum from its downward position to its stabilization point.

CHAPTER 3

MATHEMATICAL MODELING OF RIP AND ELECTRICAL SYSTEM

3.1. Parameters and Their Symbols Needed for Modeling

A Rotary inverted pendulum is an underactuated mechanical system. It consists of a rigid rod called a pendulum, which is rotating, freely in a vertical plane with the objectives of swinging up and balancing the pendulum in the inverted position. At that point, the pendulum is joined to a rotating arm that is mounted on the shaft of the servomotor. Therefore, the pivot arm rotated in the horizontal plane by the servomotor while the pendulum hangs downwards. Rotary inverted pendulum contains both mechanical and electrical subsystems modeling. Parameters needed for modeling RIP are shown below in Table 3.1.

Table 3. 1. System parameters

Parameter symbols	Description	Unit
l_p	Length of pendulum	m
l_a	Length of arm	M
m_p	Mass of pendulum	Kg
m_a	Mass of arm	Kg
g	Acceleration due to gravity	m/s^2
V_a	Armature voltage	V
i_m	Motor Armature current	A
R_m	Motor Armature resistance	Ω
L_a	Armature inductance	H
e_m	Motor back emf	V
K_m	Motor torque constant	Nm/A

K_t	Motor back-emf constant	Vs/rad
ω	Rated motor speed	rad/s
η_m	Motor efficiency	--
η_g	Gear efficiency	--
β	Servo Feedback amplifier gain	--
A	Servo Amplifier gain	--
θ	An angular position of the arm	rad
α	An angular position of the pendulum	rad
l_1	Length of the pendulum from the center of mass	m
l_2	Length of arm from the center of mass	m
J_p	Moment of inertia of the pendulum	$Kg.m^2$
J_a	Moment of inertia of the arm	$Kg.m^2$
U	The Potential energy of RIP	J
K	The Kinetic energy of RIP	J

3.2. Requirements Needed for Modeling

There are two types of criteria or requirements for modeling a rotary inverted pendulum. These are functional and additional requirements [9].

3.2.1. Functional Requirement

Functional requirements are necessary condition, which must be fulfilled for making the system operational. These are

1. Capable of stabilizing RIP from its downward position to its upward position.
2. Capable of keeping the rotating arm freely without any disturbance.

3.3.2. Other Requirement

These requirements are desirable requirements but they are not necessary requirements.

1. The system starts in the state of equilibrium that means the initial conditions are assumed zero $x(0) = 0$.

2. The pendulum deflection is restricted within few degrees in the up-right position to satisfy the linearity property may be in range of ± 15.66.
3. The Pendulum can be subjected to small disturbance input.
4. Stabilize the pendulum with less than 4 degrees (0.0697radian).
5. Swing up the pendulum in less than 2 seconds.
6. Rotating the arm by keeping the pendulum stable by displacing the arm at an angle θ and the pendulum at an angle α .

3.3. Mathematical Modeling and State Space Representation of RIP

Lagrange's equation of motion was used to determine the non-linear system model. Then, the non-linear mathematical model should be linearized to determine the linearized system model in which the model represented the pendulum in equilibrium point or upright position. Therefore, the linear approximation method was used in the linearization of a nonlinear mathematical model. After that, the linearized mathematical model was converted into a state-space model to determine the dynamic model of the arm and pendulum as well. However, the system is incapable of stabilizing in the upright position without a controller. Hence, the upright dynamic model is required to convert in the downward dynamic model for validation purposes [37].

RIP is the second class of underactuated systems with two degrees of freedom which can be transformed into non-triangular quadratic norm with actuated variables [38].

Linearization of the dynamics of the underactuated configuration variable is done using change of control. This is applied under the condition that the number of unactuated variables is less than or equal to the number of actuated variables. This procedure is called non- collocated partial feedback linearization. It is used to obtain a non-triangular normal form for an underactuated system with kinetic symmetry's linearization of such underactuated system depends on the change of coordinate.

Consider the energy of the underactuated mechanical system with the following equation.

$$E[q;\dot{q}] = \frac{1}{2}\begin{bmatrix} \dot{q}_1 \\ \dot{q}_2 \end{bmatrix}^T \begin{bmatrix} m_{11}(q) & m_{12}(q) \\ m_{21}(q) & m_{22}(q) \end{bmatrix} \begin{bmatrix} \dot{q}_1 \\ \dot{q}_2 \end{bmatrix} - U(q) \tag{3.1}$$

where q_1 and q_2 are actuated and un-actuated configuration vector (q) is an inertial matrix.

From Equation (3.1) the generalized momentum is

$$p_1 = \frac{\partial E}{\partial q_1} = m_{11}(q)\dot{q}_1 + m_{12}(q)\dot{q}_2 \tag{3.2}$$

$$p_2 = \frac{\partial E}{\partial q_2} = m_{21}(q)\dot{q}_1 + m_{22}(q)\dot{q}_2 \tag{3.3}$$

The normalized momentum conjugate q_1 and q_2 with respect to q_1 can be

$$c_1 = m_{11}(q)P_1 = \dot{q}_1 + m_{11}(q)m_{12}(q)\dot{q}_2 \tag{3.4}$$

$$c_2 = m_{21}(q)P_2 = \dot{q}_1 + m_{21}(q)m_{22}(q)\dot{q}_2 \tag{3.5}$$

where c_1 and c_2 are defined wherever m_{21} is invertible i. e $m_{21} = m_{12}$.

From the normalized momentum, conjugate $c = c(q.\dot{q})$ becomes normalized momentum if the generalized momentum configuration function $h(q)$ such that $\dot{h}(q) = c$. With this expression rotary, inverted pendulum dynamics can be expressed as non-triangular quadratic form.

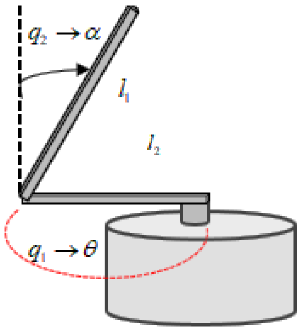

Figure 3. 1.Schematic diagram of RIP with coordinate transformation

Using the generalized coordinate, $(\theta, \alpha) \mapsto (q_1, q_2)$ the dynamics of RIP from Figure 3.1 above can be derived as follows. The position of the rotating arm and pendulum from the generalized coordinate respectively becomes:

$$\begin{bmatrix} x_a \\ y_a \\ z_a \end{bmatrix} = \begin{bmatrix} l_2 \cos(q_1) \\ l_2 \sin(q_1) \\ 0 \end{bmatrix} \tag{3.6}$$

$$\begin{bmatrix} x_p \\ y_p \\ z_p \end{bmatrix} = \begin{bmatrix} l_a \cos(q_1) - l_1 \sin(q_1)\sin(q_2) \\ l_a \sin(q_1) + l_1 \cos(q_1)\sin(q_2) \\ l_1 \cos(q_2) \end{bmatrix} \tag{3.7}$$

From Equation (3.6) and (3.7) the linear velocity of a rotating arm and pendulum respectively become

$$\begin{bmatrix} \dot{x}_a \\ \dot{y}_a \\ \dot{z}_a \end{bmatrix} = \begin{bmatrix} -l_2 \sin(q_1)\dot{q}_1 \\ l_2 \cos(q_1)\dot{q}_1 \\ 0 \end{bmatrix} \tag{3.8}$$

$$\begin{bmatrix} \dot{x}_p \\ \dot{y}_p \\ \dot{z}_p \end{bmatrix} = \begin{bmatrix} -l_a \sin(q_1)\dot{q}_1 - l_1 \cos(q_1)\sin(q_2)\dot{q}_1 - l_1 \cos(q_2)\sin(q_1)\dot{q}_2 \\ l_a \cos(q_1)\dot{q}_1 - l_1 \sin(q_1)\sin(q_2)\dot{q}_1 + l_1 \cos(q_1)\cos(q_2)\dot{q}_2 \\ -l_1 \sin(q_2)\dot{q}_2 \end{bmatrix} \tag{3.9}$$

After calculating the velocity, kinetic energy of the system with respect to the generalized coordinate q.

$$K(q) = K(q)_{translational} + K(q)_{rotational} \tag{3.10}$$

$$K(q) = \frac{1}{2} m_p \begin{bmatrix} \dot{x}_p \\ \dot{y}_p \\ \dot{z}_p \end{bmatrix}^2 + \frac{1}{2} m_a \begin{bmatrix} \dot{x}_a \\ \dot{y}_a \\ \dot{z}_a \end{bmatrix}^2 + \frac{1}{2} J_p \dot{q}_2^{\,2} + \frac{1}{2} J_a \dot{q}_1^{\,2} \tag{3.11}$$

$$= \frac{1}{2} m_p \begin{bmatrix} \left[-l_a \sin(q_1)\dot{q}_1 - l_1 \cos(q_1)\sin(q_2)\dot{q}_1 - l_1 \cos(q_2)\sin(q_1)\dot{q}_2\right]^2 + \\ \left[l_a \cos(q_1)\dot{q}_1 - l_1 \sin(q_1)\sin(q_2)\dot{q}_1 + l1\cos(q_1)\cos(q_2)\dot{q}_2\right]^2 + \left[-l_1 \sin(q_2)\dot{q}_2\right]^2 \end{bmatrix} +$$
$$\frac{1}{2} m_a \left[\left[-l_a \sin(q_1)\dot{q}_1\right]^2 + \left[l_a \cos(q_1)\dot{q}_1\right]^2\right] + \frac{1}{2} J_p \dot{q}_2^{\,2} + \frac{1}{2} J_a \dot{q}_1^{\,2}$$

After simplification the final equation of kinetic energy as

$$K(q) = \frac{1}{2}\left(m_a l_2^{\,2} + J_a + m_p l_a^{\,2} + m_p l_1 \sin^2(q_2)\right)\dot{q}_1^{\,2} + m_p l_1 \cos(q_2)\dot{q}_1\dot{q}_2 + \frac{1}{2}\left(m_p l_1^{\,2} + J_p\right)\dot{q}_2^{\,2} \tag{3.12}$$

Similarly, the potential energy of RIP with respect to the generalized coordinate become

$$U(q) = U(q_2) = m_p g l_1 \cos(q_2) \tag{3.13}$$

From the kinetic and potential energy, understand that rotational inverted pendulum only depends on coordinate q_2 .from this it is possible to say that q_1 is an external variable and q_2 is a shape variable. The required kinetic and potential energy are calculated then apply Euler Lagrange for the dynamic system as expressed in Equation (3.1).

$$E(q_1, q_2) = K(q) - U(q) \tag{3.14}$$

From Equation (3.12) the inertial matrix become

$$\begin{aligned} m_{11} &= m_a l_a^{\ 2} + J_a + m_p (l_a^{\ 2} + l_1 \sin^2(q_2)) \\ m_{12} &= m_{21} = m_p l_1 l_a \cos(q_2) \\ m_{22} &= m_p l_1^{\ 2} + J_p \end{aligned} \tag{3.15}$$

The Euler equation of Equation (3.1) become

$$E = \frac{1}{2} \begin{bmatrix} \dot{q}_1 \\ \dot{q}_2 \end{bmatrix}^T \begin{bmatrix} m_a l_a^{\ 2} + J_a + m_p (l_a^{\ 2} + m_p l_1 \sin^2(q_2)) & m_p l_1 l_a \cos(q_2) \\ m_p l_1 l_a \cos(q_2) & m_p l_1^{\ 2} + J_p \end{bmatrix} \begin{bmatrix} \dot{q}_1 \\ \dot{q}_2 \end{bmatrix} - m_p g l_1 \cos(q_2) \tag{3.16}$$

Finally, apply the Euler Lagrange equation of the dynamic system as

$$\frac{d}{dt} \frac{\partial E}{\partial q} - \frac{\partial E}{\partial q} = \begin{bmatrix} T \\ 0 \end{bmatrix} \tag{3.17}$$

After applying the Lagrange equation, the motion of rotation of the pendulum becomes

$$m_{11}(q_2)\ddot{q}_1 + m_{12}(q_2)\ddot{q}_2 + m_p l_1^2 \sin(2q_2)\,\dot{q}_1\dot{q}_2 - m_p l_1 l_a \sin(q_2)\dot{q}_2^{\ 2} = T \tag{3.18}$$

$$m_{21}(q_2)\ddot{q}_1 + m_{22}(q_2)\ddot{q}_2 - \frac{1}{2} m_p l_1^2 \sin(2q_2)\dot{q}_1^{\ 2} - m_p g l_1 \sin(q_2) = 0 \tag{3.19}$$

where, T is the torque applied to the motor

From the output of Euler Lagrange, the state space representation of a rotary inverted pendulum can be determined as follows.

Equation (3.18) and (3.19) can be rewritten as:

$$m_{11}(q_2)\ddot{q}_1 + m_{12}(q_2)\ddot{q}_2 = T + m_p l_1 l_a \sin(q_2)\dot{q}_2^{\ 2} - m_p l_1^{\ 2} \sin(2q_2)\dot{q}_1\dot{q}_2 \tag{3.20}$$

$$m_{21}(q_2)\ddot{q}_1 + m_{22}(q_2)\ddot{q}_2 = \frac{1}{2} m_p l_1^2 \sin(2q_2)\dot{q}_1^2 + m_p g l_1 \sin(q_2) \tag{3.21}$$

$\ddot{q}_1$ and $\ddot{q}_2$ become

$$\begin{bmatrix} \ddot{q}_1 \\ \ddot{q}_2 \end{bmatrix} = \begin{bmatrix} m_{11}(q) & m_{12}(q) \\ m_{21}(q) & m_{22}(q) \end{bmatrix}^{-1} \begin{bmatrix} T + m_p l_1 l_a \sin(q_2)\dot{q}_2^2 - m_p l_1^2 \sin(2q_2)\dot{q}_1\dot{q}_2 \\ \frac{1}{2} m_p l_1^2 \sin(2q_2)\dot{q}_1^2 + m_p g l_1 \sin(q_2) \end{bmatrix} \tag{3.22}$$

$$\begin{bmatrix} m_{11}(q) & m_{12}(q) \\ m_{21}(q) & m_{22}(q) \end{bmatrix}^{-1} = \frac{1}{m_{11}(q)m_{22}(q) - m_{21}(q)m_{12}(q)} \begin{bmatrix} m_{22}(q) & -m_{21}(q) \\ -m_{12}(q) & m_{11}(q) \end{bmatrix} \tag{3.23}$$

Then from Equation (3.22)

$$\ddot{q}_1 = \frac{m_{22}(q)\begin{pmatrix} T + m_p l_1 l_a \sin(q_2)\dot{q}_2^2 - \\ m_p l_1^2 \sin(2q_2)\dot{q}_1\dot{q}_2 \end{pmatrix} - m_{21}(q)\begin{pmatrix} \frac{1}{2} m_p l_1^2 \sin(2q_2)\dot{q}_1^2 + \\ m_p g l_1 \sin(q_2) \end{pmatrix}}{m_{11}(q)m_{22}(q) - m_{12}(q)m_{21}(q)} \tag{3.24}$$

$$\ddot{q}_2 = \frac{-m_{12}(q)\begin{pmatrix} T + m_p l_1 l_a \sin(q_2)\dot{q}_2^2 - \\ m_p l_1^2 \sin(2q_2)\dot{q}_1\dot{q}_2 \end{pmatrix} + m_{11}(q)\begin{pmatrix} \frac{1}{2} m_p l_1^2 \sin(2q_2)\dot{q}_1^2 + \\ m_p g l_1 \sin(q_2) \end{pmatrix}}{m_{11}(q)m_{22}(q) - m_{12}(q)m_{21}(q)} \tag{3.25}$$

Substitute the value of inertial matrix from Equation (3.15) to Equation (3.21) and (3.22) then the state space representation of the system becomes:

$$\dot{x}_1 = x_2$$

$$\dot{x}_2 = \frac{\left(m_p l_1^2 + J_p\right)\begin{pmatrix} m_p l_1 l_a \sin(x_3)x_4^2 - \\ m_p l_1^2 \sin(2x_3)x_2 x_4 \end{pmatrix} - \left(m_p l_1 \cos(x_3)\right)\begin{pmatrix} \frac{1}{2} m_p l_1^2 \sin(x_3)x_2^2 + \\ m_p g l_1 \sin(x_3) \end{pmatrix} + \left(m_p l_1^2 + J_p\right)T}{\left(m_a l_a^2 + J_a + m_p(l_a^2 + l_1 \sin^2(x_3))\right)\left(m_p l_1^2 + J_p\right) - \left(m_p l_1 \cos(x_3)\right)^2} \tag{3.26}$$

$$\dot{x}_3 = x_4$$

$$\dot{x}_4 = \frac{-\left(m_p l_1 \cos(x_3)\right)\begin{pmatrix} m_p l_1 l_a \sin(x_3) x_4^2 - \\ m_p l_1^2 \sin(2x_3) x_2 x_4 \end{pmatrix} + \begin{pmatrix} m_a l_2^2 + J_a + m_p l_a^2 \\ + m_p l_1 \sin^2(x_3) \end{pmatrix}\begin{pmatrix} \frac{1}{2} m_p l_1^2 \sin(2x_3) x_2^2 \\ + m_p g l_1 \sin(x_3) \end{pmatrix} - \begin{pmatrix} m_p l_1 * \\ \cos(x_3) \end{pmatrix}}{\left(m_a l_a^2 + J_a + m_p (l_a^2 + l_1 \sin^2(x_3))\right)\left(m_p l_1^2 + J_p\right) - \left(m_p l_1 \cos(x_3)\right)^2}$$

The above long equation expressed in Equation (3.23) in condensed form

$$\begin{aligned}
a &= \left(m_p l_1^2 + J_p\right)\begin{pmatrix} m_p l_1 l_a \sin(x_3) x_4^2 - \\ m_p l_1^2 \sin(2x_3) x_2 x_4 \end{pmatrix} - \left(m_p l_1 \cos(x_3)\right)\begin{pmatrix} \frac{1}{2} m_p l_1^2 \sin(2x_3) x_1^2 + \\ m_p g l_1 \sin(x_3) \end{pmatrix} \\
r &= -\left(m_p l_1 \cos(x_3)\right)\begin{pmatrix} m_p l_1 l_a \sin(x_3) x_4^2 - \\ m_p l_1^2 \sin(2x_3) x_2 x_4 \end{pmatrix} + \begin{pmatrix} m_a l_2^2 + J_a + m_p l_a^2 \\ + m_p l_1 \sin^2(x_3) \end{pmatrix}\begin{pmatrix} \frac{1}{2} m_p l_1^2 \sin(2x_3) x_2^2 + \\ m_p g l_1 \sin(x_3) \end{pmatrix} \\
z &= \left(m_a l_a^2 + J_a + m_p (l_a^2 + l_1 \sin^2(x_3))\right)\left(m_p l_1^2 + J_p\right) - \left(m_p l_1 \cos(x_3)\right)^2 \\
\mu &= m_p l_1^2 + J_p \\
v &= m_p l_1 \cos(x_3)
\end{aligned} \tag{3.27}$$

Then the state space equation become

$$\begin{bmatrix} \dot{x}_1 \\ \dot{x}_2 \\ \dot{x}_3 \\ \dot{x}_4 \end{bmatrix} = \begin{bmatrix} x_2 \\ \frac{a}{z} \\ x_4 \\ \frac{r}{z} \end{bmatrix} + \begin{bmatrix} 0 \\ \frac{\mu}{z} \\ 0 \\ \frac{v}{z} \end{bmatrix} T \qquad 3.28)$$

3.3.1. Mathematical Modeling for Electrical System

DC motor in this thesis is used to drive the rotating arm by receiving signals from the control input. The arm is rotated by controlling the output torque of the motor. There are two methods to control the torque applied to the motor, which is armature voltage control and armature current control. The Armature current needs a controllable current source proportional to the control signal. Similarly, armature voltage needs a controllable voltage source proportional to the control signal [39].

In this system, a servo motor amplifier is used to control the torque of the DC motor by generating a control signal proportional to the input signal.

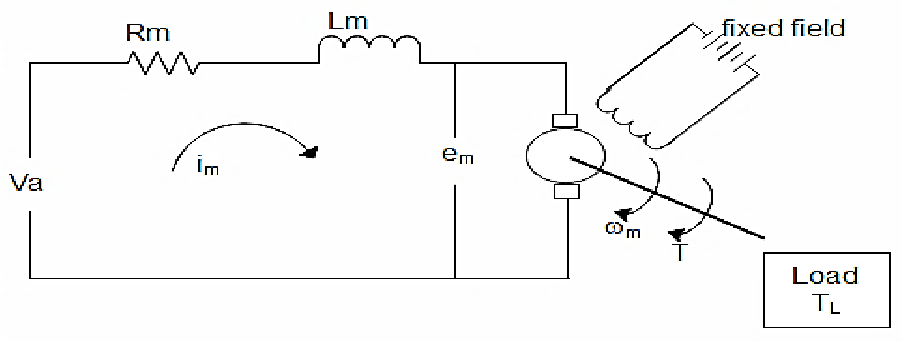

Figure 3. 2. Armature control DC motor

From Figure 3.2 above the dynamics of input voltage and output, torque can be derived using Kirchhoff's voltage law:

$$V_a = L_m \frac{d\,i}{d\,t} + R_m i_m + e_m \tag{3.29}$$

$$T = K_g \eta_m K_t i_m \tag{3.30}$$

Assuming that there is no effect of armature inductance then Equation (3.29) become

$$V_a = R_m i_m + e_m \tag{3.31}$$

Then the velocity tangent to the motor shaft can be derived with similarity $\omega = K_g \dot{\theta}$ and $e_m = K_m \omega = K_m K_g \dot{\theta}$ by substituting Equation (3.31) to (3.30)

$$V_a = R_m i_m + K_m K_g \dot{\theta} \tag{3.32}$$

From this, the relation between the input voltage and output torque can be derived from Equation (3.32)

$$i_m = \frac{V_a - K_m K_g \dot{\theta}}{R_m} \tag{3.33}$$

From Equation (3.30)

The torque $T = K_g \eta_m K_t i_m$ then the output torque become

$$T = K_g \eta_m K_t \left(\frac{V_a - K_m K_g \dot{\theta}}{R_m} \right) \tag{3.34}$$

However, this is not the actual torque since there is mechanical loss and efficiency of the gear system, therefore the actual torque of the rotating pendulum becomes.

$$T = K_g \eta_m \eta_g K_t \left(\frac{V_a - K_m K_g \dot{\theta}}{R_m} \right) \tag{3.35}$$

The armature voltage control is shown in Figure 3.3

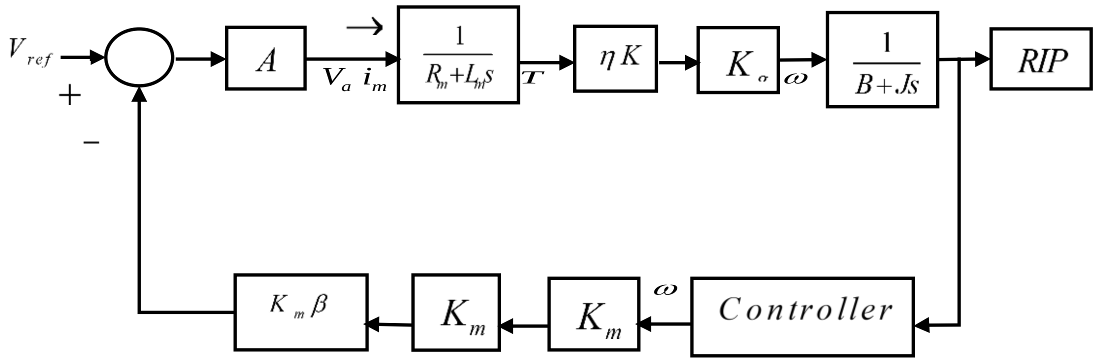

Figure 3. 3. Overall system block diagram

From the above Figure 3.3 the reference voltage can be variable i.e. zero or periodic. The armature voltage at the end of the DC motor is the difference between the reference voltage and the signal coming from the controller as a voltage source. Moreover, the servo feedback gain is used to increase the intensity of the error signal.

$$V_a = A\left(V_{ref} - \beta\,\omega\right) \tag{3.36}$$

Then drive the torque to drive the motor as voltage control. From Equation (3.33) there is

$$V_a = R_m i_m + K_m K_g \dot{\theta} = R_m i_m + K_m K_g \omega \tag{3.37}$$

Substitute Equation (3.36) into (3.37) and become

$$R_m i_m + K_m K_g \omega = A\left(V_{ref} - \beta\,\omega\right) \tag{3.38}$$

From Equation (3.33)

There is $i_m = \dfrac{T}{K_g \eta_m K_t}$ then substitute into Equation (3.37)

$$R_m \left(\frac{T}{K_g \eta_m K_t} \right) + K_m K_g \omega = A\left(V_{ref} - \beta\,\omega\right) \tag{3.39}$$

$$\left(\frac{T}{K_g \eta_m K_t} \right) = \frac{AV_{ref} - A\beta\omega - K_m K_g \omega}{R_m}$$

Finally, the required torque for rotating the arm by considering loss become

$$T = \frac{\left(AV_{ref} - \left(A\beta + K_m K_g\right)\omega\right) K_g \eta_m \eta_g K_t}{R_m} \tag{3.40}$$

Similarly, it is possible to find current control. From Equation (3.31) with $\omega = \dot{\theta}$ Substitute Equation (3.37) into Equation (3.36)

$$i_m = \frac{A\left(V_{ref} - \beta\,\omega\right) - K_m K_g \omega}{R_m} \tag{3.41}$$

At the minimum requirement of the reference voltage, the armature current is depending on the angular velocity of the rotating arm and Equation (3.40) become.

$$i_m = \frac{-A\beta\,\omega - K_m K_g \omega}{R_m} \tag{3.42}$$

Since at minimum requirement V_{ref} is zero. Then from Equation (3.33) $T = K_g \eta_m K_t i_m \Rightarrow$

$i_m = \dfrac{T}{K_g \eta_m K_t}$ and substitute into Equation (3.42) the output torque by considering loss

become

$$\frac{T}{K_g \eta_m K_t} = \frac{-A\beta\,\omega - K_m K_g \omega}{R_m} \Rightarrow T = \left(\frac{-A\beta\,\omega - K_m K_g \omega}{R_m} \right) K_g \eta_m \eta_g K_t \tag{3.43}$$

N.B. when applying the current control method, the voltage-controlled source is used, and similarly, when applying the voltage control method, use the current-controlled source.

CHAPTER 4

LINEARIZATION AND CONTROLLER DESIGN METHODS

4.1. Jacobean Linearization

Consider a nonlinear dynamic time-invariant system

$$\dot{x} = f\left(x(t), u(t)\right) \qquad (4.1)$$
$$y = h\left(x(t), u(t)\right)$$

where, f is a function mapping $R^n XR^m \rightarrow R^n$**,** A point $\overline{x}$ is an equilibrium point if there is a specific input $\overline{u} \in R_n$ which is an equilibrium input such that

$$f\left(\overline{x}, \overline{u}\right) = 0_n \qquad (4.2)$$

Assume $\overline{x}$ is an equilibrium point (with an equilibrium input $\overline{u}$) and consider starting the system in Equation (4.1) from the initial condition $x(t_0) = \overline{x}$, and applying the input $u(t) = \overline{u}$ for all $t \geq t_0$, then

$$x(t) = \overline{x},\ For\ all\ t \geq t_0 \qquad (4.3)$$

And the time at any stability region.

4.1.1. Approximation Variables:

Suppose $\left(\overline{x}, \overline{u}\right)$ is an equilibrium point and input respectively. It is known that if the system started at $x(t_0) = \overline{x}$, and applies the constant input $u(t) = \overline{u}$ then the state of the system will remain fixed at the point $x(t) = \overline{x}$, for all t.but when starting away from the equilibrium point in small difference, then some deviation exist. So the deviation variables needed are represented below[40].

$$\delta_x(t) = x(t) - \overline{x}$$
$$\delta_u(t) = u(t) - \overline{u} \qquad (4.4)$$

To relate the variable $x(t)$ and $u(t)$ substitute Equation (4.4) into Equation (4.1) will give

$$\dot{\delta}_x(t) = f\left(\bar{x} + \delta_x(t), \bar{u} + \delta_u(t)\right) \tag{4.5}$$

This is the exact value of variables with time. Then to remove the higher-order value of deviation use Taylor expansion in the right side of Equation (4.5) to neglect the higher-order.

$$\dot{\delta}_x(t) = f\left(\bar{x}, \bar{u}\right) + \left.\frac{\partial f}{\partial x}\right|_{\substack{x=\bar{x} \\ u=\bar{u}}} \delta_x(t) + \left.\frac{\partial f}{\partial u}\right|_{\substack{x=\bar{x} \\ u=\bar{u}}} \delta_u(t) \tag{4.6}$$

However, $f\left(\bar{x}, \bar{u}\right) = 0$ since it is an equilibrium point and Equation (4.6) becomes.

$$\dot{\delta}_x(t) = \left.\frac{\partial f}{\partial x}\right|_{\substack{x=\bar{x} \\ u=\bar{u}}} \delta_x(t) + \left.\frac{\partial f}{\partial u}\right|_{\substack{x=\bar{x} \\ u=\bar{u}}} \delta_u(t) \tag{4.7}$$

The above equations approximately governs the deviation variables $\delta_x(t)$ and $\delta_u(t)$ by neglecting second order and higher as long as they remain small. It became a linear time-invariant differential equation since the derivative δ_x is a linear combination of the δ_x variables and the deviation input δ_u. Then the matrix can be derived as

$$A = \left.\frac{\partial f}{\partial x}\right|_{\substack{x=\bar{x} \\ u=\bar{u}}} \in R^{n\times n} \ \text{ and } \ B = \left.\frac{\partial f}{\partial u}\right|_{\substack{x=\bar{x} \\ u=\bar{u}}} \in R^{n\times m} \tag{4.8}$$

This matrix is constant.it can be defined as a linear system combination

$$\dot{\delta}_x(t) = A\delta_x(t) + B\delta_u(t) \tag{4.9}$$

Equation (4.9) is the **Jacobian linearization** of the original nonlinear system described in Equation (4.1).

N.B. all the above procedures can also work for the output y for the system with non-linearity.

For a small value of δ_x and δ_u, the linear equation approximately governs the relationship between the deviation variable δ_u and δ_x .For small δ_u (i.e., while remains close to $\bar{u}$), and while δ_x remains small (i.e. while $x(t)$ remains close to $\bar{x}$), the variables δ_x and δ_u are related by the differential Equation (4.9).

In some rigid bodies problems considered in different underactuated system, problems are treated by making a small-angle estimation, taking θ and its derivatives $\dot{\theta}$ and $\ddot{\theta}$ very small so that certain terms were ignored $\left(\dot{\theta}^2, \ddot{\theta}\sin\theta\right)$ and other terms are simplified $\left(\sin\theta \approx \theta, \cos\theta \approx 1\right)$. In the context of this discussion, the linear model obtained was, the Jacobian linearization around the equilibrium point $\theta = 0, \dot{\theta} = 0$ .but this all approximation depends on the controlled body in which the model is applied.

4.2. Linear Quadratic Gaussian Control

Linear Quadratic Gaussian (LQG) control could be a present-day state-space method for designing optimal dynamic controllers. It enables the regulation performance, control effort; take into account processes and mismeasurement noise. Like pole placement, LQG design requires a state-space demonstration of the plant[41].

As explained above this system is a nonlinear system but LQG control is mostly applied with the linearized dynamical system, so any component used by LQG is linearized by the above linearization method.

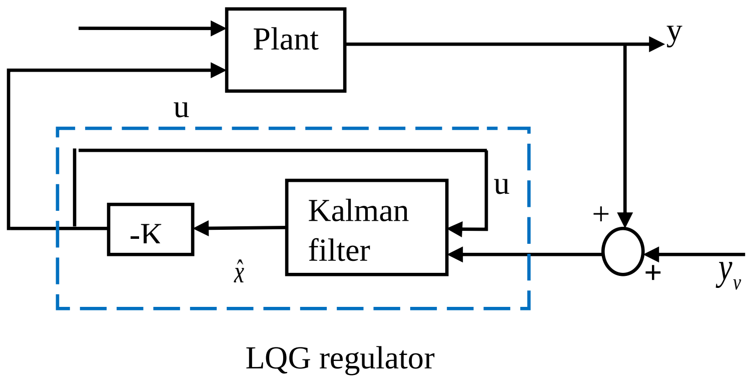

Figure 4. 1.Block diagram of LQG control

LQG is state space control and it can be derived as the regulator state-space equation as

$$\dot{\hat{x}} = \left[A + LC - \left(B - LD\right)K\right]\hat{x} + Ly_v \tag{4.10}$$

$$u = -K\,\hat{x} \tag{4.11}$$

where, A, B, C, D are state matrices, L is Kalman gain, u is control input, K feedback gain, y measured output, and $\hat{x}$ is Kalman filter.

The point is to regulate the output y around zero. The plant is subject to disturbances and is driven by controls. The controller depends on the noisy estimations $y_v = y + v$ to produce these controls. The plant state and estimation conditions are of the form

$$\begin{aligned} \dot{x} &= Ax + Bu + Gw \\ y_v &= Cx + Du + Hw + v \end{aligned} \tag{4.12}$$

where v and w are white noises

The LQG regulator consists of an optimal state-feedback gain and a Kalman state estimator LQE. It can design these two components independently as shown next.

4.2.1. Optimal State-Feedback Gain

In LQG control, the regulation performance is measured by a quadratic performance criterion of the form

$$J(u) = \int_0^{\infty} \left\{ x^T Q x + 2x^T N x + u^T R u \right\} \tag{4.13}$$

where Q, N and R are weighting matrix which is user-specified and defines the trade-off between regulation performance (how fast the output goes to zero) and control effort. The first design step seeks a state feedback law that minimizes the cost function. This gain is called the LQ-optimal gain.

4.2.2. Kalman State Estimator

As for pole placement, the LQ-optimal state feedback $u = -Kx$ is not implementable without full state measurement. However, this can derive a state estimator $\hat{x}$, such that $u = -K\hat{x}$ remains optimal for the output-feedback problem. The Kalman filter generates this state estimate.

$$\dot{\hat{x}} = A\hat{x} + Bu + L(y_v - C\hat{x} - Du) \tag{4.14}$$

In addition, the noise variance data are $E(ww^T) = Q_n, E(vv^T) = R_n, E(wv^T) = N_n$.

This Determines the Kalman gain L through an algebraic Riccati equation. The Kalman filter is an optimal estimator when dealing with Gaussian white noise. Specifically, it minimizes the asymptotic covariance of the estimation error $x-\hat{x}$.

$$\lim_{t\to\infty} E((x-\hat{x})(x-\hat{x})^T)$$

The goal is to regulate the plant output y around zero.

4.3. Adaptive Inverse Control

Consider the plant with non-linearity $N(.)$ at the input of the linear part of the plant $G(D)$

$$y(t) = G(D)u(t) \tag{4.15}$$

where the system input is expressed as

$$u(t) = N(\upsilon(t)) \tag{4.16}$$

where $G(D)$ a rational transfer is function, and D, represents Laplace transform in s-domain for continuous-time system and z-domain for discrete-time systems.

The main control objective is to avoid the effect of non-linearity and use the easiest scheme of linear control methods to ensure the desired performance of the system [15].

To achieve these objectives two processes should be required,

- Avoidance of such nonlinearities for which such compensator can be used is required.
- Adaptive law that can exactly update the compensator parameter is required.

4.3.1. Nonlinearity Clarification

Parameterized model for all non-linearity's can be defined as,

$$u(t) = N(\upsilon(t)) = N(\theta^*;\upsilon(t)) \tag{4.17}$$

$$= -\theta^*\omega^{*T}(t) + \alpha^*_s(t) \tag{4.18}$$

where $\theta^* \in R^{n\theta}$ unknown parameter vector of non-linearity. While $\omega^*(t)$ and $\alpha^*_s(t)$ are unknown signals, whose components are determined by their flow in the non-linearity $N(.)$ The importance of adaptive inverse control method is to remove the effect of non-linearity, where the inverse characteristics $NI(.)$ are parametrized by $\theta(t)$ which is an estimation of θ^*.the system is derived by $u_d\ (t)$ which is the desired control signal from feedback law.

There are criteria's which are applied to inverse control law, these are

- Parameters in the system should be adapted.
- This parameter should stay in a pre-specified region to implement the inverse control law.

All this can be fulfilled by

- The parameter error model
- Parameter projection function needed for commanding the parameter to keep in range of defined boundary.

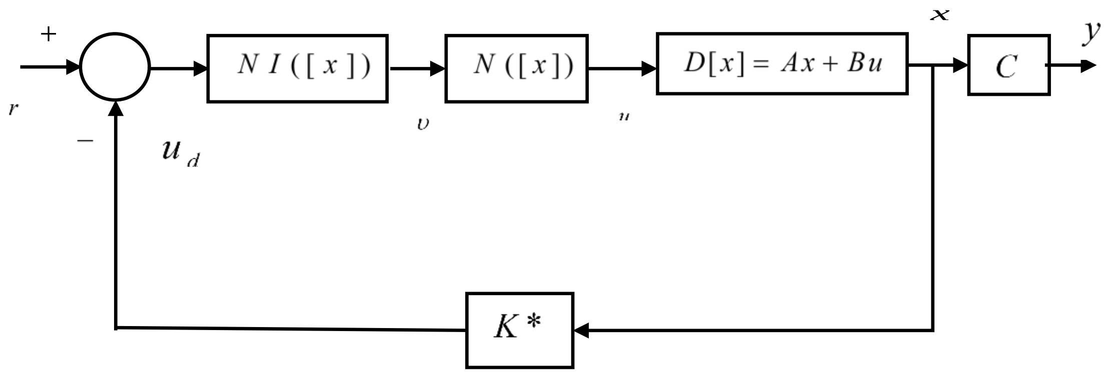

Figure 4. 2. State feedback inverse control

As shown from Figure 4.2 the control law can be derived as;

$$u_d(t) = -K^* x(t) + r(t) \tag{4.19}$$

Lemma: Inverse model: -A desirable inverse $\upsilon(t) = NI(u_d(t))$ should be parametrized by $-\theta^T(t)\,\omega(t) + \alpha_s(t)$, where $\omega(t) \in R^{n\theta}$ and $\alpha_s(t) \in R$ known signals. These components are determined by their flow through the non-linearity inverse model. If $u_d(t)$ is bounded then, $\upsilon(t), \omega\ (t)$ and $\alpha_s(t)$ is bounded. Therefore

$$\upsilon(t) = NI(u_d(t)) \tag{4.20}$$

$$u(t) = u_d(t) + (-\theta^* \omega^{*T}(t) + \alpha^*_s(t) - (-\theta^T(t)\omega(t) + \alpha_s(t)) \quad (4.21)$$

From Equation (4.18) there is

$$u(t) = -\theta^{*T}(t)\omega^*(t) + \alpha^*_s(t) \quad (4.22)$$

The feedback gain K^* on the block diagram of Figure 4.2 can be selected using any method like linear quadratic regulator so that $(A - BK^*)$ is stabilizable.

Using Equation (4.19) the closed-loop response of the system of Figure 4.2 is derived as

$$y(t) = C[DI - A - Bk^*]^{-1} B([r](t) + [(\theta - \theta^*)\omega] d_N(t) + \varepsilon_o(t) \quad (4.23)$$

Equation (4.23) can be reduced by letting $W_d(t) = C[DI - A - Bk^*]^{-1} B$ and if $d_N(t) = 0$ and the inverse cancels the non-linearity $(\theta = \theta^*)$. The total response of Equation (4.23) become

$$y(t) = W_d(t)[r](t) + \varepsilon_o(t) \quad (4.24)$$

Then the reference model of the system can be derived by neglecting the effect of $\varepsilon_o(t)$ and Equation (4.24) become

$$y_m(t) = W_m(t)[r](t) \quad (4.25)$$

To express quantitatively the disturbance signal $d_N(t)$, subtract Equation (4.21) from Equation (4.18).

$$\begin{aligned} u(t) &= u_d(t) + (-\theta^{*T}\omega^*(t) + \alpha^*_s(t) - (-\theta^T(t)\omega(t) + \alpha_s(t)) \\ &= u_d(t) + \theta^{*T}\omega^*(t) + (\tilde{\theta}^T(t) + \theta^{*T})\omega(t) + \alpha^*_s(t) - \alpha_s(t) \\ &= u_d(t) + \theta^{*T}\omega^*(t) + (\omega(t) - \omega^*(t))\theta^{*T} + \alpha^*_s(t) - \alpha_s(t) \end{aligned} \quad (4.26)$$

From Equation (4.26) $(\omega(t) - \omega^*(t))\theta^{*T} + \alpha^*_s(t) - \alpha_s(t)$ is the disturbance signal $d_N(t)$ and the final equation becomes.

$$u(t) = u_d(t) + \theta^{*T}\omega^*(t) + d_N(t) \quad (4.27)$$

As seen from $(\omega(t)-\omega^*(t))\theta^{*T} + \alpha^*_s(t)-\alpha_s(t)$, $d_N(t)$ =0, if $\omega(t)=\omega^*(t)$ and $\alpha^*_s(t)=\alpha_s(t)$.

To drive the reference model with disturbance, consider again Figure 4.2.

$$\begin{aligned} y(t) &= W_m(D)[r](r)+W_m(D)[(\theta(t)+\theta^*)^T\omega](t)+W_m(D)[d_N](t)+\varepsilon_o(t) \\ &= W_m(D)[r](r)+W_m(D)[\tilde{\theta}^T\omega](t)+W_m(D)[d_N](t)+\varepsilon_o(t) \end{aligned} \tag{4.28}$$

Consider $W(D)=W_m(D)$ and Using Equation (4.25) the output error is derived as

$$\begin{aligned} y(t)-y_m(t) &= (W_m(D)[r](r)+W_m(D)[\tilde{\theta}^T\omega](t)+W_m(D)[d_N](t)+\varepsilon_o(t)) \\ &\quad -(W_d(t)[r](t)+\varepsilon_o(t)) \end{aligned} \tag{4.29}$$

Canceling like terms and Equation (4.29) become

$$y(t)-y_m(t)=W_m(D)[\theta(t)-\theta^*)^T\omega](t)+W_m(D)[d_N](t) \tag{4.30}$$

$$y(t)-y_m(t)=W_m(D)[\theta^T\omega](t)-\theta^{*T}W_m(D)[\omega](t)+W_m(D)[d_N](t) \tag{4.31}$$

Then calculate the estimated error as

$$\varepsilon(t)=y(t)-y_m(t)+\zeta(t) \tag{4.32}$$

where,

$$\zeta(t)=\theta^T(t)\xi(t)-W_m(D)[\theta^T\omega](t) \text{ and } \xi(t)=W_m(D)[\omega](t) \tag{4.33}$$

Substitute Equation (4.33) into Equation (4.32) and become:

$$\varepsilon(t)=y(t)-y_m(t)+\theta^T(t)W_m(D)[\omega](t)-W_m(D)[\theta^T\omega](t) \tag{4.34}$$

By considering, Equation (4.31) and Equation (4.34) can be reduced as:

$$\begin{aligned} \varepsilon(t) &= \theta^T(t)-\theta^{*T}-\theta^{*T}(t)W_m(D)[\omega](t)+W_m(D)[d_N](t) \\ &= (\theta^T(t)-\theta^*)^T(t)W_m(D)[\omega](t)-W_m(D)[d_N](t) \end{aligned} \tag{4.35}$$

If $d_N(t)$ =0, then estimation error becomes:

$$\begin{aligned}\varepsilon(t) &= (\theta^T(t)-\theta^*)^T(t)W_m(D)[\omega](t) \\ &= \tilde{\theta}^T W_m(D)[\omega]\,(t)\end{aligned} \tag{4.36}$$

In the time domain the error is:

$$\varepsilon(t) = \tilde{\theta}^T \xi(t) + d_N(t) \tag{4.37}$$

This is linear $\tilde{\theta}(t)$ with bounded error due to the uncertainty of non-linearity $N(.)$.

Lyapunov Adaptive Law Design Method with Continuous Time: The closed-loop state-Space representation of the general system shown in Figure 4.2 is

$$\dot{x}(t) = Ax(t) + Br(t) + B(\tilde{\theta}\,\omega(t) + d_N(t)) \tag{4.38}$$

$$y(t) = C\,x(t) \tag{4.39}$$

If $d_N(t) = 0$ that means $\theta(t) = \theta$ with the control signal of Equation (4.19) then the system becomes,

$$\dot{x}(t) = (A - Bk^*)\,x(t) + Br(t) \tag{4.40}$$

$$y(t) = C\,x(t) \tag{4.41}$$

From this, the reference model can be derived as,

$$\dot{x}_m(t) = (A - Bk^*)\,x_m(t) + Br(t) \tag{4.42}$$

$$y_m(t) = C\,x_m(t) \tag{4.43}$$

With this method, the error can also be calculated as follows,

Let $\tilde{x}(t) = x(t) - x_m(t)$ and $e(t) = y(t) - y_m(t)$ then the above equation become

$$\dot{\tilde{x}}(t) = (A - Bk^*)\,\tilde{x}(t) + B(\tilde{\theta}^T\omega\,(t) + d_N(t)) \tag{4.44}$$

$$e(t) = C\,\tilde{x}(t) \tag{4.45}$$

To develop adaptive law for the given system, consider the following Lyapunov function as

$$v(\tilde{x},\tilde{\theta}) = \frac{1}{2}(\tilde{x}^T P\,\tilde{x} + \tilde{\theta}^T\,\Gamma^{-1}\tilde{\theta}) \tag{4.46}$$

where, $\Gamma = diag[\gamma_1, \gamma_2, ...\gamma_{n\theta}]$, and γ_i's are any positive real numbers for continuous-time systems and $0 < \gamma_i < 2$ to the discrete-time systems. While p is any positive definite matrix, $P = P^T > 0$ satisfy Lyapunov equation stated on Equation (4.47).

$$P(A - Bk^*) + (A - Bk^*)T\,P = -2Q \tag{4.47}$$

where Q is any positive definite matrix, $Q = Q^T > 0$.

Let us take the derivative of Equation (4.46) of Lyapunov function as

$$\begin{aligned}\dot{v} &= \frac{1}{2}[\frac{d}{dt}(\tilde{x}^T P\,\tilde{x} + \tilde{\theta}^T\Gamma^{-1}\tilde{\theta})] \\ &= \tilde{x}^T P\,\dot{\tilde{x}} + \tilde{\theta}^T\Gamma^{-1}\dot{\tilde{\theta}}\end{aligned} \tag{4.48}$$

Then substitute $\dot{\tilde{x}}(t)$ with $(A - Bk^*)\tilde{x}(t) + B(\tilde{\theta}^T\omega(t)) + d_N(t)$ and Equation (4.48) gives

$$\begin{aligned}\dot{v} &= \tilde{x}^T P((A - Bk^*)\,\tilde{x} + B(\tilde{\theta}^T\omega + d_N) + \tilde{\theta}^T\Gamma^{-1}\dot{\tilde{\theta}} \\ &= \tilde{x}^T P\,(A - Bk^*)\,\tilde{x} + \tilde{x}^T PB(\tilde{\theta}^T\omega + d_N) + \tilde{\theta}^T\Gamma^{-1}\dot{\tilde{\theta}}\end{aligned} \tag{4.49}$$

Since $Q = P(A - Bk^*)$ Equation (4.49) becomes

$$\dot{v} = -\tilde{x}^T Q\,\tilde{x} + \tilde{x}^T P\,B(\tilde{\theta}^T\omega + d_N) + \tilde{\theta}^T\Gamma^{-1}\dot{\tilde{\theta}} \tag{4.50}$$

After this step, select an adaptive law for the system as

$$\dot{\tilde{\theta}} = -\Gamma\omega(t)\,\tilde{x}^T(t)P\,B + f_\theta(t) \tag{4.51}$$

If $d_N(t) = 0$,

$$\tilde{x}^T P\,B\,\tilde{\theta}^T\omega + \tilde{\theta}^T\,\Gamma^{-1}\dot{\tilde{\theta}} = 0 \tag{4.52}$$

Equation (4.49) can be reduced as

$$\dot{v} = -\tilde{x}^T Q\,\tilde{x} \le 0 \tag{4.53}$$

This shows that v is bounded and $\tilde{y} = y - y_m \in L^2$ i.e $\tilde{y}$ and $\tilde{\theta}$ are bounded, similarly y and θ are also bounded. But if $d_N(t) \neq 0$, use the parameter projection law $f_\theta(t)$ expressed as

$$f_\theta(t) = \begin{cases} 0 & if\ \theta_i \in [\theta_i^a, \theta_i^b]\ or \\ & if\ \theta_i = \theta_i^a\ and\ g_i(t) \geq 0\ or \\ & if\ \theta_i = \theta_i^b\ and\ g_i(t) \leq 0 \\ -g_i(t) & otherwise \end{cases} \tag{4.54}$$

where $g_i(t)$ stands for;

$$g_i(t) = -\Gamma\omega(t)\tilde{x}^T PB \tag{4.55}$$

And $[\theta_i^a, \theta_i^b]$ is an appropriate span of parameters, with θ_i^a is minimum boundary value and θ_i^b is maximum boundary value. Similarly, adaptive law on Equation (4.51) and the derivative of Lyapunov function becomes considered in [15].

$$\begin{aligned} \dot{v} &= \tilde{x}^T P((A - Bk^*)\tilde{x} + B(\tilde{\theta}^T\omega + d_N) + \tilde{\theta}^T\Gamma^{-1}(-\Gamma\omega\tilde{x}^T PB + f_\theta) \\ &= \tilde{x}^T P(A - Bk^*)\tilde{x} + \tilde{x}^T PB(\tilde{\theta}^T\omega + d_N) + \tilde{\theta}^T\Gamma^{-1}(-\Gamma\omega\tilde{x}^T PB + f_\theta) \\ &= \tilde{x}^T PQ\tilde{x} + \tilde{x}^T PB(\tilde{\theta}^T\omega + d_N) + \tilde{\theta}^T\Gamma^{-1}(-\Gamma\omega\tilde{x}^T PB + f_\theta) \\ &= \tilde{x}^T PQ\tilde{x} + \tilde{x}^T PB\tilde{\theta}^T\omega + \tilde{x}^T PBd_N - \tilde{\theta}^T\Gamma^{-1}\Gamma\omega\tilde{x}^T PB + \tilde{\theta}^T\Gamma^{-1}f_\theta \end{aligned} \tag{4.56}$$

The condensed or final simplified form of Equation (4.56) becomes

$$\dot{v} = \tilde{x}^T Q\tilde{x} + \tilde{x}^T PBd_N + \tilde{\theta}^T\Gamma^{-1}f_\theta \tag{4.57}$$

There is an additional condition that Γ must fulfill which is $\tilde{\theta}^T\Gamma^{-1}f_\theta(\mathrm{t}) \leq 0$ .from Equation (4.52), for each $(\theta_i(t) - \theta_i^*)f_i(t) \leq 0$ θ_i, for $i = 1,2,3,.......,n\theta$. i.e., $\tilde{\theta}^T\Gamma^{-1}f_\theta(\mathrm{t}) \leq 0$, $d_N(t)$, and $x(t)$ are bounded. Equation (4.43) shows that $x_m(t)$ bounded and Equation (4.27) indicates $u_d(t)$ also bounded. At the end of the inverse control theorem, $\omega(t), \alpha(t), \upsilon(t)$ are all bound. Since all closed-loop signals are bounded the output error

$e(t) = y(t) - y_m(t)$ and $\dot{\theta}(t)$ are bounded. That means square error: $\int_{t1}^{t2} e^2(t)dt \le \gamma_o + k_o \int_{t1}^{t2} d_N^2(t)$ for some constant $\gamma_o, k_o > 0$

4.4. Application to Linear Quadratic Gaussian Control

The linear quadratic Gaussian (LQG) is the standard technique for the control design of output or partial state information. Consider a state observer which is constructed using the Kalman optimal estimation method as [42]:

$$\begin{aligned} \dot{\hat{x}} &= A\hat{x} + L(y - \hat{y}) + Bu \\ \hat{y} &= C\,\hat{x} \end{aligned} \tag{4.58}$$

where, $\hat{x}$ is the estimated state vector, L is Kalman filter gain, and $\hat{y}$ is estimated output.

In an adaptive linear quadratic Gaussian (LQG), control the main objective is designing a closed-loop observer model that tracks a reference model expressed as:

$$\dot{x} = A_m\, x_m + B_m\, r \tag{4.59}$$

Consider an ideal controller for a closed-loop system

$$u^* = K_x^*\hat{x} + K_y^*(\mathrm{y} - \hat{\mathrm{y}}) + K_r^*\mathrm{r} \tag{4.60}$$

N.B. variables expressed in adaptive and Lyapunov design are changed with their appropriate symbol used in LQG unless it follows similar steps.

Substitute Equation (4.60) into Equation (4.56) and become

$$\begin{aligned} \dot{\hat{x}} &= A\,\hat{x} + L\,(y - \hat{y}) + B\,K_x^*\hat{x} + B\,K_y^*(y - \hat{y}) + B\,K_r^*\mathrm{r} \\ &= A\,\hat{x} + L\,(y - \hat{y}) + (K_x^*\hat{x} + K_y^*(y - \hat{y}) + K_r^*\mathrm{r})B \end{aligned} \tag{4.61}$$

where,

$$\mathrm{A} + \mathrm{B}K_x^* = A_m, B\,K_r^* = B_m \text{ and } B\,K_y^* = -L \tag{4.62}$$

Then chose a continuous-time adaptive controller as

$$u = K_x(t)\,\hat{x} + K_y(\mathrm{t})\,(y - \hat{y}) + K_r(\mathrm{t})\,\mathrm{r} \tag{4.63}$$

where $\tilde{K}_x = K_x - K_x^*, \tilde{K}_y = K_y - K_y^*, \tilde{K}_r = K_r - K_r^*$ an estimation error of is $K_x(t), K_y(t)$ and $K_r(t)$.substituting Equation (4.62) and the above estimation error into Equation (4.61) it become:

$$\dot{\hat{x}} = A\hat{x} + B_m r + B\tilde{K}_x\hat{x} + B\tilde{K}_y(y-\hat{y}) + B\tilde{K}_r \mathrm{r} \tag{4.64}$$

Assume $e = x_m - \hat{x}$ be the tracking error, which is the subtraction of Equation (4.64) from Equation (4.59), and with error derivative, it becomes

$$\begin{aligned}\dot{e} = \dot{x}_m - \dot{\hat{x}} &= (A_m x_m + B_m r) - (A\hat{x} + B_m r + B\tilde{K}_x\hat{x} + B\tilde{K}_y(y-\hat{y}) + B\tilde{K}_r \mathrm{r})\\ &= A_m(x_m - \hat{x}) - B\tilde{K}_x\hat{x} - B\tilde{K}_y(y-\hat{y}) \text{-} B\tilde{K}_r \mathrm{r})\\ &= A_m e - B\tilde{K}_x\hat{x} - B\tilde{K}_y(y-\hat{y}) \text{-} B\tilde{K}_r \mathrm{r})\end{aligned} \tag{4.65}$$

The choose an adaptive law for $K_x(t), K_y(t)$ and $K_r(t)$ using optimal control modification given by

$$\dot{K}_x^T = \Gamma_x\hat{x}(e^T P + v_x\hat{x}^T K_x^T B^T P A_m^{-1})B \tag{4.66}$$

$$\dot{K}_y^T = \Gamma_y(y-\hat{y})[e^T P + v_y(y-\hat{y})^T K_y^T B^T P A_m^{-1}]B \tag{4.67}$$

$$\dot{K}_r^T = \Gamma_r r(e^T P + v_r r^T K_r^T B^T P A_m^{-1})B \tag{4.68}$$

With initial conditions $K_x(0) = \bar{K}_x, K_y(0) = \bar{K}_y, K_r(0) = \bar{K}_r$, $\Gamma_x = \Gamma_x^T > 0, \Gamma_y = \Gamma_y^T > 0$ and $\Gamma_r = \Gamma_r^T > 0$ are positive gains, $v_x > 0, v_y > 0,$ and $v_r > 0,$ are modification parameters. In addition, $P = P^T > 0$ is the solution of the Lyapunov equation.

$$PA_m + A_m^T P = -Q \tag{4.69}$$

where $Q = Q^T > 0$.

For an adaptive augmentation regulator design where the reference model is zero, the adaptive controller is given by

$$u = \bar{K}_x\hat{x} + \Delta\bar{K}_x\hat{x} + K_y(y-\hat{y}) \tag{4.70}$$

where $\bar{K}_x$ is derived from the LQR design of the full state equation and the adaptive laws for $\Delta\bar{K}_x$ and $K_y(t)$ are given by

$$\Delta\dot{K}_x^T = -\Gamma_x \hat{x}\hat{x}^T (P - v_x \Delta K_x^T B^T P A_m^{-1}) B \qquad (4.71)$$
$$\dot{K}_y^T = -\Gamma_y (y-\hat{y})[x^T P + v_y (y-\hat{y})^T K_y^T B^T P A_m^{-1}] B \qquad (4.72)$$

To check the stability of adaptive law, use the cost function of the Lyapunov equation. Chose a Lyapunov cost function as it is known that

$J(A,B;K) = trace\, P(A,B;K)$ refer to [43] then it becomes

$$v = \hat{x} P \hat{x}^T + trace(\Delta\tilde{K}_x \Gamma_x^{-1} \Delta\tilde{K}_x^T) + trace(\tilde{K}_y \Gamma_y^{-1} \tilde{K}_y^T) \qquad (4.73)$$

The derivative of the Lyapunov equation is

$$\dot{v} = -\hat{x} Q \hat{x}^T + 2v_x \hat{x}^T \Delta K_x^T B^T P A_m^{-1} B \Delta\tilde{K}_x \hat{x} + 2v_y (y-\hat{y})^T K_y^T B^T P A_m^{-1} B \tilde{K}_y (y-\hat{y}) \qquad (4.74)$$

Let $PA_m^{-1} = M + N$. where,

$$M = \frac{1}{2}(PA_m^{-1} + A_m^{-T} P) = -\frac{1}{2} A_m^{-T} Q A_m^{-1} \qquad (4.75)$$

$$N = \frac{1}{2}(PA_m^{-1} - A_m^{-T} P) \qquad (4.76)$$

From this $N = -N^T$ which implies $z^T N z = 0$. and substitute Equation (4.75) and (4.76) into Equation (4.74)

$$\dot{v} = -\hat{x} Q \hat{x}^T - v_x \hat{x}^T \Delta K_x^T B^T A_m^{-1} B \Delta\tilde{K}_x \hat{x} - v_y (y-\hat{y})^T K_y^T B^T A_m^{-1} B \tilde{K}_y (y-\hat{y})$$
$$= +2v_x \hat{x}^T \Delta K_x^{*T} B^T P A_m^{-1} B \Delta\tilde{K}_x \hat{x} + 2v_y (y-\hat{y})^T K_y^{*T} B^T P A_m^{-1} B \tilde{K}_y (y-\hat{y}) \qquad (4.77)$$

Check the boundedness of the Lyapunov equation

$$\dot{v} \le -a_1 \|\hat{x}\|^2 - a_2 v_x \|\hat{x}\|^2 \left(\|\Delta\tilde{K}_x\| - a_3 \|\Delta K_x^*\|\right)^2 - v_y a_2 \|y-\hat{y}\|^2 \left(\|\tilde{K}_y\| - a_3 \|K_y^*\|\right)^2$$
$$+ v_x a_2 a_3^2 \|\hat{x}\|^2 \|\Delta K_x^*\|^2 + v_y a_2 a_3^2 \|y-\hat{y}\|^2 \|K_y^*\|^2 \qquad (4.78)$$

where $a_1 = \lambda_{\min}(Q), a_2 = \lambda_{\min}(B^T Q A_m^{-1} B), a_3 = \dfrac{\lambda_{\min}(B^T P A_m^{-1} B)}{a_2}$ from these values

$\dot{v} \le 0$ if

$$\|\hat{x}\| \ge a_3 \|y-\hat{y}\| \|K_y^*\| \sqrt{\frac{v_y a_2}{a_1 - v_x a_2 a_3 \|\Delta K_x^*\|^2}} = \rho \qquad (4.79)$$

$$\|\Delta \tilde{K}_x\| \ge a_3 \|\Delta K_x^*\| + \sqrt{a_3^2 \|\Delta K_x^*\|^2 + \frac{v_y a_3^2 \|y-\hat{y}\|^2 \|K_y^*\|^2}{v_x \|\hat{x}\|^2}} = k \qquad (4.80)$$

$$\|\tilde{K}_y\| \ge a_3 \|K_y^*\| + \sqrt{a_3^2 \|K_y^*\|^2 + \frac{v_y a_3^2 \|\hat{x}\|^2 \|\Delta K_x^*\|^2}{v_y \|y-\hat{y}\|^2}} = \sigma \qquad (4.81)$$

From Equation (4.76), $a_1 - v_x a_2 a_3 \|\Delta K_x^*\|^2 > 0$ this implies that,

$v_x < \dfrac{a_1}{a_2 a_3 \|\Delta K_x^*\|^2}$ .so all signals are uniformly bounded with an ultimate bound

$$\lim_{t\to\infty} \|\hat{x}\| \le \sqrt{\frac{\lambda_{\max}(P)\rho^2 + \lambda_{\max}\Gamma_x^{-1} k^2 + \lambda_{\max}\Gamma_y^{-1}\sigma^2}{\lambda_{\min}(P)}} \qquad (4.82)$$

From the above proof, we see that adaptive optimal control modification regulator does not exactly result in $\hat{x}(t) \to 0$ as $t \to \infty$. This is because the optimal control modification provides robustness by seeking an optimal solution of $\hat{x}(t)$ bounded away from the origin. The proximity $\hat{x}(t)$ is controlled by the modification parameters v_x and v_y . By $v_x = 0$ and $v_y = 0$, recover the standard model reference adaptive control which results in $\hat{x}(t) \to 0$ as $t \to \infty$. The optimal control modification has a linear limiting property under fast adaptation with large adaptive gains.[44] In the theoretical limit as $\Gamma \to \infty$, then

$$B\Delta K_x = \frac{1}{v_x} B (B^T A_m^{-T} PB)^{-1} B^T P \qquad (4.83)$$

$$BK_y y = \frac{1}{v_y} B (B^T A_m^{-T} PB)^{-1} B^T P \hat{x} \qquad (4.84)$$

Using this limiting property, the estimated stability margin closed-loop system become

$$\dot{x} = Ax + B\bar{K}_x\hat{x} + \left(\frac{1}{v_x} + \frac{1}{v_y}\right)B(B^T A_m^{-T} PB)^{-1} B^T P\,\hat{x} \tag{4.85}$$

$$\hat{x} = \left[Ax + B\bar{K}_x + \left(\frac{1}{v_x} + \frac{1}{v_y}\right)P^{-1}A_m^T P - LC\right]\hat{x} + LCx \tag{4.86}$$

CHAPTER 5

SWING-UP CONTROLLER DESIGN

The swing-up control strategy is based on the mechanical energy of the system. This mechanical energy contains, the potential energy reference, and total energy is at the place where the pendulum is at rest, as depicted in Figure 5.1. This reference potential energy is

$$E_r = m_p g\, l_p \tag{5.1}$$

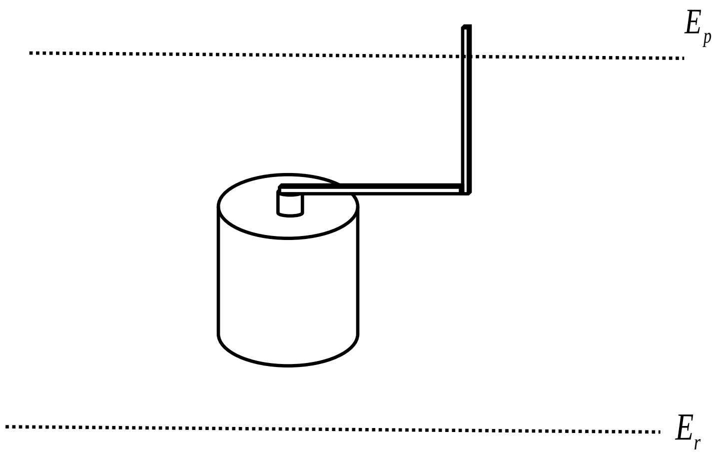

Figure 5. 1.Potential energy reference

The energy-based approach attempts to swing the pendulum upright by using the total energy of the system as a feedback quantity. The pendulum is controlled in such a way that its energy is driven towards a value equal to the steady-state upright position[45]. Ignoring friction and accepting the pendulum as an unbending body, the equation of motion of the pendulum is

$$J_p\, \ddot{\alpha} - m_p g\, l_p \sin(\alpha) + mu\, l_p \cos(\alpha) = 0 \tag{5.2}$$

where g is the acceleration of gravity and *u (=ng)* is the maximum acceleration of the pivot. The parameter *n* is dimension-free. Normalized variables are useful to characterize the properties of a system. Introduce $\omega_o = \sqrt{\frac{mgL}{J_p}}$ which is the frequency of small oscillations around the downward position. The equation of motion is then characterized by two parameters only. As indicated in the figure the potential energy of the pendulum at upright position corresponds to the energy reference

$$E_r = 2m_p g\, l_p \tag{5.3}$$

Choose the energy of the system as zero in the upright position, and normalize it by $m_p g l_p$, *which* is the energy required to raise the pendulum from the hanging down position to the horizontal position. The normalized energy can be then written as

$$E_p = \frac{1}{2} J_p \dot{\alpha}^2 + 2m_p g\, l_p (1\text{-}\cos(\alpha)) \tag{5.4}$$

Swinging up the pendulum will particularly concern controlling the energy such that the pendulum comes to its heteroclinic orbits. These orbits are found by investigating the case where the energy of the pendulum is equal to $E*$, i.e.

$$\begin{aligned} &E_r = E_p \\ &2m_p g\, l_p = \frac{1}{2} J_p \dot{\alpha}^2 + 2m_p g\, l_p (1\text{-}\cos(\alpha)) \end{aligned} \tag{5.5}$$

Solving $\dot{\alpha}$ yields the expression for the heteroclinic orbits.

$$\dot{\alpha} = \sqrt{\frac{g}{l_p}(1\text{-}\cos(\alpha))} \tag{5.6}$$

Heteroclinic orbits are trajectories that connect two stable equilibrium points of a system (i.e., there exists an equilibrium point on either side of heteroclinic orbits). The blue line in Figure 5.2 represents the heteroclinic orbit of a pendulum. In addition, the two smaller circle in the right and left side are the equilibrium points. Inside heteroclinic orbits, the trajectory moves away from the unstable equilibrium point on one side and moves toward it on the other side. Outside Heteroclinic orbits, the energy of the system is greater than reference energy; this shows that if there is no friction the system will continue on the path. However, if there is friction it loses the energy and ends up on the next stable equilibrium point. For an Inverted pendulum on a cart for zero friction if the system energy is greater than reference energy the pendulum continues rotating or swings back and forth continuously and never stops. However, if there is friction it will end up at one of its stable equilibrium points (*nπ;* 0).

The process of driving a pendulum from its pedant position, where the energy of the system is minimum to an inverted position where the energy of the system is maximum is known as Swing-up. The main objective of this process is to add energy to the system so that the system reaches its unstable equilibrium point, for control purposes.

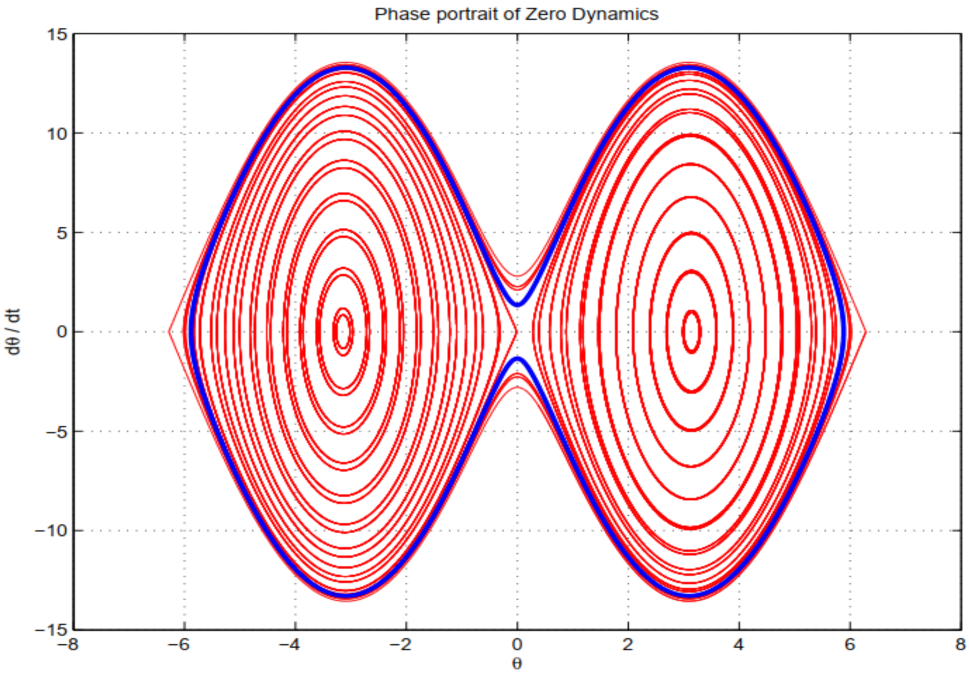

Figure 5. 2. Hetero clinic orbit in pendulum natural dynamics

To derive the control strategy, take the derivative of Equation (5.4) gives

$$\dot{E} = \dot{\alpha}\,(J_p\ddot{\alpha} + \frac{1}{2} m_p g\, l_p \sin(\alpha)) \tag{5.7}$$

To introduce the pivot acceleration u and eventually, our control variable, solve α in Equation (5.2) and obtain as

$$\sin(\alpha) = \frac{1}{m_p\, g\, l_p}\left(-2J_p\ddot{\alpha} + m_p g\, l_p\ \cos(\alpha)\right) \tag{5.8}$$

Then substitute Equation (5.8) into Equation (5.7) gives

$$\dot{E} = \frac{1}{2} m_p\, l_p\, u\, \dot{\alpha}\ \sin(\alpha)) \tag{5.9}$$

The pendulum will swing up to the desired reference energy E_r and acceleration u becomes

$$u = (E - E_r\, \dot{\alpha} \cos(\alpha)) \tag{5.10}$$

By setting the reference energy to the pendulum potential energy, i.e., $E^* = E$ the control will swing the link to its upright position. For energy to change quickly the magnitude of the control signal must be large. as a result, the following swing-up controller is designed as

$$u = sat_{u_{max}} \left(\mu\, (E - E_r) sign(\dot{\alpha} \cos\alpha) \right) \tag{5.11}$$

where μ is tunable control gain and $sat_{u_{max}}$ function saturates the control signal at a maximum acceleration of the pendulum pivot u_{max}.

5.2. Energy Based PD based Swing-up Controller Design (EBPDSC)

A Swing-up controller will derive the position of the arm to drive from the stable downward position of the pendulum.it makes sense that by applying the DC motor and by moving the arm back and forth strongly enough, the energy is gradually added to the RIP system, so the pendulum it can be swing up to an unstable position

Many different control algorithms (trajectory tracking, energy-based method, and rectangular reference input swing-up type, adaptive or intelligent strategy) can be used to perform the swing-up control. Here a positive feedback GA tuned PD controller with an energy-based approach is used because of its simple structure, effectiveness, and easy tuning [46].

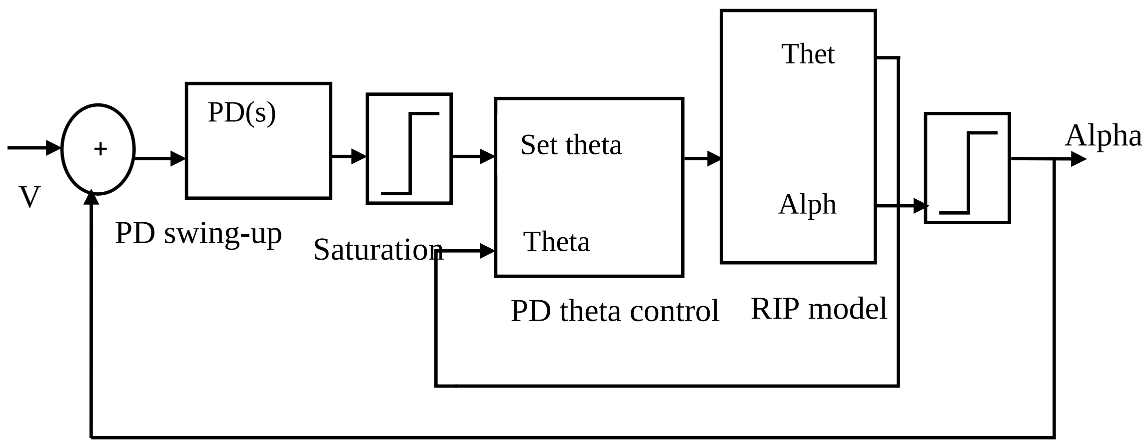

Figure 5. 3. Block diagram of PD swing-up control of RIP

The block control diagram consists of two loops as shown in Figure 5.3. The inner loop performs the position control of the arm, while the outer loop specifies the desired trajectory for the arm along to swing the pendulum to the balancing position.

For the servo arm to track the desired position, a positive feedback PD control law is designed as

$$u_m(t) = k_p * \theta + k_d * \dot{\theta} \qquad (5.12)$$

The position PD controller offers the voltage applied to the motor so that angle of the arm θ tracks the desired position θ_d .the tuning parameters of conventional PD parameter k_p and k_d have randomly selected and tuned with GA to achieve the desired performance for the inner loop and outer loop.

Within the external loop, for swing-up, the pendulum a positive feedback PD control loop was chosen. This positive feedback loop increases the energy provided to the pendulum and has a role in destabilizing the system because the downward position of the pendulum is stable. The value of the tuning PD parameters $k_{p\alpha}$ and $k_{d\alpha}$ plays a key role in bringing up the pendulum smoothly. These parameters (the proportional and derivative constants) can be tuned to alter the positive damping within the system. Moreover, the command provided by the swung-up controller (desired angle of pivot arm) must be limited in the range $\pm 180^o$ to ensure that the arm does not reach a position that will cause a collision.

$$\theta_d(t) = k_{p\alpha} * \alpha + k_{d\alpha} * \qquad (5.13)$$

The energy of the system is given to the outer loop PD controller to get a perfect stabilizing point.

5.3. Swinging (Switching) Condition

As the pendulum goes to the upright position of equilibrium point, the stabilizing controller must take over the swing-up controller. Therefore, there must be a switching mechanism for swinging up the pendulum. The requirements of the switching up of the controller for its stabilization are

- The change in the range of the pendulum must be in the range of $E^* - E \le \frac{1}{2}\left|E^*\right|$.
- The angle of the pendulum must be in range $|\alpha| < \frac{\pi}{6}$.

According to the above criteria, it is possible to select the controller for applying to the system. i.e. If one or both of the criteria is fulfilled the output of the swing up controller to the system unless the output of stabilizing controller is applied to the system. However, anyone should remind that both controllers do not apply to the system at the same time. That means if one of the controllers is applied, the other should be passive or eliminated from the system.

CHAPTER 6

STABILIZING CONTROLLER DESIGN

6.1. Approximate Linearization, Stability, and Controllability Checking

6.1.1. Linearization about an Equilibrium Point of Nonlinear System

Given the nonlinear system of an underactuated mechanical system

$$f(x,u) \tag{6.1}$$

From topic (4.1) the approximate linearization of a nonlinear underactuated model which is the Furuta pendulum is based on Tayler series expansion of the model around the equilibrium point $\bar{x},\bar{u}$ and rotating only the first-order terms.[43]

For the system containing n-states n -states $x_1, x_2.....x_n$ and n - inputs $u_1, u_2.....u_n$ the Tayler series can be expressed as

$$y-\bar{y} = (x_1-\bar{x}_1)\left.\frac{\partial f}{\partial x_1}\right|_{x=\bar{x}} + (x_2-\bar{x}_2)\left.\frac{\partial f}{\partial x_2}\right|_{x=\bar{x}} + ... + (x_n-\bar{x}_n)\left.\frac{\partial f}{\partial x_n}\right|_{x=\bar{x}}$$
$$+ (u_1-\bar{u}_1)\left.\frac{\partial f}{\partial u_1}\right|_{u=\bar{u}} + (u_2-\bar{u}_2)\left.\frac{\partial f}{\partial u_2}\right|_{u=\bar{u}} + ... + (u_n-\bar{u}_n)\left.\frac{\partial f}{\partial u_n}\right|_{u=\bar{u}} \tag{6.2}$$

Depending on the topic described in Equation (4.1) eliminate the higher-order term and write as general case as

$$y-\bar{y} = f(\bar{x},\bar{u}) + \left.\frac{\partial f}{\partial x}\right|_{\substack{x=\bar{x}\\u=\bar{u}}} + \left.\frac{\partial f}{\partial x_2}\right|_{\substack{x=\bar{x}\\u=\bar{u}}} \tag{6.3}$$

Then from the nonlinear model expressed in Equation (3.18) and (3.19)

$$m_{11}(q_2)\ddot{q}_1 + m_{12}(q_2)\ddot{q}_2 + m_p l_1^2 \sin(2q_2)\dot{q}_1\dot{q}_2 - m_p l_1 l_a \sin(q_2)\dot{q}_2^2 = T \tag{6.4}$$

$$m_{21}(q_2)\ddot{q}_1 + m_{22}(q_2)\ddot{q}_2 - \frac{1}{2} m_p l_1^2 \sin(2q_2)\dot{q}_1^2 - m_p g l_1 \sin(q_2) = 0 \tag{6.5}$$

Equation (6.4) and (6.5) consists of pendulum rotation angle α and arm rotational angle θ and from the above Equation (6.4) and (6.5) the coordinate transform is represented as

$(q_1, q_2) \rightarrow (\theta, \alpha)$ Expressed in Chapter 3.

Then the equation of motion as a function of $\theta, \dot{\theta}, \alpha, \dot{\alpha}$ with becomes

$$
\begin{gathered}
m_{11} = m_a l_a{}^2 + J_a + m_p l_a{}^2 + m_p l_1 \sin^2(q_2) \\
m_{12} = m_{21} = m_p l_1 l_a \cos(q_2) \qquad (6.6) \\
m_{22} = m_p l_1{}^2 + J_p
\end{gathered}
$$

$$
T = K_g \eta_m \eta_g K_t \frac{V_a}{R_m} - \frac{K_g^2 \eta_m \eta_g K_t K_m \dot{\theta}}{R_m} \text{ with } K_u = \frac{K_g \eta_m \eta_g K_t}{R_m} \text{ and } K_\theta = \frac{K_g^2 \eta_m \eta_g K_t K_m}{R_m}
$$

Become

$$
\begin{aligned}
f(\theta, \dot{\theta}, \alpha, \dot{\alpha}) = {} & (m_a l_a{}^2 + J_a + m_p l_a{}^2 + m_p l_1 \sin^2(\alpha))\ddot{\theta} + m_p l_1 l_a \cos(\alpha)\ddot{\alpha} \\
& + m_p l_1^2 \sin(2\alpha)\dot{\theta}\dot{\alpha} - m_p l_1 l_a \sin(\alpha)\dot{\alpha}^2 - K_u u + K_\theta \dot{\theta} \qquad (6.7)
\end{aligned}
$$

$$
\begin{aligned}
f(\theta, \dot{\theta}, \alpha, \dot{\alpha}) = {} & m_p l_1 l_a \cos(\alpha)\ddot{\theta} + (m_p l_1{}^2 + J_p)\ddot{\alpha} - \frac{1}{2} m_p l_1{}^2 \sin(2\alpha)\dot{\theta}^2 \\
& - m_p g l_1 \sin(\alpha) \qquad (6.8)
\end{aligned}
$$

Linearization for the Upright Position: From Equation (6.7) the linearization about unstable equilibrium $x_{eq} = [0\ 0\ \pi\ 0]^T$ then it becomes

$$
\bar{f}_1(0\ 0\ \pi\ 0) = (m_a l_a{}^2 + J_a + m_p l_a{}^2)\ddot{\theta} + m_p l_1 l_a \ddot{\alpha} - K_u u \qquad (6.9)
$$

Then the partial derivative to each variable at equilibrium unstable position become

$$
\left.\frac{\partial f_1}{\partial \theta}\right|_{x=\bar{x}} = 0, \left.\frac{\partial f_1}{\partial \dot{\theta}}\right|_{x=\bar{x}} = \mathrm{b}_1, \left.\frac{\partial f_1}{\partial \alpha}\right|_{x=\bar{x}} = 0, \left.\frac{\partial f_1}{\partial \dot{\alpha}}\right|_{x=\bar{x}} = 0, \qquad (6.10)
$$

Therefore, the linearized equation of motion for rotation is given as

$$
(m_a l_a{}^2 + J_a - m_p l_a{}^2)\ddot{\tilde{\theta}} + m_p l_1 l_a \ddot{\tilde{\alpha}} - K_u u + (b_1 + K_\theta)\dot{\tilde{\alpha}} = 0 \qquad (6.11)
$$

From Equation (6.8) the linearization about unstable equilibrium $x_{eq} = [0\ 0\ \pi\ 0]^T$ become

$$\bar{f}_2(0\ 0\ \pi\ 0) = -m_p l_1 l_a \ddot{\theta} + (m_p l_1^2 + J_p)\ddot{\alpha} \tag{6.12}$$

Then the partial derivative to each state is then

$$\left.\frac{\partial f_2}{\partial \theta}\right|_{x=\bar{x}} = 0, \left.\frac{\partial f_2}{\partial \dot{\theta}}\right|_{x=\bar{x}} = 0, \left.\frac{\partial f_2}{\partial \alpha}\right|_{x=\bar{x}} = \text{-}m_p l_1 g, \left.\frac{\partial f_2}{\partial \dot{\alpha}}\right|_{x=\bar{x}} = 0, \tag{6.13}$$

So, the linearized equation of motion of rotation become

$$-m_p l_1 l_a \ddot{\tilde{\theta}} + (m_p l_1^2 + J_p)\ddot{\tilde{\alpha}} + b_2 \dot{\tilde{\alpha}} - m_p l_1 \mathrm{g} \tilde{\alpha} = 0 \tag{6.14}$$

The linearized equation of the input is

$$\left.\frac{\partial f_1}{\partial u}\right|_{u=\bar{u}} = K_u, and, \left.\frac{\partial f_2}{\partial u}\right|_{u=\bar{u}} = 0 \tag{6.15}$$

The final linearized model of pendulum motion in the upright position become with considering viscous friction b_1 and b_2

$$\begin{bmatrix} (m_a l_a^2 + J_a + m_p l_a^2) & -m_p l_1 l_a \\ -m_p l_1 l_a & (m_p l_1^2 + J_p) \end{bmatrix} \begin{bmatrix} \ddot{\tilde{\theta}} \\ \ddot{\tilde{\alpha}} \end{bmatrix} + \begin{bmatrix} b_1 + K_\theta & 0 \\ 0 & b_2 \end{bmatrix} \begin{bmatrix} \dot{\tilde{\theta}} \\ \dot{\tilde{\alpha}} \end{bmatrix}$$
$$+ \begin{bmatrix} 0 & 0 \\ 0 & -m_p l_1 g \end{bmatrix} \begin{bmatrix} \tilde{\theta} \\ \tilde{\alpha} \end{bmatrix} = \begin{bmatrix} K_u \\ 0 \end{bmatrix} u \tag{6.16}$$

As described in the Topic 3.3 the coordinate rotation variables are substituted at equilibrium with

$$q_1 = \tilde{x}_1 = \tilde{\theta}, and\ \dot{\tilde{x}}_1 = \tilde{x}_2 \Rightarrow \ddot{\tilde{x}}_1 = \dot{\tilde{x}}_2$$
$$q_2 = \tilde{x}_3 = \tilde{\alpha}, and\ \dot{\tilde{x}}_3 = \tilde{x}_4 \Rightarrow \ddot{\tilde{x}}_3 = \dot{\tilde{x}}_4$$

Therefore, the corresponding state variable state rotation coordinate become

$$\left[\dot{\tilde{x}}_1, \dot{\tilde{x}}_2, \dot{\tilde{x}}_3, \dot{\tilde{x}}_4\right]^T = \left[\dot{\tilde{\theta}}, \ddot{\tilde{\theta}}, \dot{\tilde{\alpha}}, \ddot{\tilde{\alpha}}\right]^T \tag{6.17}$$

Then to get the state matrices to consider Equation (6.10) and (6.13) in terms of state variable χ

$$(m_a l_a{}^2 + J_a + m_p l_a{}^2)\dot{\tilde{x}}_2 + m_p l_1 l_a \dot{\tilde{x}}_4 - K_u u + (b_1 + K_\theta)\tilde{x}_2 = 0 \tag{6.18}$$

$$-m_p l_1 l_a \dot{\tilde{x}}_2 + (m_p l_1{}^2 + J_p)\dot{\tilde{x}}_4 + b_2 \tilde{x}_4 - m_p l_1 \mathrm{g}\,\tilde{\mathrm{x}}_3 = 0 \tag{6.19}$$

From the beginning let $\dot{\tilde{x}}_1 = \tilde{x}_2$ and $\dot{\tilde{x}}_3 = \tilde{x}_4$ and From Equation (6.18)

$$\dot{\tilde{x}}_4 = \frac{m_p l_1\,\mathrm{g}\,\tilde{x}_3 + m_p\, l_1\, l_a \dot{\tilde{x}}_2 - b_2 \tilde{x}_4}{m_p l_1{}^2 + J_p} \qquad (6.20$$

Substitute Equation (6.19) into (6.17) becomes

$$(m_a l_a{}^2 + J_a + m_p\, l_a{}^2)\dot{\tilde{x}}_2 + m_p l_1 l_a \left(\frac{m_p l_1 \mathrm{g}\,\tilde{\mathrm{x}}_3 + m_p l_1 l_a \dot{\tilde{x}}_2 - b_2 \tilde{x}_4}{m_p l_1{}^2 + J_p} \right) - K_u u + K_\theta = 0 \tag{6.21}$$

$$\dot{\tilde{x}}_2 = \frac{K_u u\left(m_p\, l_1{}^2 + J_p\right) - (b_1 + K_\theta)\left(m_p\, l_1{}^2 + J_p\right)\tilde{x}_2 + m_p^2\, l_1{}^2 l_a g\,\tilde{x}_3 - m_p l_1 l_a b_2\,\tilde{x}_4}{\left(m_a\, l_a{}^2 + J_a + m_p\, l_a{}^2\right)\left(m_p l_1{}^2 + J_p\right) - m_p^2\, l_1^2 l_a^2} \tag{6.22}$$

Similarly, from Equation (6.18)

$$\dot{\tilde{x}}_2 = \frac{(m_p l_1{}^2 + J_p)\,\dot{\tilde{x}}_4 + b_2\,\tilde{x}_4 - m_p l_1\,\mathrm{g}\, m\,\tilde{x}_3}{m_p l_1\, l_a} \tag{6.23}$$

Substitute Equation (6.22) into Equation (6.17)

$$(m_a l_a{}^2 + J_a + m_p\, l_a{}^2)\left(\frac{(m_p\, l_1{}^2 + J_p)\,\dot{\tilde{x}}_4 + b_2 \tilde{x}_4 - m_p l_1 \mathrm{g}\, m\,\tilde{x}_3}{m_p l_1 l_a} \right) + m_p\, l_1\, l_a\, \dot{\tilde{x}}_4 - K_u u$$

$$+ (b_1 + K_\theta)\tilde{x}_2 = 0 \tag{6.24}$$

Then $\dot{\tilde{x}}_2$ become

$$\dot{\tilde{x}}_4 = \frac{K_u u\, m_p l_1 l_a - \left(b_1 + K_\theta\right) m_p l_1 l_a\, \tilde{x}_2 + \left(m_a l_a{}^2 + J_a + m_p l_a{}^2\right) m_p l_1\, \mathrm{g}\,\tilde{x}_3 - \left(m_p l_1{}^2 + J_p\right) b_2 \tilde{x}_4}{\left(m_a l_a{}^2 + J_a + m_p l_a{}^2\right)\left(m_p l_1{}^2 + J_p\right) - m_p^2 l_1^2 l_a^2} \tag{6.25}$$

For simplification let

$$a = m_p l_1{}^2 + J_p, b = m_a l_a{}^2 + J_a + m_p l_a{}^2, c = m_p^2 l_1^2 l_a^2,\ d = m_p^2 l_1{}^2 l_a g, e = m_p l_1 l_a,\ f = m_p l_1 \mathrm{g}$$

Then the state space representation in the upright position become

$$\begin{bmatrix} \dot{\tilde{x}}_1 \\ \dot{\tilde{x}}_2 \\ \dot{\tilde{x}}_3 \\ \dot{\tilde{x}}_4 \end{bmatrix} = \begin{bmatrix} 0 & 1 & 0 & 0 \\ 0 & \dfrac{-(b_1+K_\theta)a}{ab-c} & \dfrac{d}{ab-c} & \dfrac{eb_2}{ab-c} \\ 0 & 0 & 0 & 1 \\ 0 & \dfrac{-(b_1+K_\theta)}{ab-c} & \dfrac{af}{ab-c} & \dfrac{ab_2}{ab-c} \end{bmatrix} \tilde{x} + \begin{bmatrix} 0 \\ \dfrac{K_u a}{ab-c} \\ 0 \\ \dfrac{K_u e}{ab-c} \end{bmatrix} \tilde{u} \tag{6.26}$$

$$\tilde{y} = \begin{bmatrix} 0 & 1 & 0 & 0 \\ 0 & 0 & 0 & 1 \end{bmatrix} \begin{bmatrix} \tilde{x}_1 \\ \tilde{x}_3 \end{bmatrix}$$

Linearization for the Downward Position: Linearization of the downward position is around the stable $x_{eq} = [0\ 0\ 0\ 0]^T$ and from Equation (6.7) and (6.8)

$$\bar{f}_1(0\ 0\ 0\ 0) = (m_a l_a{}^2 + J_a + m_p l_a{}^2)\ddot{\theta} + m_p l_1 l_a \ddot{\alpha} - K_u u + K_\theta \dot{\theta} \tag{6.27}$$

Then the partial derivative to each state become

$$\left.\frac{\partial f_1}{\partial \theta}\right|_{x=\bar{x}} = 0, \left.\frac{\partial f_1}{\partial \dot{\theta}}\right|_{x=\bar{x}} = b_1 + K_\theta, \left.\frac{\partial f_1}{\partial \alpha}\right|_{x=\bar{x}} = 0, \left.\frac{\partial f_1}{\partial \dot{\alpha}}\right|_{x=\bar{x}} = 0, \tag{6.28}$$

The linearized equation becomes

$$(m_a l_a{}^2 + J_a + m_p l_a{}^2)\ddot{\tilde{\theta}} + m_p l_1 l_a \ddot{\tilde{\alpha}} - K_u u + (b_1 + K_\theta)\dot{\tilde{\theta}} = 0 \tag{6.29}$$

And from Equation (6.8)

$$\bar{f}_2(0\ 0\ 0\ 0) = -m_p l_1 l_a \ddot{\theta} + (m_p l_1^2 + J_p)\ddot{\alpha} \tag{6.30}$$

The partial derivative to each variable becomes

$$\left.\frac{\partial f_2}{\partial \theta}\right|_{x=\bar{x}} = 0, \left.\frac{\partial f_2}{\partial \dot{\theta}}\right|_{x=\bar{x}} = b, \left.\frac{\partial f_2}{\partial \alpha}\right|_{x=\bar{x}} = m_p g l_1, \left.\frac{\partial f_2}{\partial \dot{\alpha}}\right|_{x=\bar{x}} = b_2, \tag{6.31}$$

The linearized equation of rotational motion is then

$$m_p l_1 l_a \ddot{\tilde{\theta}} + (m_p l_1^2 + J_p)\ddot{\tilde{\alpha}} + b_2 \dot{\tilde{\alpha}} + m_p l_1 g \tilde{\alpha} = 0 \tag{6.32}$$

Then the final linearized model of the pendulum in the downward position become

$$\begin{bmatrix} (m_a l_a{}^2 + J_a + m_p l_a{}^2) & m_p l_1 l_a \\ m_p l_1 l_a & (m_p l_1{}^2 + J_p) \end{bmatrix} \begin{bmatrix} \ddot{\tilde{\theta}} \\ \ddot{\tilde{\alpha}} \end{bmatrix} + \begin{bmatrix} b_1 + K_\theta & 0 \\ 0 & b_2 \end{bmatrix} \begin{bmatrix} \dot{\tilde{\theta}} \\ \dot{\tilde{\alpha}} \end{bmatrix} + \begin{bmatrix} 0 & 0 \\ 0 & m_p l_1 g \end{bmatrix} \begin{bmatrix} \tilde{\theta} \\ \tilde{\alpha} \end{bmatrix} = \begin{bmatrix} K_u \\ 0 \end{bmatrix} u \tag{6.33}$$

Similarly, to the above steps put the linearized model in state-space form Equation (6.31) can be written as

$$(m_a l_a{}^2 + J_a + m_p l_a{}^2)\, \dot{\tilde{x}}_2 + m_p l_1 l_a \dot{\tilde{x}}_4 + (b_1 + K_\theta)\, \tilde{x}_2 = K_u u \tag{6.34}$$

$$m_p l_1 l_a \dot{\tilde{x}}_2 + (m_p l_1{}^2 + J_p)\, \dot{\tilde{x}}_4 + b_2\, \tilde{x}_4 + m_p l_1 \mathrm{g}\, \tilde{x}_3 = 0 \tag{6.35}$$

From Equation (6.33)

$$\dot{\tilde{x}}_4 = \frac{-b_2 \tilde{x}_4 - m_p l_1\, \mathrm{g}\, \tilde{x}_3 - m_p l_1 l_a\, \dot{\tilde{x}}_2}{m_p l_1{}^2 + J_p} \tag{6.36}$$

Substitute Equation (6.34) into (6.32)

$$(m_a l_a{}^2 + J_a + m_p l_a{}^2)\, \dot{\tilde{x}}_2 + m_p l_1 l_a \left(\frac{-b_2 \tilde{x}_4 - m_p l_1 \mathrm{g}\, \tilde{x}_3 - m_p l_1 l_a \dot{\tilde{x}}_2}{m_p l_1{}^2 + J_p} \right) + (b_1 + K_\theta) \tilde{x}_2 = K_u u \tag{6.37}$$

From this rearrangement $\dot{\tilde{x}}_2$ becomes

$$\dot{\tilde{x}}_2 = \frac{K_u u \left(m_p l_1{}^2 + J_p \right) - \left(b_1 + K_\theta \right) \left(m_p l_1{}^2 + J_p \right) \tilde{x}_2 + m_p l_1 l_a b_2\, \tilde{x}_4 + m_p^2 l_1{}^2 l_a g\, \tilde{x}_3}{\left(m_a l_a{}^2 + J_a + m_p l_a{}^2 \right) \left(m_p l_1{}^2 + J_p \right) - m_p^2 l_1{}^2 l_a^2} \tag{6.38}$$

Similarly, from Equation (6.33)

$$\dot{\tilde{x}}_2 = \frac{-b_2 \tilde{x}_4 - m_p l_1\, \mathrm{g}\, \tilde{x}_3 - (m_p l_1{}^2 + J_p)\, \dot{\tilde{x}}_4}{m_p l_1 l_a} \tag{6.39}$$

$$(m_a l_a{}^2 + J_a + m_p l_a{}^2) \left(\frac{-b_2 \tilde{x}_4 - m_p l_1 \mathrm{g} \tilde{x}_3 - (m_p l_1{}^2 + J_p) \dot{\tilde{x}}_4}{m_p l_1 l_a} \right) + m_p l_1 l_a \dot{\tilde{x}}_4 + (b_1 + K_\theta) \tilde{x}_2 = K_u u \tag{6.40}$$

Rearranging this $\dot{\tilde{x}}_4$ become

$$\dot{\tilde{x}}_4 = \frac{K_u u m_p l_1 l_a - \left(b_1 + K_\theta\right) m_p l_1 l_a \tilde{x}_2 + \left(m_a l_a{}^2 + J_a + m_p l_a{}^2\right) b_2 \tilde{x}_4 + m_p l_1 \mathrm{g} \begin{pmatrix} m_a l_a{}^2 + J_a \\ + m_p l_a{}^2 \end{pmatrix} \tilde{x}_3}{-\left(m_a l_a{}^2 + J_a + m_p l_a{}^2\right)\left(m_p l_1^2 + J_p\right) + m_p^2 l_1^2 l_a^2} \tag{6.41}$$

For simplification let

$$a = m_p l_1^2 + J_p \,, b = m_a l_a{}^2 + J_a + m_p l_a{}^2 \,, c = m_p^2 l_1^2 l_a^2$$
$$d = m_p^2 l_1^2 l_a g \,, e = m_p l_1 l_a \,, f = m_p l_1 \mathrm{g}$$

Then the state space representation in the downward position become

$$\begin{bmatrix} \dot{\tilde{x}}_1 \\ \dot{\tilde{x}}_2 \\ \dot{\tilde{x}}_3 \\ \dot{\tilde{x}}_4 \end{bmatrix} = \begin{bmatrix} 0 & 1 & 0 & 0 \\ 0 & \dfrac{-(b_1 + K_\theta) a}{ab - c} & \dfrac{d}{ab - c} & \dfrac{e b_2}{ab - c} \\ 0 & 0 & 0 & 1 \\ 0 & \dfrac{-(b_1 + K_\theta)}{-ab + c} & \dfrac{af}{-ab + c} & \dfrac{a b_2}{-ab + c} \end{bmatrix} \tilde{x} + \begin{bmatrix} 0 \\ \dfrac{K_u a}{ab - c} \\ 0 \\ \dfrac{K_u e}{-ab + c} \end{bmatrix} \tilde{u} \tag{6.42}$$

$$\tilde{y} = \begin{bmatrix} 0 & 1 & 0 & 0 \\ 0 & 0 & 0 & 1 \end{bmatrix} \begin{bmatrix} \tilde{x}_1 \\ \tilde{x}_3 \end{bmatrix} \quad \text{where,}$$

$$A = \begin{bmatrix} 0 & 1 & 0 & 0 \\ 0 & \dfrac{-(b_1 + K_\theta) a}{ab - c} & \dfrac{d}{ab - c} & \dfrac{e b_2}{ab - c} \\ 0 & 0 & 0 & 1 \\ 0 & \dfrac{-(b_1 + K_\theta)}{-ab + c} & \dfrac{d}{ab - c} & \dfrac{e b_2}{ab - c} \end{bmatrix}, B = \begin{bmatrix} 0 \\ \dfrac{K_u a}{ab - c} \\ 0 \\ \dfrac{K_u e}{-ab + c} \end{bmatrix}, C = \begin{bmatrix} 0 & 1 & 0 & 0 \\ 0 & 0 & 0 & 1 \end{bmatrix} \tag{6.43}$$

6.2. System Stability

As presented at the beginning of Section 6.1, Equations (6.10) and (6.13) express the local

Stability of the internal dynamics, and the zero dynamics respectively. The matrix expressed in Equation (6.42) is called the Jacobian matrix. This matrix exhibits a characteristics polynomials equation for proving the stability of the whole system defined as

$$\left|A - sI_4\right| = \left\|\begin{bmatrix} -s & 1 & 0 & 0 \\ 0 & \frac{-(b_1+K_\theta)a}{ab-c} - s & \frac{d}{ab-c} & \frac{eb_2}{ab-c} \\ 0 & 0 & -s & 1 \\ 0 & \frac{-(b_1+K_\theta)}{ab-c} & \frac{af}{ab-c} & \frac{ab_2}{ab-c} - s \end{bmatrix}\right\| \tag{6.44}$$

$$= s^4 - \left(\frac{-(b_1+K_\theta)a}{ab-c} + \frac{ab_2}{ab-c}\right)s^3 + \left(\frac{-(b_1+K_\theta)a}{ab-c} * \frac{ab_2}{ab-c} - \left(\frac{af}{ab-c} + \frac{eb_2}{ab-c} * \frac{-(b_1+K_\theta)}{ab-c}\right)\right)s^2$$
$$+ \left(\frac{-(b_1+K_\theta)a}{ab-c} * \frac{af}{ab-c} - \frac{d}{ab-c} * \frac{-(b_1+K_\theta)}{ab-c}\right)s \tag{6.45}$$

The linearized system above is stable around the equilibrium point $x = 0$ if A is a Hurwitz matrix. Based on Hurwitz's criterion and the results of the calculations, the constraint condition of the controller parameters is determined as

$$\frac{ab_2}{ab-c} > \frac{(b_1+K_\theta)a}{ab-c} \tag{6.46}$$

$$\frac{-(b_1+K_\theta)a}{ab-c} * \frac{ab_2}{ab-c} > \left(\frac{af}{ab-c} + \frac{eb_2}{ab-c} * \frac{-(b_1+K_\theta)}{ab-c}\right) \tag{6.47}$$

$$\frac{-(b_1+K_\theta)a}{ab-c} * \frac{af}{ab-c} > \frac{d}{ab-c} * \frac{-(b_1+K_\theta)}{ab-c} \tag{6.48}$$

From the above Equation (4.46), (4.47) and (4.48) it is clear that the stability of the system exist when the criteria's expressed in this three equation are satisfied.

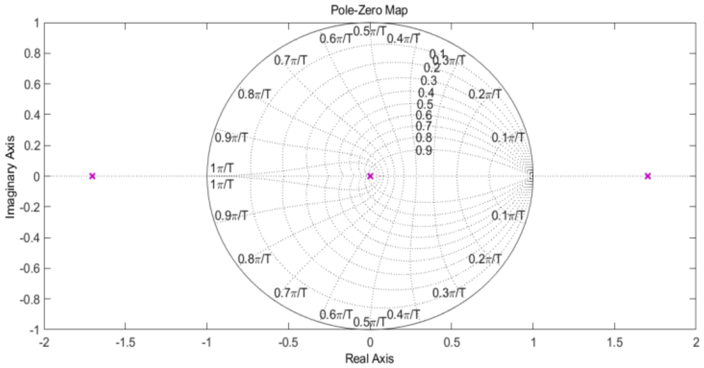

Figure 6. 1.Pole-Zero map for the linear plant

From Figure 6.1, there is one zero at the imaginary axis this is due to consideration of viscous friction. Therefore, if Equations (46)-(48) among the control parameters are maintained, then the zero dynamics is stable around the equilibrium point $x = 0$, which leads to the local stability of the internal dynamics of Equation (6.7) and (6.8).and the MATLAB script to determine pole and zero is given in appendix A.

6.3. System Controllability

Assume that the mapping f is continuously differentiable in a neighborhood of a point $(\bar{x}, \bar{u})$ for which

$$f(\bar{x}, \bar{u}) = 0 \tag{6.49}$$

If the linearized system is controllable then the system $\dot{x} = Ax + Bu$ is locally controllable at the point $\bar{x}$ and an arbitrary time $T > 0$.

An already linearized system is controllable if the pair (A, B) where $A \in M(n, n)$ $B \in M(n, m)$ is controllable. i.e, the controllability matrix $C_o = [B, AB, A^2B, A^3B]$ is controllable when the determinant of $|C_o| \neq 0$. MATLAB script to determine the controllability of the system is given in appendix A.

6.4. Adaptive Linear Quadratic Gaussian Based Stabilizing Controller Design (ALQGSC)

Consider linearized the dynamic model of RIP with the system, which is controllable by applying the control concept of Section (4.3).For the upward position of the pendulum, the system as expressed in

$$\dot{\tilde{x}}_1 = \tilde{x}_2$$

$$\dot{\tilde{x}}_4 = \frac{K_u u\, m_p l_1 l_a - (b_1 + K_\theta) m_p l_1 l_a \tilde{x}_2 + \left(m_a l_a{}^2 + J_a + m_p l_a{}^2\right) m_p l_1 g \tilde{x}_3 - \left(m_p l_1{}^2 + J_p\right) b_2 \tilde{x}_4}{\left(m_a l_a{}^2 + J_a + m_p l_a{}^2\right)\left(m_p l_1{}^2 + J_p\right) - m_p^2 l_1^2 l_a^2}$$

$$\dot{\tilde{x}}_3 = \tilde{x}_4$$

$$\dot{\tilde{x}}_2 = \frac{K_u u\left(m_p l_1{}^2 + J_p\right) - (b_1 + K_\theta)\left(m_p l_1{}^2 + J_p\right)\tilde{x}_2 + m_p^2 l_1^2 l_a g \tilde{x}_3 - m_p l_1 l_a b_2 \tilde{x}_4}{\left(m_a l_a{}^2 + J_a + m_p l_a{}^2\right)\left(m_p l_1{}^2 + J_p\right) - m_p^2 l_1^2 l_a^2} \tag{6.50}$$

The new state of the system is $y = [x_1\ x_2\ x_3\ x_4]^T$. Then apply the concept described in Chapter 4. The state feedback gain $K = [k_1\ k_2\ k_3\ k_4]^T$ for the linearized equation, designed using a linear quadratic regulator. A design parameter Γ is a 4x4 diagonal matrix and P and Q is a 4x4 positive definite matrix. γ is the diagonal elements of Γ and can be any positive number that satisfies the criteria stated in Section 4.The baseline LQR and Kalman filter controller is augmented with $L1$ adaptive controller [46] and the control input is expressed as

$$u_{in} = u_{ad} + u_{lqg} \tag{6.51}$$

Where $u_{lqg} = k_{lqr}\hat{x}$, $k_{lqr} = R^{-1}B^T P$ and P is determined from the MATLAB script in appendix C.

Baseline Controller (LQR+KF). This section explains the design of a baseline controller, which compensates for the linear and known part of system dynamics. The linearized model of the original dynamics is considered at nominal conditions. Since the L1, adaptive controller contains a mechanism for integral control, an LQR+KF is considered. In this thesis, L_1 adaptive controller is considered; this controller consists of three parts for the control parameter.

State Predictor: consider the following state predictor as

$$\dot{\hat{x}}(t) = A_m \hat{x}(t) + B_m(\hat{\omega}u(t) + \hat{\theta}^T x(t) + \hat{\sigma}(t))$$
$$y(t) = C^T \hat{x}(t) \tag{6.52}$$

Where $\hat{x}(t)$ is the measured state predictor vector, $u(t)$ is the control input, A_m is Hurwitz n x n matrix, and as described in section 4 $\hat{\omega}$ is unknown constant with known sign $\hat{\theta}$ is a vector of time-varying parameters.

Adaptation Law: the following projection-based adaptation laws described in section 4.3 govern the adaptive process.

$$\begin{aligned}
\dot{\hat{\omega}}(t) &= \Gamma proj\,(\hat{\omega}(t), -\tilde{x}^T(t)PB_m u(t)), \hat{\omega}(0) = \hat{\omega}_o \\
\dot{\hat{\theta}}(t) &= \Gamma proj\,(\hat{\theta}(t), -\tilde{x}^T(t)PB_m \|x(t)\|), \hat{\theta}(0) = \hat{\theta}_o \\
\dot{\hat{\sigma}}(t) &= \Gamma proj\,(\hat{\sigma}(t), -\tilde{x}^T(t)PB_m), \hat{\sigma}(0) = \hat{\sigma}_o
\end{aligned} \tag{6.53}$$

Where $\hat{\omega} \in \mathbb{R}, \hat{\theta} \in \mathbb{R}$ and $\hat{\sigma} \in \mathbb{R}$ adaptive parameters are estimates of $\omega(t), \theta(t)$ and $\sigma(t)$ respectively. $\tilde{x} = \hat{x} - x$ Is the prediction error and $p = p \geq 0$ is the solution of the Lyapunov equation: $A_m^T P + PA_m + Q = 0$ for chosen positive definite matrix Q and the projection operator is defined in section 4.3. Above stated, projection-based adaptation law ensures that the parameters are confined to their respective bounds i.e. $\hat{\omega}(t) \in \Omega$, $\|\hat{\theta}(t)\|_\infty \leq \theta_b$ and $\|\hat{\sigma}(t)\|_\infty \leq \theta_b$

Control Law: adaptive control law is generated as an output of the following feedback system.

$$k\,D(s)(\hat{\eta}(s) - k_g\, r(s)) \tag{6.54}$$

where $r(s)$ and $\hat{\eta}(s)$ are Laplace transform of $r(t)$ and $\hat{\eta}(t) = \hat{\omega}u(t) + \hat{\theta}^T x(t) + \hat{\sigma}(t)$ respectively; $k_g = -1 \big/ C^T A_m B$; and $k \geq 0$ and D(s) are feedback gain and strictly proper transfer function leading to a strictly proper stable satisfying $C(s) = \omega k\,D(s) \big/ 1 + \omega k\,D(s)$ $\forall \omega \in \Omega_o$ the choice of k and D(s) needs to ensure the norm condition of L1 adaptive control inferred in[47]

Reference Model: The choice of the reference model (A_m, B_m) plays a key part in controller design. A_m is chosen to be a Hurwitz matrix of appropriate dimensions, which ensures that the pair (A_m, C) is observable. The choice of Am dictates the response characteristics of a reference model, thus it must be ensured that the eigenvalue A_m corresponding to acceptable damping and natural frequencies.

$A_m = \begin{bmatrix} -2 & -1 & 0 & 0 \\ -1 & -1 & 0 & 0 \\ -1 & 0 & -2 & 1 \\ 0 & 0 & 1 & -1 \end{bmatrix}$, $B_m = \begin{bmatrix} 1 \\ 0 \\ 1 \\ 0 \end{bmatrix}$ This matrix is controllable so used as a reference model.

The low pass filter that gives good control action is given by

$$D(s) = \frac{1}{s(\frac{s}{100}+1)} \begin{bmatrix} 1 & 0 \\ 0 & 1 \end{bmatrix}$$

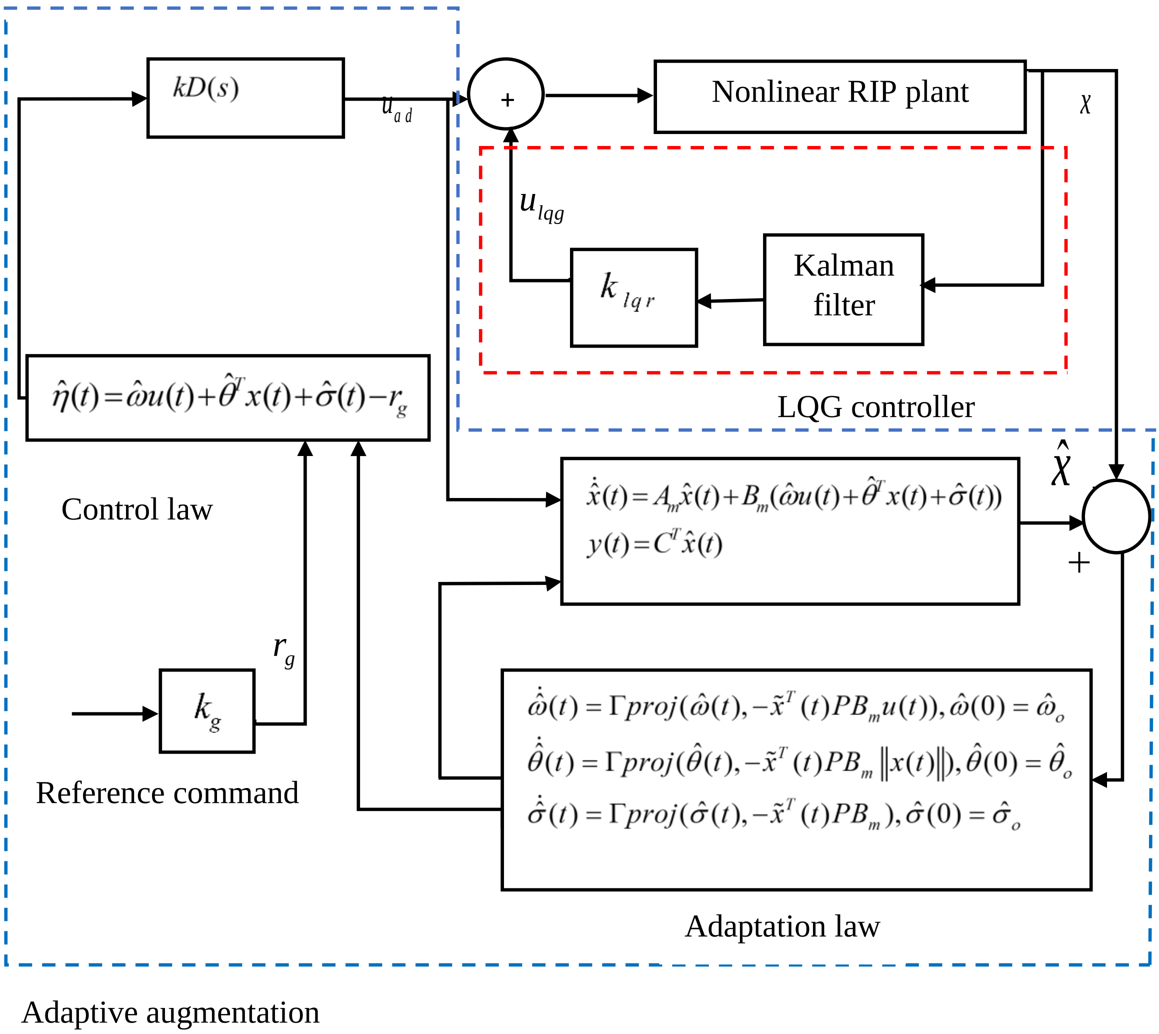

Figure 6. 2. Adaptive LQG controller architecture

CHAPTER 7

RESULTS AND DISCUSSIONS

7.1. Model Validation and Open-loop Dynamics

Simulation is performed using MATLAB/SIMULINK with 3D animation. A rotary inverted pendulum is shown in Figure 7.1 is designed using VREALM software in MATLAB to understand the system validation in Simulink. After designing in this software then exported to MATLAB/SIMULINK using VR sink. Where the system validation is tested before applying the controllers.

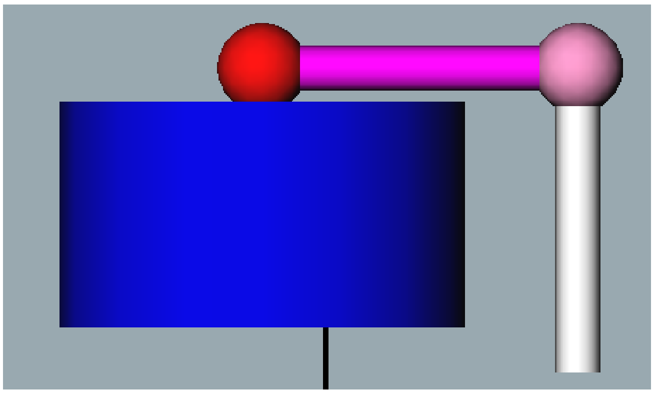

Figure 7. 1.MATLAB/SIMULINK 3D body imported from VREALM

For testing, the validation of the model a signal of 15.66 degrees is applied to the pendulum angle as a disturbance for allowing natural movement with time. As shown from the result below in Figures 7.1 and 7.2 both the pendulum and the rotating arm starts to rotate from the initial angle of 0 degrees.

The arm rotates continuously slowly until the running time finishes. The pendulum starts to fall to the downward position and run back and forth with decreasing swinging angle and amplitude until stops its motion to the down ward position. In this case, the pendulum is unstable in the upright position while moving back and forth from it. After converging, the pendulum is stable in the downward position. This all behavior is happened in the physical model due to viscous friction. In this way, the validation of the system can be investigated.

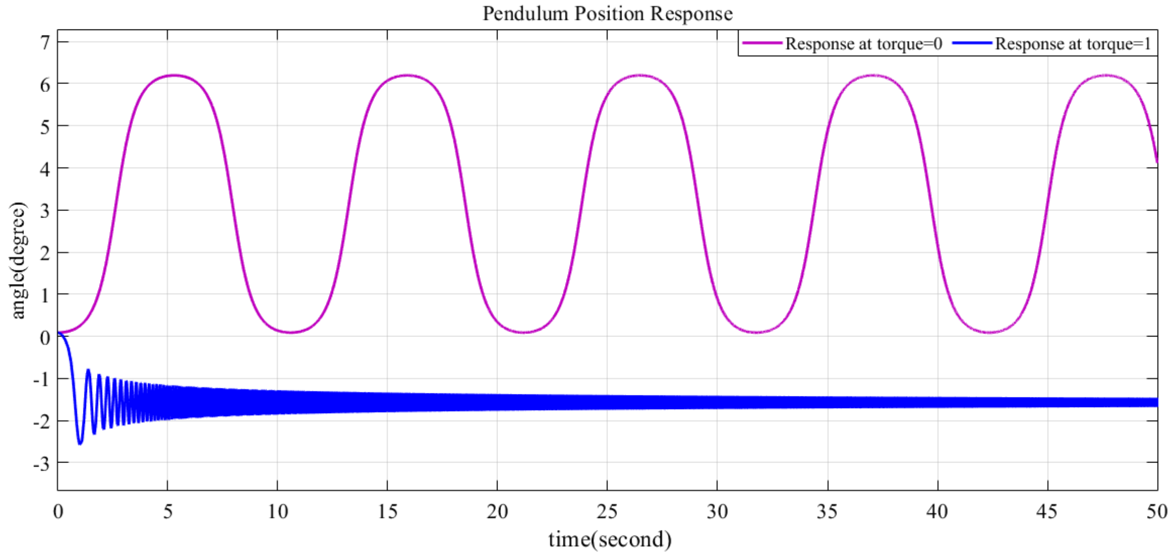

Figure 7. 2.Pendulum angular position in its natural dynamics (without controller)

Figure 7.2 shows that the response of open-loop behavior of pendulum with and without the applied torque from the motor with 15.66 degree or 0.0873 radian initial angle as a disturbance. In the open-loop response at torque equal to zero, the pendulum rotates freely without any retardation, shown in the pink color. The response of open loop system also has slow motion with low velocity. The total torque generated from the motor is approximated as one calculated from the estimated motor parameter. As the torque is applied to the system, the pendulum starts to rotate with rotating angular velocity with increasing frequency. It seems that as time increases the rotation of the pendulum become increases as shown in the graph represented with blue color.

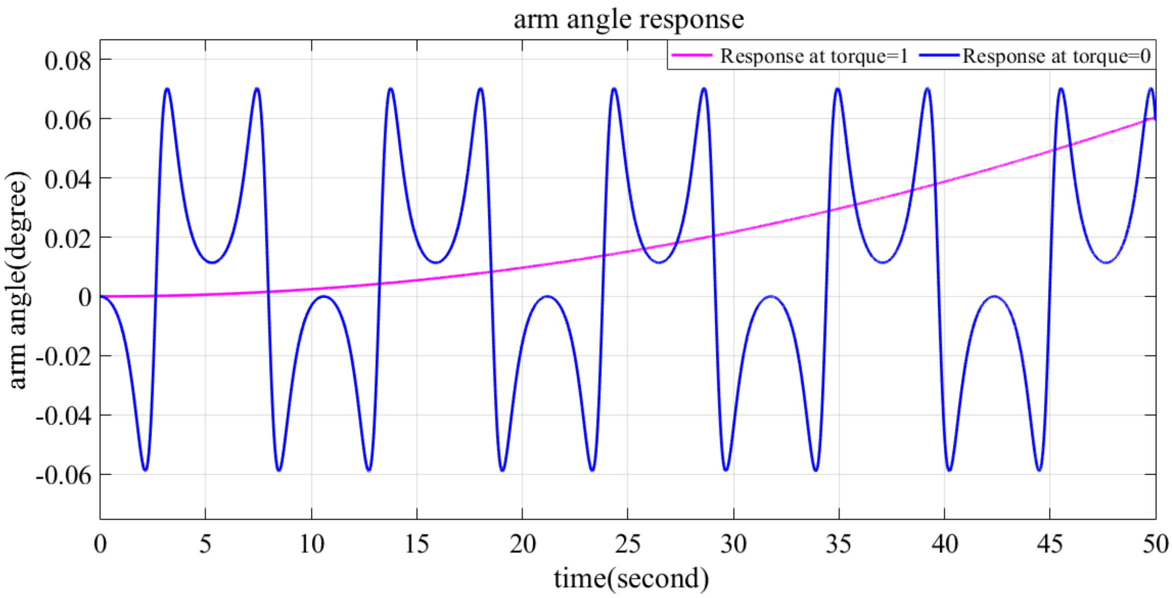

Figure 7. 3.Arm angular position in its natural dynamics (without controller)

As shown in Figure 7.3 the motion of the rotating arm has a different path with and without the applied torque. Without the applied torque, the arm rotates freely in its path but when torque is applied, the freewheeling motion of the arm is restricted in some path followed. From Figure 7.3, the arm rotation is freewheeling at zero torque but when torque is applied arm is restricted to follow some path almost with having constant velocity.

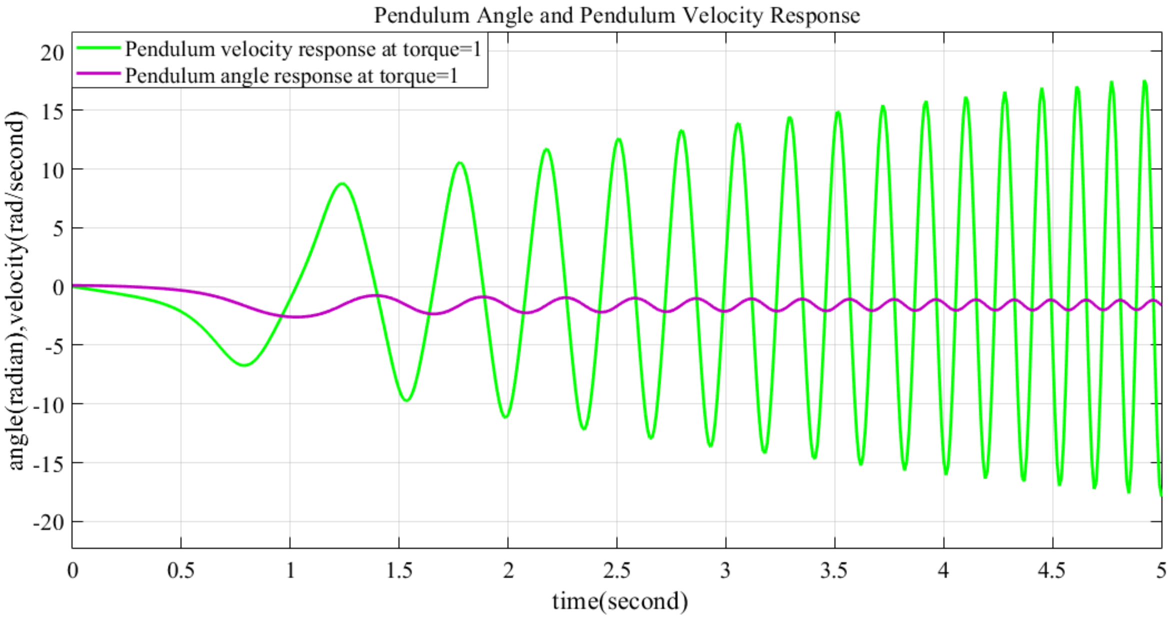

Figure 7.4. Pendulum angular position and velocity in its natural dynamics (without controller)

From Figure 7.4 the velocity and angle of the pendulum are represented in the same plot for indicating the behavior of RIP in the 3D body. As shown in the Figure 7.4, the amplitude of the velocity of the pendulum increases while the amplitude of the angle of the pendulum become decreases with time. This indicates that the integrability of the system for control action.

The velocity of the angular velocity of the arm is almost street line as shown in Figure 7.5, which can be the slope of the arm position response with the applied torque. This is because of the integration of arm angular velocity or the derivative of arm position. At the open-loop response, the arm velocity response and its position response differ only in smoothness of their response. The position response is smooth with a semi-circle with a vertical line in shape whereas the angular velocity has a sharp corner and the path is not smooth like position response. Figure 7.6 indicates that the pendulum rotates at a slow speed whereas the rotation of the pendulum when applying torque have fast response.

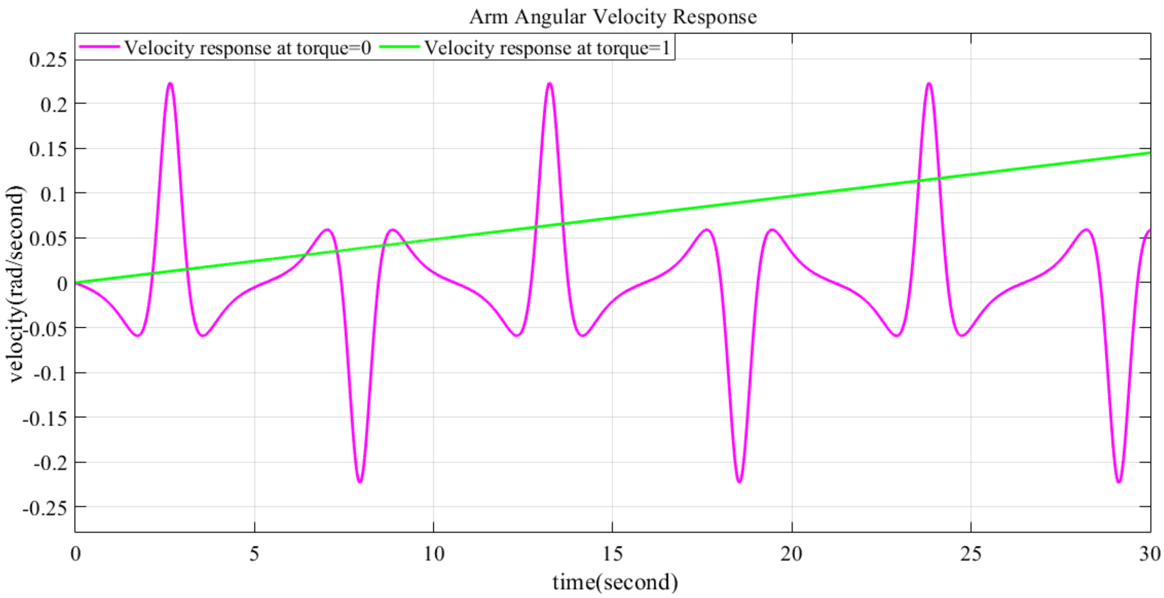

Figure 7. 5. Arm angular velocity in its natural dynamics (without controller)

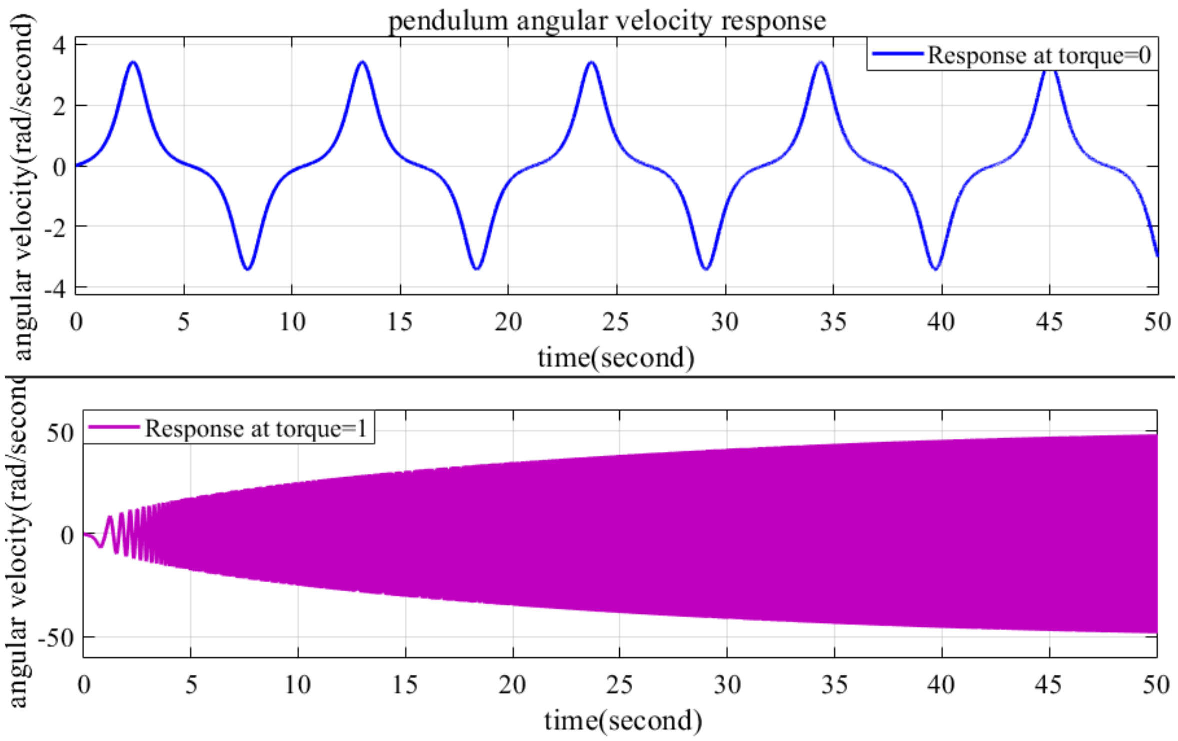

Figure 7. 6. Pendulum angular velocity in its natural dynamics (without controller)

7.2. Response of the System with Adaptive ALQGSC

The dynamics of the system response with adaptive LQG-based stabilizing controller depends on the design parameters described in chapter 4.the change in the design parameters has its effect on the whole system. For the change of some parameters, the controllability of the system may change. Tuning this changing parameter is needed for designing an adaptive controller (using the inverse method) based on LQG control.

The tuning of parameters is done manually by looking at the response of the system in each parameter. The value of the Q matrix is selected depending on the system stability from the response. This system is selected as below from the stable response of the system.

N.B. The parameters of matrix P and Q are selected only when they are positive definite that satisfy Lyapunov Equation (4.47).

Therefore, the first step of selecting P and Q matrix is checking its positive definiteness from reference [15].

$$Q = \begin{bmatrix} 1 & 0 & 0 & 0 \\ 0 & 1 & 0 & 0 \\ 0 & 0 & 10 & 0 \\ 0 & 0 & 0 & 100 \end{bmatrix}$$

With the eigenvalues of Q become $eig(Q) = \begin{bmatrix} 1 \\ 1 \\ 10 \\ 100 \end{bmatrix}$

P is determined by solving the Lyapunov equation described in 4.45

$$P = \begin{bmatrix} 245.98 & -0.27 & -65.93 & 0.67 \\ -0.25 & 0 & 0.01 & 0 \\ -659.36 & 0.12 & 99.59 & -2.61 \\ 67.7 & 0 & -26.12 & 0 \end{bmatrix}$$

With eigenvalues of P $\quad eig(P) = \begin{bmatrix} 394.05 \\ -48.05 \\ -0.10 \\ 0.02 \end{bmatrix}$

The design parameter, which is adaptation gain in the L1 adaptive control structure, can have different values in $\hat{\omega}, \hat{\theta}$ and $\hat{\sigma}(t)$ adaptation law but for simulation purposes, the input to three projections Γ matrix element is similar and selected described in 4.3.

$$\Gamma = \begin{bmatrix} 1.5 & 0 & 0 & 0 \\ 0 & 1.5 & 0 & 0 \\ 0 & 0 & 1.5 & 0 \\ 0 & 0 & 0 & 0.5 \end{bmatrix}$$

The time-varying initial condition and projection maximum and minimum values are determined in Table 7.1. Below.

Table 7. 1. Time-varying parameters

Parameters	Initial condition	Minimum value	Maximum value
Mass of arm	0.059 Kg	0.06Kg	3Kg
Length of arm	0.215m	0.1m	0.4m
Mass of pendulum	0.059Kg	0.005Kg	2.5Kg
Length of pendulum	0.113m	0.08m	0.35m

All the above parameters are adapted or predicted in the predictor model. Adaptation and control law has no significant change on the system rather than substituting the correct state. In addition, the projection operator bounds are $\theta_{\max-\delta} = 10, \theta_{\max-\theta} = 40$ and $\theta_{\max-\omega} = 0.95$ with the projection operator centered at $\omega = 1.5$ initial conditions are all zero.

The feedback gain is selected as k=100. The other parameters of LQG design are determined in the MATLAB script described in Appendix C.

Constraints that affect the physical system are shown in Table 7.2 below.

Table 7. 2. Physical parameter constraints

Parameters	Value
Arm viscous friction(b1)	0.0865(rad/sec)
Pendulum viscous friction(b2)	0.0529(rad/sec)

By using all the above parameters, the performance of the system can be tested using a different mass of the pendulum and arm.

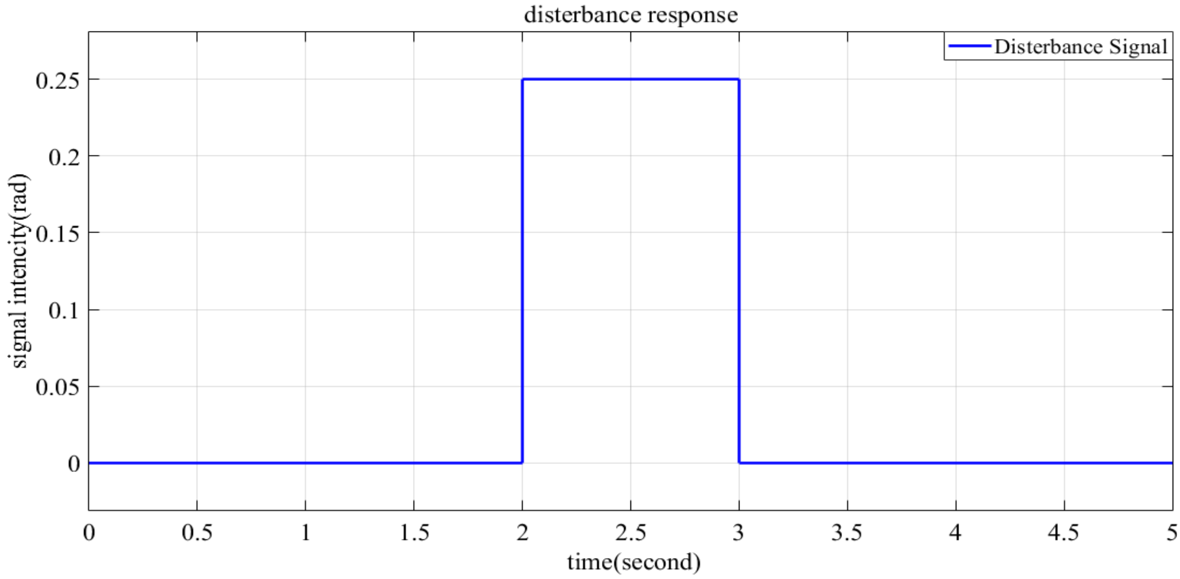

Figure 7. 7. Disturbance signal

Disturbance signal is built in the signal builder. This signal is important for starting the pendulum for swinging or stabilizing toward the upright position.

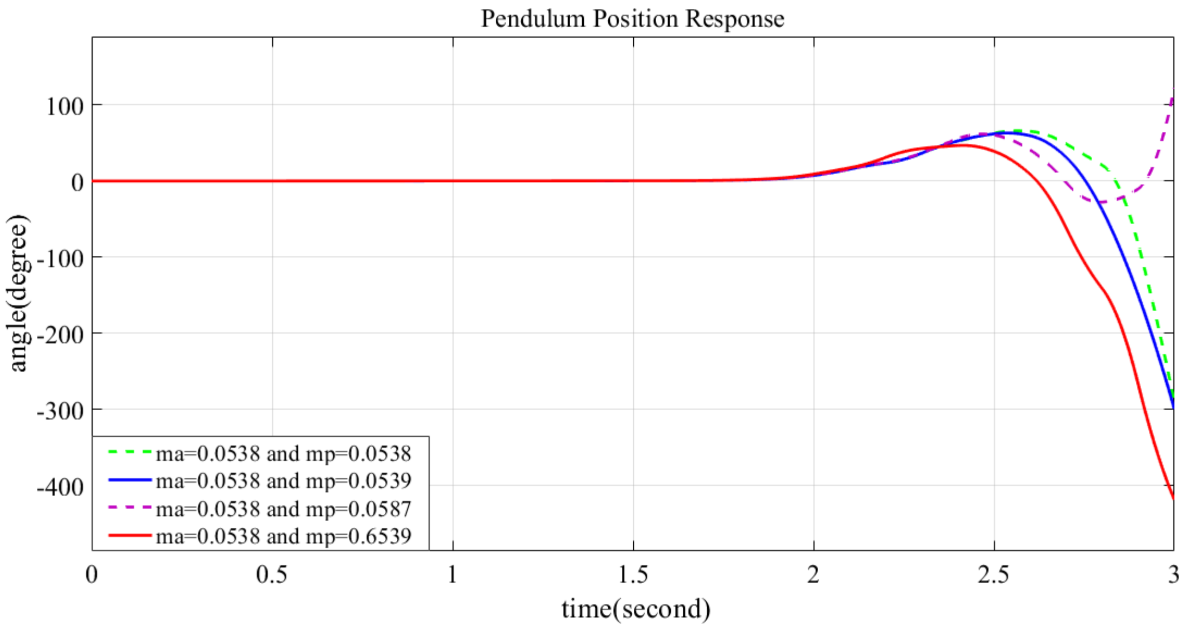

Figure 7. 8. Pendulum position response with ALQGSC

The response shown in Figure 7.8 above and 7.9 below indicates that the response of arm and pendulum position with the same mass of arm and with different mass of pendulum. From Figure 7.8, the response from four different masses of pendulum is almost have similar settling time approximately from t=0 to t=1.85. This is done by adapting these different masses of pendulum. Since the controller is stabilizing the control action starts immediately at time zero as soon as applying the control signal. However, after this time the response from different masses have different path since the controller finish the time of control action and the pendulum goes downward with unstable signal.

Similarly, from Figure 7.9 it is clear that the response of arm position has the same stable point with different mass value of pendulum and with the same mass value of arm. The only difference is the settling time of arm. After this time the stability of arm become, diverge.

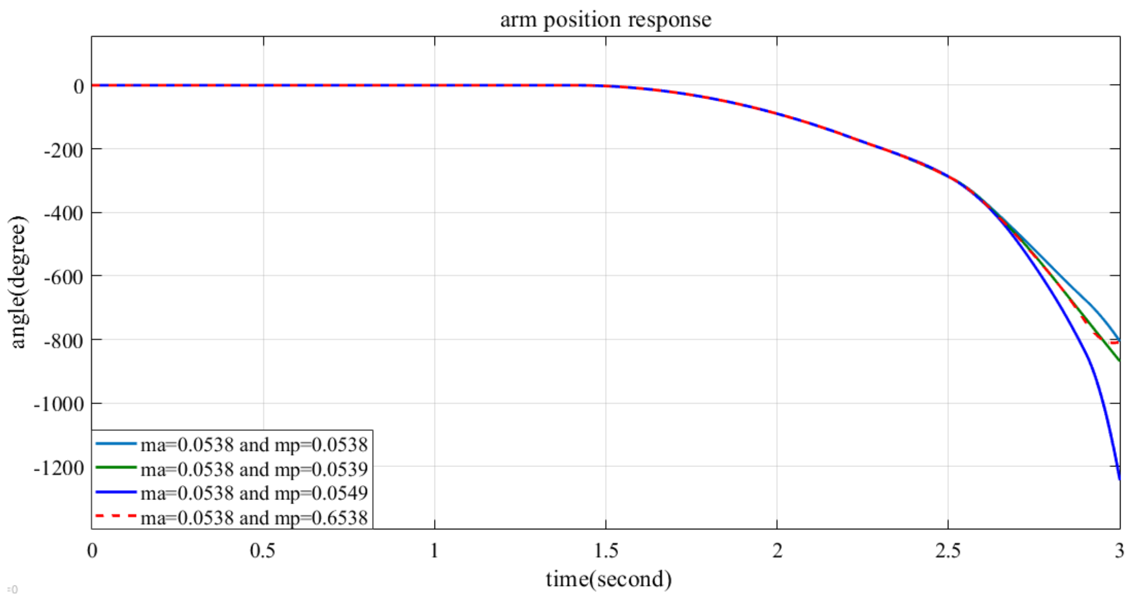

Figure 7. 9. Arm position response with ALQGSC

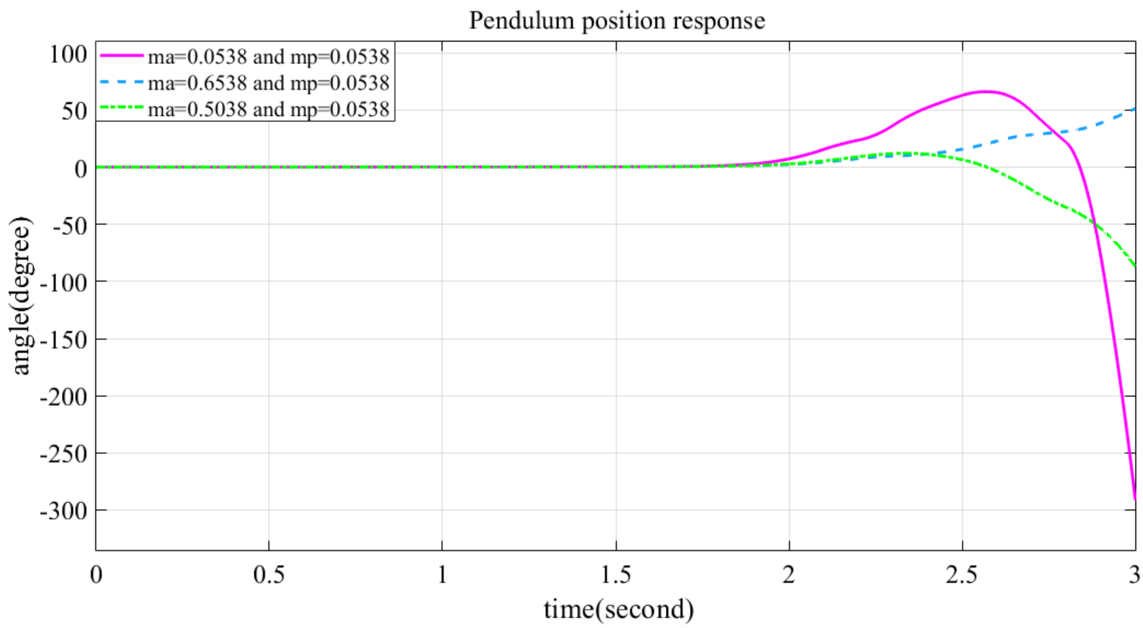

Figure 7. 10. Pendulum position response with ALQGSC

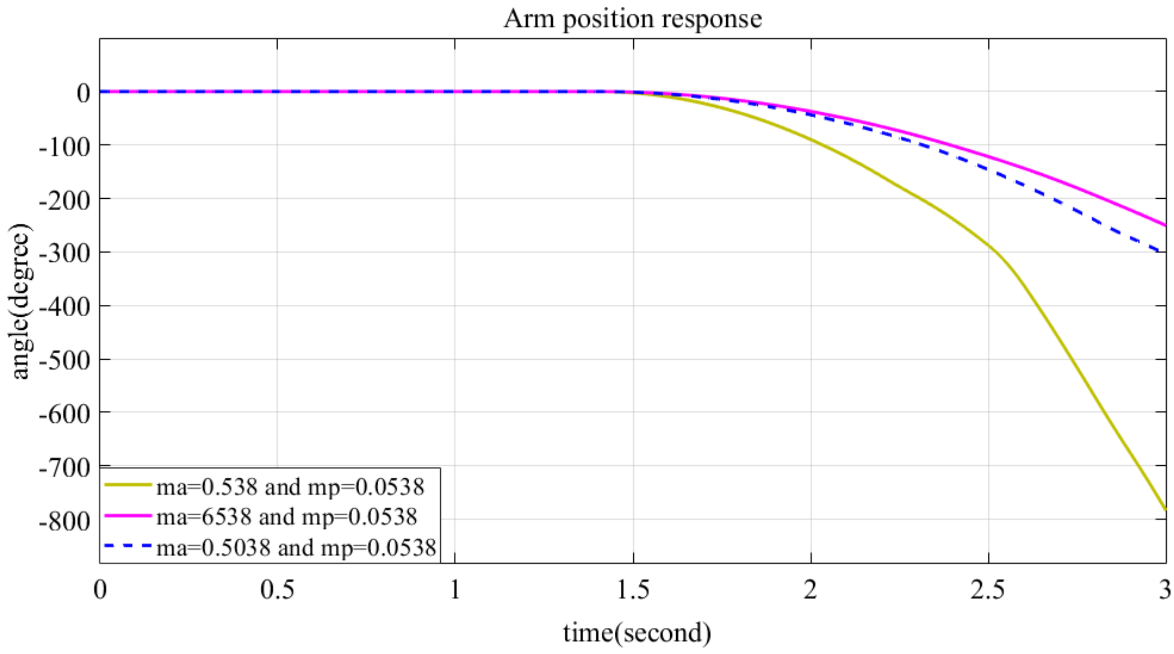

Figure 7. 11. Arm position response with ALQGSC

From Figures 7.10 and 7.11 different masses of the arm with a constant mass of the pendulum are adapted for checking the performance of stabilizing controller. From the graph even if there is some difference around the unstable position but at the stable region, all mass has almost the same response with Figure 7.8 and 7.9**.** Whatever the value of parameter changes in the system they are adjusted for proper controlled position and velocity in the whole system with adaptive mechanism.

7.3. Response of the System with Energy-based GA tuned PDSC

In an energy-based swing-up controller, the input to the PD controller is fixed with the energy compensation of the system. The pendulum swings depending on the potential energy and reference energy variation. This variable energy is then given to the PD controller for making swing up and good stable property of RIP.

With similar initial parameters of RIP system used in stabilizing controller and the new parameters used in the energy, input design described is shown in Table 7.3 below. This parameter is used to convert the acceleration generated from energy to torque and the voltage signal. The response of ESUPDC is described in Figures 7.7, 7.8, 7.9, and 7.10 below.

The value of PD parameters for the pendulum is K_p =0.2, K_d =0.05 and for arm K_p =100, K_d =2.5 these values are determined from the tuning of the genetic algorithm.

Table 7. 3.Motor parameter constraints

Parameters	Values
Motor back-emf constant K_t	0.00768 Vs/rad
Motor torque constant K_m	Nm/A
Gear box constant	70 $Nm\Omega rad/Vs$
Gear efficiency	0.69
Motor efficiency	0.9

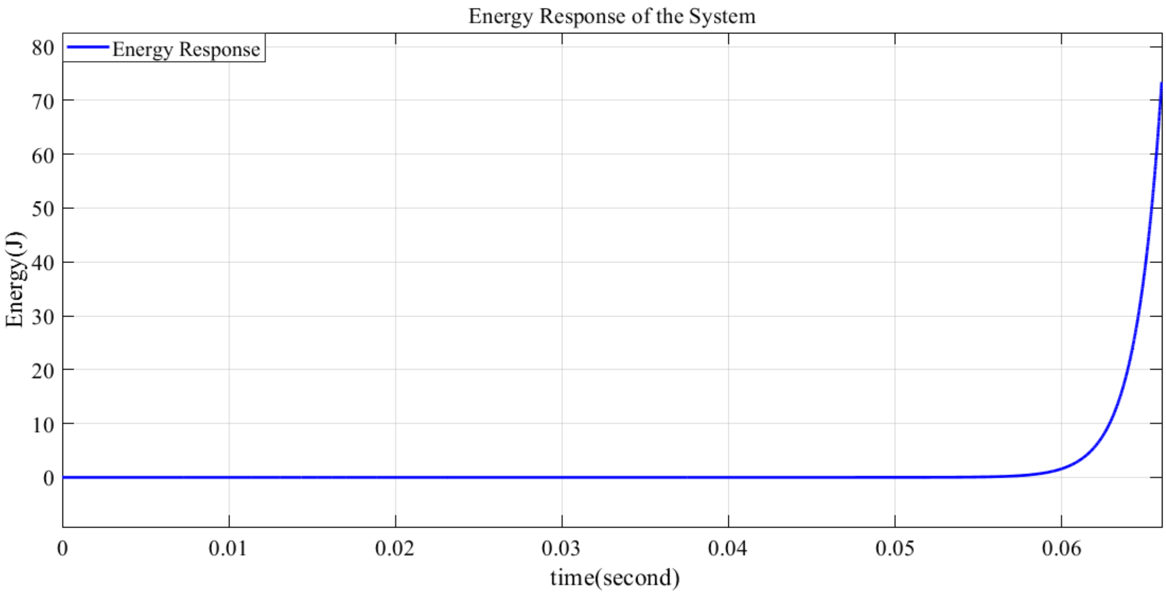

Figure 7. 12. Energy input response with PD controlled angle input

The energy of the system is calculated from the motor parameter and this energy signal is given to the PD controller for giving exact swinging up of the pendulum at a specific position. Since the output of the pendulum angle is given to the energy of the system, the response of energy output is almost stable.

From figure, 7.13 and 7.14 below the arm position response is different in EBPDSUC and PDSUC. From this result the output response from EBPDSUC have best stable response with some unstable point. When the total energy equal to the reference energy of the system the arm angle to the unstable point become reduced as indicated in the red line, but when the reference energy equals to zero the arm angle at the unstable point increases as indicated in the black line.

In addition, from Figure 7.14 the response of the arm position has some sinusoidal oscillation and have almost similar response at zero input and step input response.it takes more time to get exact stable region in PDSUC when compared to EBPDSUC.

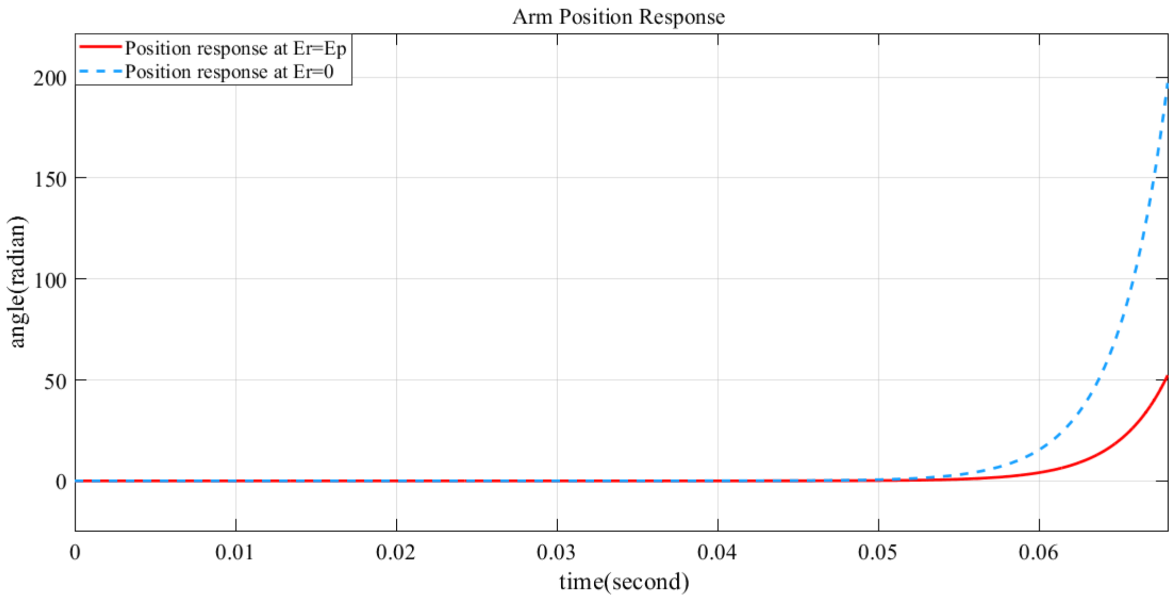

Figure 7. 13. Arm position response with EBPDSUC

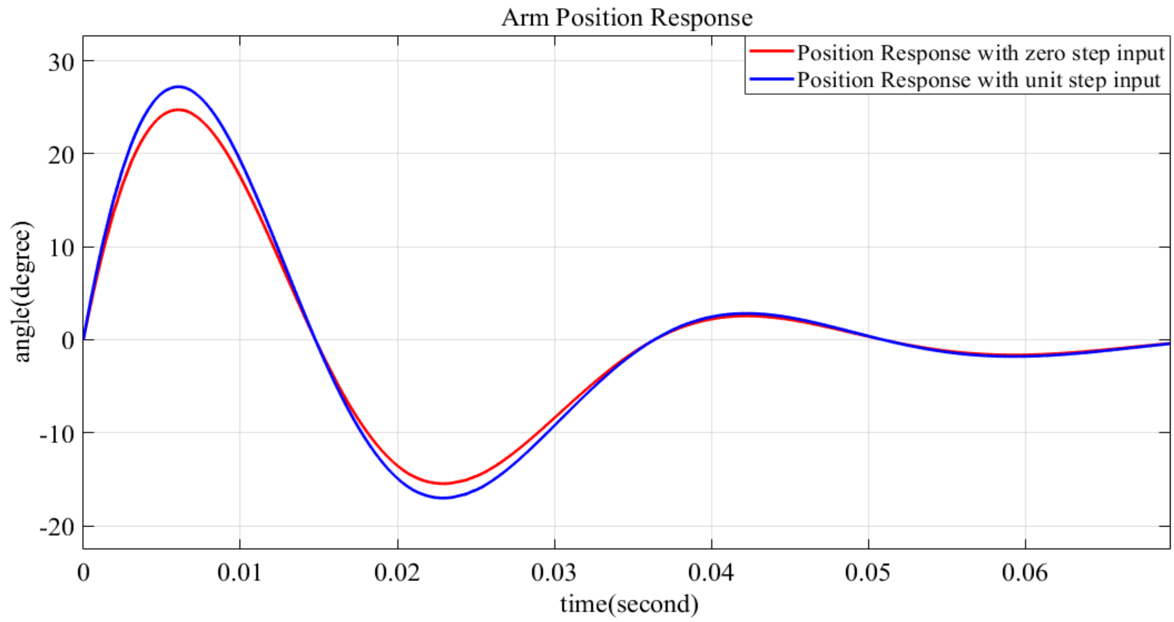

Figure 7. 14. Arm position response with only PDSUC

From Figure 7.15 and 7.16 below the pendulum position have different response with EBPDSUC and PDSUC.As shown in Figure 7.15 above the pendulum position response with EBPDSUC have exact stable region with some settling time difference at $E_r = E_p$ and

$E_r = 0$.at $E_r = 0$ the position response of pendulum is slower than at $E_r = E_p$ as represented in pink color. In addition, from Figure 7.16 below the response of the pendulum position with PDSUC is not good and have no good stable region. Even if it may be stable but it will take more, time to get the stable region. The difference of the input step and zero input is in amplitude only.

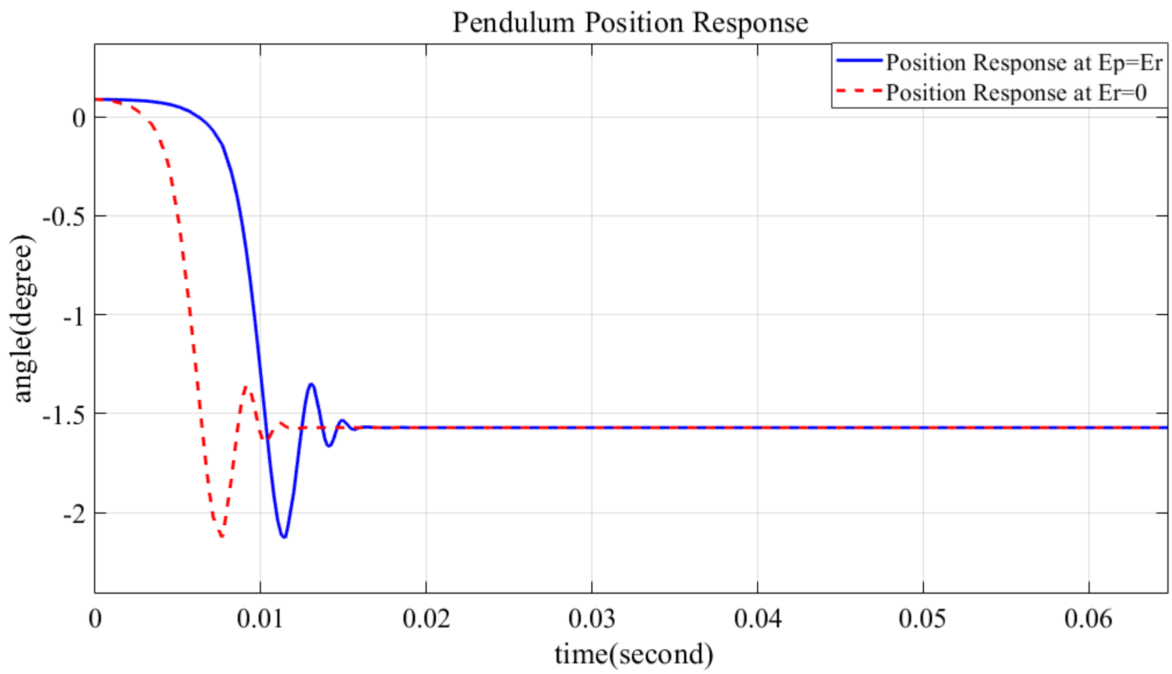

Figure 7. 15. Pendulum position response with EBPDSUC

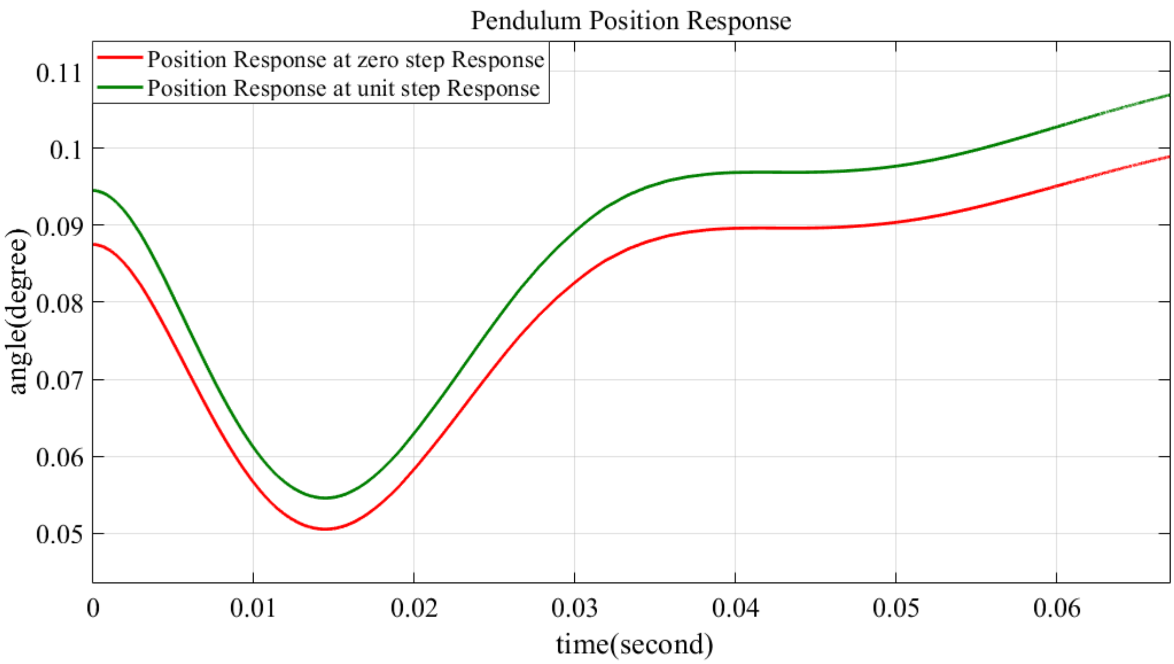

Figure 7. 16. Pendulum position response with only PDSUC

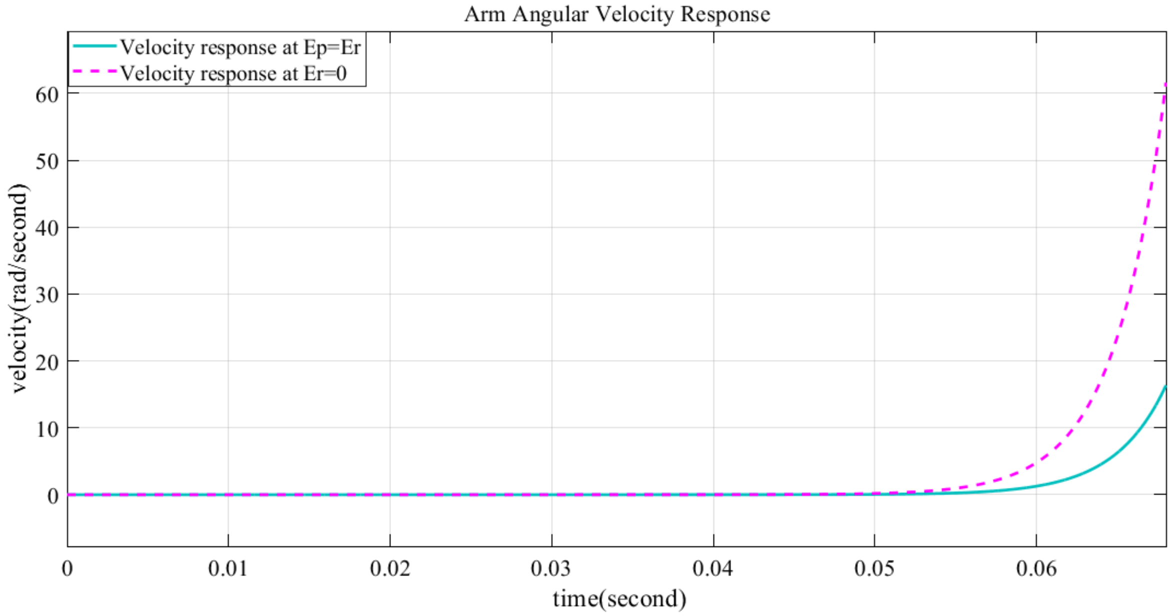

Figure 7. 17. Arm angular velocity response with EBPDSWC

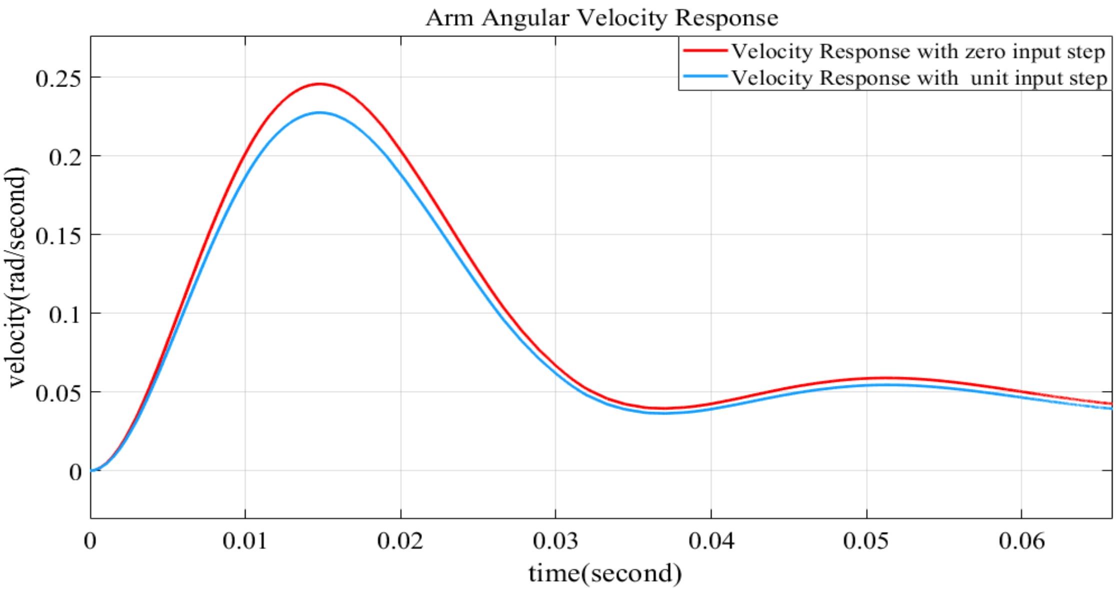

Figure 7. 18. Arm angular velocity response with only PDSUC

From Figure 7.17 and 7.18 the output angular velocity response with EBPDSUC and PDSUC have different stability region.in Figure 7.17 angular velocity have good stable response with different magnitude at $E_r = E_p$ and $E_r = 0$ as indicated in cyan and hot pink color respectively. In Figure 7.18, the arm angular velocity response with PDSUC have higher overshoot at the start of the simulation. It may take more time than EBPDSUC to be perfectly stable.

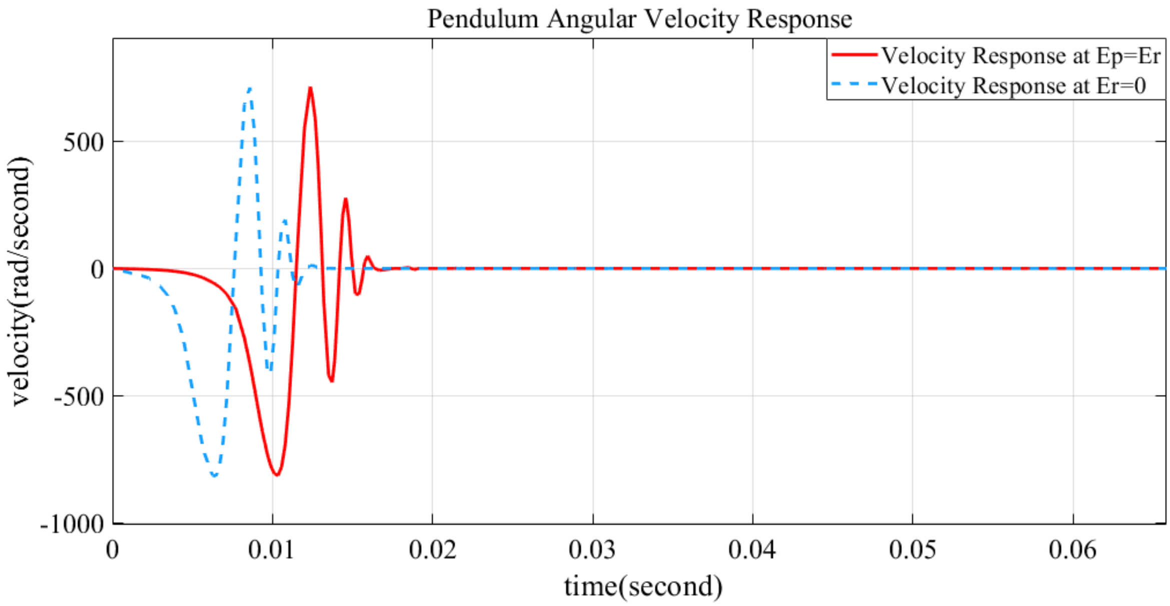

Figure 7. 19. Pendulum angular velocity response with EBPDSUC

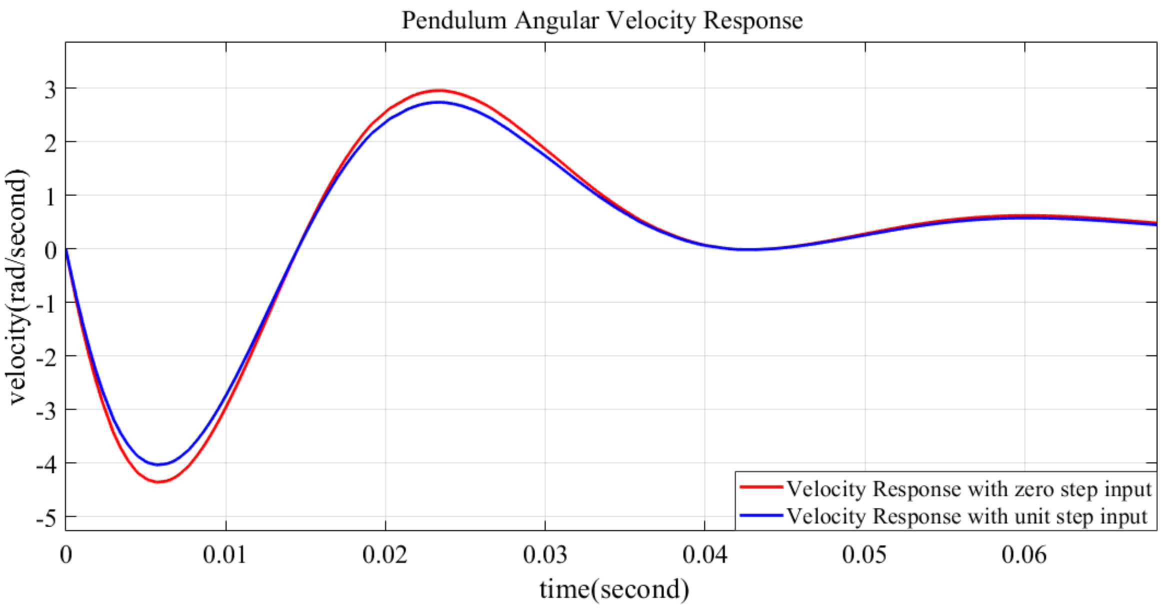

Figure 7. 20. Pendulum angular velocity response with PDSUC

Figure 7.19 and 7.20 are the angular velocity response of pendulum. The response of Figure 7.19 has similar response with pendulum position response except its amplitude and velocity and position value. However, the velocity response of pendulum in Figure 7.20 has good output response compared to the pendulum position response.

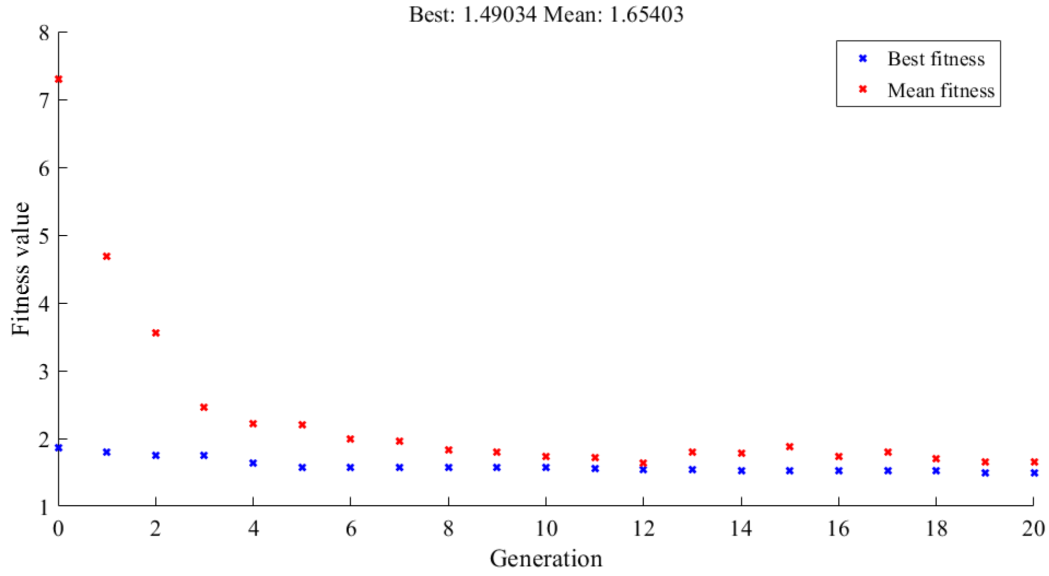

Figure 7. 21. GA Tuning output Response

Figure 7.21 shows that the response of genetic algorithm response of tuning the parameters of PD controller. The dotted line represented in red color is the mean fitness value with the value of 1.65403 and the line represented in black color is best fitness value with the value of 1.49034.

8. CONCLUSION AND RECOMMENDATION

8.1. Conclusion

This thesis contains the application of Linear Quadratic Gaussian in rotary inverted pendulum for stabilization problem and energy compensation PD swing up controller to control the swing up of pendulum problem. With having the system in two parts arm and the pendulum subsystem integrating with adaptive inverse control to stabilize the rotary inverted pendulum in the upright position. While EBNSUC is used to swing up the pendulum from the pendant position to its inverted (upright) position, the ALQGSC is used to stabilize the Rotary inverted pendulum to the upright position. The simulation result shows promising the result under the different arm and pendulum mass shown above Figure 7.2 with the disturbance apply up to $\pm$15.66 for applying ALQDSC.

The combined controller of adaptive and LQG controller adapts different mass of arm and pendulum for determining the performance of adaptive LQG controller. Compared to the controllers expressed in [4], [5], [6] and [17] for controlling the stabilizing and swing up control ALQGSC and EBNPDSUC are more effective and better.

A Swing up controller contains the outer loop for controlling the pivoted arm and the inner loop for controlling the swing up of the pendulum. The best stability of the PD swing-up controller is done using energy compensation for giving input to the PD controller. The torque applied to the system is also calculated from the motor parameter and the input is given as voltage for the PD controller. Parameters of PD controller are tuned by genetic algorithm for giving a better response. An Energy of the system is given to the pendulum angle control as an input to the outer loop of the PD controller and giving an on-off signal for swinging up of the pendulum.

8.2. Recommendation

The parameters used in this Rotary Inverted Pendulum for designing ALQGSC and EBPDSUC are randomly selected as stated in section 6.and for the energy enhancement for the input to PD controller parameters and the energy gain constant are selected manually with particular value for this thesis. Different mass values are adapted at a different time for applying ALQGSC. This takes several times to get output result from the simulation of the whole system. The genetic algorithm tuning behavior of the Simulink model of the whole system takes time may upto an hour. The author of this thesis recommends all interested researchers to design one’s systematic way of selecting designing parameters and tuning the whole system researcher may use MATLAB code with genetic algorithm for saving simulation period.

This thesis is done only in software simulation to check the validation and performance of the controllers on the system. Therefore, researcher this thesis wants to recommend implementing the hardware for checking the exact validation of controllers with enough time and sufficient resources.

In the swing up controller EBPDSUC, the simulation time is so slow. Even if EBPSSUC has the best performance at a smaller time, the simulation at a large time is very slow. As compared to only PDSUC, EBPDSUC have less simulation rate but has better performance. The researcher tries to solve this low simulation rate but did not get any attractive solution. The tuning of parameters takes more time, which makes the researcher so bored. Therefore, the researcher of the future can do this problem with enough time and knowledge

Research fund Acknowledgment

This thesis project is funded by Adama Science and Technology University under the grant number ASTU/SM-R/158/20, Adama, Ethiopia.

References

[1] K. P. Kumar, “Modeling and Controller Designing of Rotary Inverted Pendulum (RIP) -Comparison by,” vol. 2, no. 2.

[2] F. Grasser, A. D. Arrigo, S. Colombi, and A. Rufer, “JOE : A Mobile , Inverted Pendulum.”

[3] A. Kathpal and A. Singla, “SimMechanics ™ Based Modeling , Simulation and Real-Time Control of Rotary Inverted Pendulum,” no. October, 2017, doi: 10.1109/ISCO.2017.7855975.

[4] N. Mus and B. Tovornik, “Swinging Up and Stabilization of a Real Inverted Pendulum,” vol. 53, no. 2, pp. 631–639, 2006.

[5] R. Ortega, M. W. Spong, and G. Blankenstein, “Stabilization of a Class of Underactuated Mechanical Systems Via Interconnection and Damping Assignment,” vol. 47, no. 8, pp. 1218–1233, 2002.

[6] Y. C. A. Huang, “Adaptive control of rotary inverted pendulum system with time-varying uncertainties,” 2013, doi: 10.1007/s11071-013-1112-4.

[7] S. Nair, “Normal Form for Energy Shaping: Application to the Furuta Pendulum,” no. December, pp. 516–521, 2002.

[8] C. Aguilar-avelar and J. Moreno-valenzuela, “A composite controller for trajectory tracking applied to the Furuta pendulum $,” *ISA Trans.*, pp. 1–9, 2015, doi: 10.1016/j.isatra.2015.02.009.

[9] R. Sritharan and I. V Eee, “Mathematical Modeling and control of QNET Rotary inverted pendulum in MATLAB and real time implementation in LabVIEW using ELVIS,” *2018 Second Int. Conf. Inven. Commun. Comput. Technol.*, no. Icicct, pp. 1452–1457, 2018.

[10] V. S. and M. Parnichkun, “Real-Time Optimal Control for Rotary Inverted Pendulum Viroch Sukontanakarn and Manukid Parnichkun Mechatronics , School of Engineering and Technology , Asian Institute of Technology , Pathumthani , Thailand,” *Am. J. Appl. Sci.*, vol. 6, no. 6, pp. 1106–1115, 2009.

[11] P. Taylor, I. Fantoni, and R. Lozano, “Stabilization of the Furuta pendulum around

its homoclinic orbit," no. April 2013, pp. 37–41, 2010, doi: 10.1080/0020717011011226.

[12] P. X. La, L. B. Freidovich, A. S. Shiriaev, and U. Mettin, "Mechatronics New approach for swinging up the Furuta pendulum : Theory and experiments," *Mechatronics*, vol. 19, no. 8, pp. 1240–1250, 2009, doi: 10.1016/j.mechatronics.2009.07.005.

[13] A. S. Shiriaev, L. B. Freidovich, A. Robertsson, R. Johansson, and A. Sandberg, "Virtual-Holonomic-Constraints-Based Design of Stable Oscillations of Furuta Pendulum : Theory and Experiments," vol. 23, no. 4, pp. 827–832, 2007.

[14] L. T. Aguilar, I. Boiko, L. Fridman, and R. Iriarte, "Generating Self-Excited Oscillations via Two-Relay Controller," vol. 54, no. 2, pp. 416–420, 2009.

[15] "[39](Adaptive and learning systems for signal processing, communications, and control) Gang Tao - Adaptive Control Design and Analysis-Wiley-Interscience (2003)." .

[16] samarajit Ghosh, *GHOSH, SMARAJIT - Signals and Systems-Pearson Canada [distributor, Pearson Education Canada (2005_2009)*. .

[17] J. Kim, W. Shin, and R. H. Sagor, "Modeling and comparative study of linear and nonlinear controllers for rotary inverted pendulum," doi: 10.1088/1742-6596/755/1/011001.

[18] K. Furuta, M. Yamakita, and S. Kobayashi, "Swing-up control of inverted pendulum using pseudo-state feedback," vol. 206, 2016.

[19] D. Abebe, B. Submitted, C. E. Fulfillment, E. C. Engineering, and D. Shiferaw, "Design and Implementation of Feedback Linearization based Adaptive Stabilizing Controller Coupled with Fuzzy Logic Swing-up for Pendulum on a Cart," 2019.

[20] L. Chrif and Z. Meguenni, "Aircraft Control System Using LQG and LQR Controller with Optimal Estimation-Kalman Filter Design," *Procedia Eng.*, vol. 80, pp. 245–257, 2014, doi: 10.1016/j.proeng.2014.09.084.

[21] M. Fatihu, H. Jen, I. Ahmed, A. Ismail, A. Yahaya, and T. Kumbasar, "Current development on using Rotary Inverted Pendulum as a benchmark for testing linear and nonlinear control algorithms," *Mech. Syst. Signal Process.*, vol. 116, pp. 347–

369, 2019, doi: 10.1016/j.ymssp.2018.06.054.

[22] J. Aracil and F. Gordillo, “A family of smooth controllers for swinging up a pendulum,” vol. 44, pp. 1841–1848, 2008.

[23] M. Park and D. Chwa, “Swing-Up and Stabilization Control of Inverted-Pendulum Systems via Coupled Sliding-Mode Control Method,” vol. 56, no. 9, pp. 3541–3555, 2009.

[24] C. A. License, “Furuta ’ s Pendulum : A Conservative Nonlinear,” vol. 2010, 2010, doi: 10.1155/2010/742894.

[25] I. M. Gregory, C. Cao, E. Xargay, N. Hovakimyan, and X. Zou, “L1 adaptive control design for NASA AirSTAR flight test vehicle,” *AIAA Guid. Navig. Control Conf. Exhib.*, pp. 1–25, 2009, doi: 10.2514/6.2009-5738.

[26] C. Cao and N. Hovakimyan, “Design and Analysis of a Novel L1 Adaptive Control,” *IEEE Trans. Automat. Contr.*, vol. 53, no. 2, pp. 586–591, 2008.

[27] H. Seraji, “A New Class of Nonlinear PID Controllers,” *IFAC Proc. Vol.*, vol. 30, no. 20, pp. 65–71, 1997, doi: 10.1016/s1474-6670(17)44245-5.

[28] Y. Hou and K. Mei, “Vertical-Rotary Inverted Pendulum System Based on Fuzzy Control,” pp. 2804–2807, 2011.

[29] M. F. Hamza, H. J. Yap, and I. A. Choudhury, “Genetic Algorithm and Particle Swarm Optimization Based Cascade Interval Type 2 Fuzzy PD Controller for Rotary Inverted Pendulum System,” vol. 2015, 2015.

[30] S. Durand, J. F. Guerrero-Castellanos, N. Marchand, and W. F. Guerrero-Sánchez, “Event-based control of the inverted pendulum: Swing up and stabilization,” *Control Eng. Appl. Informatics*, vol. 15, no. 3, pp. 96–104, 2013.

[31] S. V. Radhamohan, A. Mona Subramaniam, and M. J. Nigam, “Fuzzy swing-up and stabilization of real inverted pendulum using single rulebase,” *J. Theor. Appl. Inf. Technol.*, vol. 14, no. 1, pp. 43–50, 2010.

[32] Ponce, “a Review of Intelligent Control Systems Applied To the Inverted-Pendulum Problem,” *Am. J. Eng. Appl. Sci.*, vol. 7, no. 2, pp. 194–240, 2014, doi: 10.3844/ajeassp.2014.194.240.

[33] T. A. Albahkali, “An impulse-momentum approach to swing-up control of double inverted pendulum on a cart,” *World Acad. Sci. Eng. Technol.*, vol. 78, no. 6, pp. 762–768, 2011, doi: 10.5281/zenodo.1084799.

[34] J. H. Christensen and R. Christiansen, “Swing Up and Stabilisation of an Inverted Pendulum on a Cart using Nonlinear Methods,” no. June, 2017.

[35] E. S. Varghese, A. K. Vincent, and V. Bagyaveereswaran, “Optimal control of inverted pendulum system using PID controller, LQR and MPC,” *IOP Conf. Ser. Mater. Sci. Eng.*, vol. 263, no. 5, 2017, doi: 10.1088/1757-899X/263/5/052007.

[36] G. Garcia and E. Mu, “G. Garcia-Chavez,” 2017.

[37] T. T. Fong, Z. Jamaludin, and L. Abdullah, “System identification and modelling of rotary inverted pendulum,” no. November 2015, 2014.

[38] A. C. Smith, “Nonlinear Control of Underactuated Mechanical Systems with Application to Robotics and by Reza Olfati-Saber,” 2001.

[39] “Power Electronics,Dr.P.S. BIMBHRA.PDF.” .

[40] E. Points and D. Variables, “Jacobian Linearizations , equilibrium points,” 2002.

[41] S. D. Patek *et al.*, “Linear Quadratic Gaussian-Based Closed-Loop Control of Type 1 Diabetes,” vol. 1, no. 6, pp. 834–841, 2007.

[42] N. Ames, M. Field, S. Ghaffarian, and M. Field, “Adaptive Linear Quadratic Gaussian Optimal Control Modification for Flutter Suppression of Adaptive Wing,” no. January, pp. 1–23, 2015.

[43] M. C. Campi and P. R. Kumar, “ADAPTIVE LINEAR QUADRATIC GAUSSIAN CONTROL :,” vol. 36, no. 6, pp. 1890–1907, 1998.

[44] A. Mathematics and S. Review, “Applications of Singular Perturbation Techniques to Control Problems Author (s): Petar V . Kokotovic Source : SIAM Review , Oct ., 1984 , Vol . 26 , No . 4 (Oct ., 1984), pp . 501-550 Published by : Society for Industrial and Applied Mathematics Stabl,” vol. 26, no. 4, pp. 501–550, 1984.

[45] N. John, M. K. Koteswara, and N. Sivakumaran, “Swing Up and Stabilization Control of a Rotary Inverted Pendulum,” 2013.

[46] T. Authors *et al.*, “6ZLQJ XS DQG VWDELOL] DWLRQ RI WKH

URWDWLRQDO LQYHUWHG SHQGXOXP XVLQJ 3 ' DQG IX]]\ 3 ' FRQWUROOHUV," vol. 12, pp. 57–64, 2014, doi: 10.1016/j.protcy.2013.12.456.

[47] chengyu cao, *Hovakimyan, Naira, and Cao, Chengyu, L1 Adaptive Control Theory: Guaranteed Robustness with Fast Adaptation Speyer, Jason L., and Jacobson, David H., Primer on Optimal Control Theory*.

Appendix

A MATLAB Script to check stability and controllability of the system

MATLAB script for checking the controllability of the system

```
mp=5.38*10^(-2);
ma=5.38*10^ (-2);
Ja=1.75*10^(-2);
Jp=1.98*10^(-2);
la=0.215;
l1=0.113;
g=9.81;
b1=0.256;
b2=0.876;
Kth=0.0589;
Ku=0.00698;
a=mp*(l1)^2+Jp;
b=ma*(la)^2+Ja+mp*(la)^2;
d=(mp)^2*(l1)^2*la;
e=mp*la*l1;
f=mp*l1*g;
s=1;c=(mp)^2*(l1)^2*(la)^2;

A=[0 1 0 0;0 -(b1+Kth)*a/(a*b-c) d/(a*b-c) e*b2/(a*b-c);
   0 0 0 1;0 -(b1+Kth)/(a*b-c) a*f/(a*b-c) a*b2/(a*b-c)];
B=[0;Ku*a/(a*b-c);0;Ku*e/(a*b-c)];
C=[1 0 0 0;0 0 1 0];
D=[0];
n=4;
eigenvalueA=eig(A)
Co=[B,A*B,A^2*B,A^3*B];
c=rank(Co);
if rank(Co)==n
   disp('system is controllable');
else
   disp('system is uncontrollable');
end
```

MATLAB script for checking the stability of the system

```
sys=idss(A,B,C,D,'Ts',0.1);
pzmap(sys)
```

B MATLAB Script for designing ALQG

MATLAB script for adaptive Linear Quadratic Gaussian controller design

```
mp=0.67;
```

```
ma=5.38*10^(-2);
Ja=5.38*10^(-2);
Jp=1.98*10^(-2);
la=0.215;
l1=0.113;
g=9.81;
b1=0.256;
b2=0.876;
Kth=0.0589;
Ku=0.00698;
a=mp*(l1)^2+Jp;
b=ma*(la)^2+Ja+mp*(la)^2;
d=(mp)^2*(l1)^2*la;
e=mp*la*l1;
f=mp*l1*g;
s=1;c=(mp)^2*(l1)^2*(la)^2;

A=[0 1 0 0;0 -(b1+Kth)*a/(a*b-c) d/(a*b-c) e*b2/(a*b-c);
   0 0 0 1;0 -(b1+Kth)/(a*b-c) a*f/(a*b-c) a*b2/(a*b-c)];
B=[0;Ku*a/(a*b-c);0;Ku*e/(a*b-c)];
C=[1 0 0 0];
D=zeros(size(C,1),size(B,2));
Q=[1 0 0 0;0 1 0 0;
   0 0 10 0;0 0 0 100];
R=0.01;
K=lqr(A,B,Q,R);
Vd=0.1*eye(4);
Vn=1;
BF=[B Vd 0*B];
sysC=ss(A,BF,C,[0 0 0 0 0 Vn]);
sysFullOutput=ss(A,BF,eye(4),zeros(4,size(BF,2)));
%%kalman filter design
[L,P,E]=lqe(A,Vd,C,Vd,Vn);
Kf=(lqr(A',C',Vd,Vn));
sysKF=ss(A-L*C,[B L],eye(4),0*[B L])%kalman filter
function [theta,sigma,omega] = AdaptiveLaw(x, x_hat,u)
      P=[245.9896   -0.2756  -65.9342    0.6771;
         -0.2756   -0.0000    0.0126    0.0000;
       -659.3417    0.1262   99.5960   -2.6124;
         67.7142    0.0000  -26.1243   -0.0000];
    Bm=[0;0.311740485235922;0;0.019889076033295];
    theta=0;sigma=0;omega=0;
    theta_min=0;theta_max=10;
    sigma_min=0;sigma_max=40;
    omega_min=0;omega_max=0.95;
    g1=P*Bm*u;
    g2=P*Bm*x;
  g3=P*Bm;
if theta>theta_min&&theta<thata_max
   theta=0;
```

```
elseif theta==theta_min&&g1>=0
   theta=0;
elseif theta==theta_max&&g1<=0
   theta=0;
else
   theta=(x_hat-x)*g1;
end
if sigma>sigma_min&&sigma<sigma_max
   sigma=0;

elseif sigma==sigma_min&&g1>=0
   sigma=0;
elseif sigma==sigma_max&&g1<=0
   sigma=0;
else
   theta=(x_hat-x)*g2;
end
if omega>omega_min&&omega<omega_max
   sigma=0;

elseif omega==omega_min&&g1>=0
   sigma=0;
elseif omega==omega_max&&g1<=0
   omega=0;
else
   theta=(x_hat-x)*g3;
end
function [dx_hat,y] = predictor(u, x_hat, theta,sigma,omega)
      Am= [0 1 0 0;3.1174 -244.9716 10.6723 45.2462;0 0 0 1;
         0.1988 -701.2194 3.34338 41.8513];
      Bm=[0;0.3117;0;0.01988];
      Cm= [1 0 0 0;0 0 1 0];
      dx_hat=Am*x_hat+Bm*(omega*u+theta'*x+sigma);
      y =Cm'*x_hat;
end
function u= ControlLaw (u, x, theta, sigma, omega, r)
  K=100;
  D= [-1 1; -1000 0];
  Kg=-0.1;
  u=K*D*((theta'*x+omega*u+sigma)-Kg*r);
end
```

C MATLAB Script to Determine Design Parameters with Initial Value

MATLAB script for determining parameters for L1 adaptation

```
mp=5.38*10^(-2);
```

```
ma=5.38*10^(-2);
Ja=1.75*10^(-2);
Jp=1.98*10^(-2);
la=0.215;
l1=0.113;
g=9.81;
b1=0.256;
b2=0.876;
Kth=0.0589;
Ku=0.00698;
a=mp*(l1)^2+Jp;
b=ma*(la)^2+Ja+mp*(la)^2;
c=(mp)^2*(l1)^2*(la)^2;
d=(mp)^2*(l1)^2*la;
e=mp*la*l1;
f=mp*l1*g;
s=1;
A=[0 1 0 0;0 -(b1+Kth)*a/(a*b-c) d/(a*b-c) e*b2/(a*b-c);
   0 0 0 1;0 -(b1+Kth)/(a*b-c) a*f/(a*b-c) a*b2/(a*b-c)]
B=[0;Ku*a/(a*b-c);0;Ku*e/(a*b-c)]
C=[1 0 0 0]
% D=zeros(size(C,1),size(B,2));
Q=[1 0 0 0;0 1 0 0;
   0 0 10 0;0 0 0 100];
R=0.01;
K=lqr(A,B,Q,R)
Am=A-B*K;
Kg=-1/C'*(Am)^(-1)*B
P=-Q/(Am'+Am)
PB=P*B
g=2.5*eye(4)
```

D MATLAB Script for GA Tuning Process

```
function Tune_ModelPD_RIP
clear all
options= optimoptions('ga','PlotFcn',@gaplotbestf);
options.PopulationSize= 30;
options.MaxGenerations= 20;  % Increase value if needed
nvar= 4;
LB= [0.0001 0.0001 0.0001 0.0001];
UB= [15 15 3 3];

[x,fval]= ga(@EvalObj,nvar,[],[],[],[],LB,UB,[],options)

% Updates Kp, Ki and Kd in simulink model workspace for verification
simulink_model= 'ModelPD_RIP';
load_system(simulink_model);
gains= get_param(simulink_model,'modelworkspace');
```

```
gains.assignin('Kpal', x(1));
gains.assignin('Kdal', x(2));
gains.assignin('Kpth', x(3));
gains.assignin('Kdth', x(4));
function obj= EvalObj(x)
% Updates the values of Kp, Ki and Kd in Simulink model workspace
simulink_model= 'ModelPD_RIP';
load_system(simulink_model);
gains= get_param(simulink_model,'modelworkspace');
gains.assignin('Kpal', x(1));
gains.assignin('Kdal', x(2));
gains.assignin('Kpth', x(3));
gains.assignin('Kdth', x(4));

simOut= sim(simulink_model,'SaveOutput','on');

% Retrieves time t and error e
t= simOut.find('t');
e= simOut.find('e');

% Calculate a performance index using the trapezoidal integration rule
n= length(e);
ee= abs(e);
obj= 0;
for i= 2:n
   stepsize= t(i)-t(i-1);
   obj= obj+0.5*(ee(i-1)+ee(i))*stepsize; % IAE
end
```

E MATLAB/SIMULINK Block Diagrams

MATLAB/SIMULINK Block Diagrams

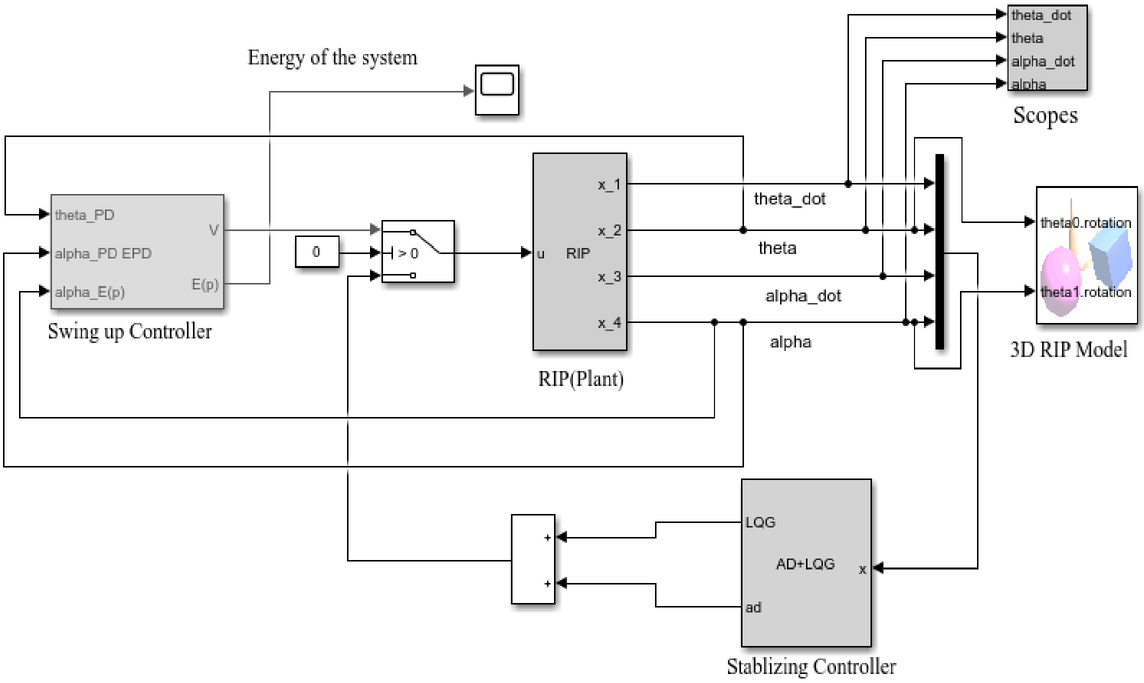

Figure D. 1.Overall System Model

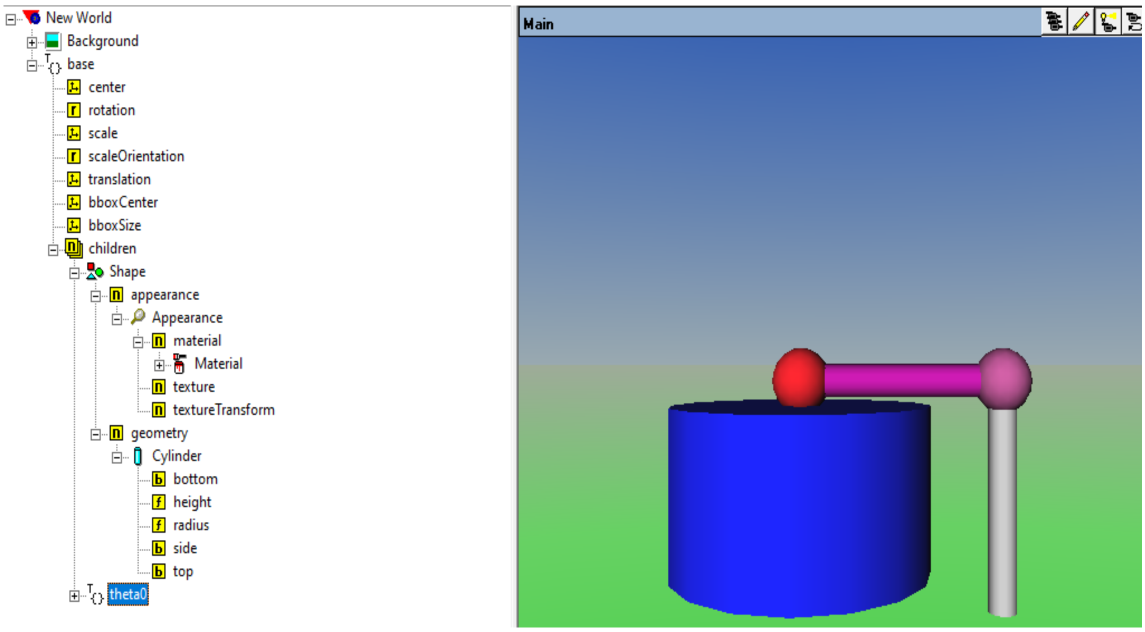

Figure D. 2.3D Multibody of RIP

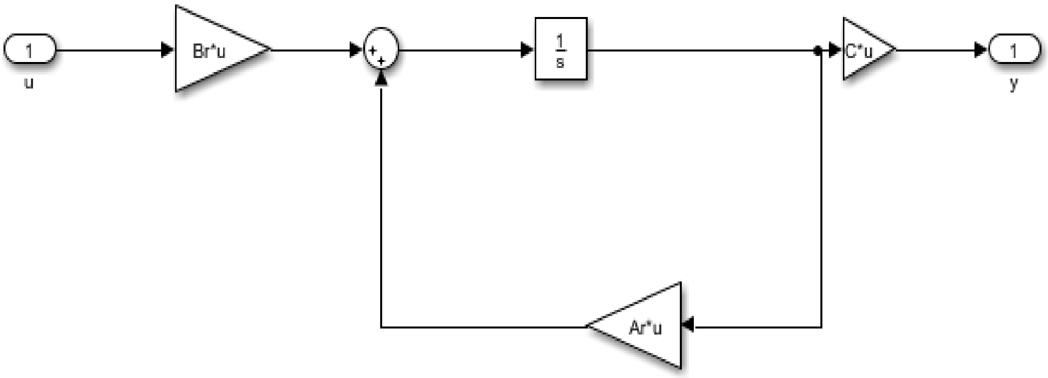

Figure D. 3.Reference Model

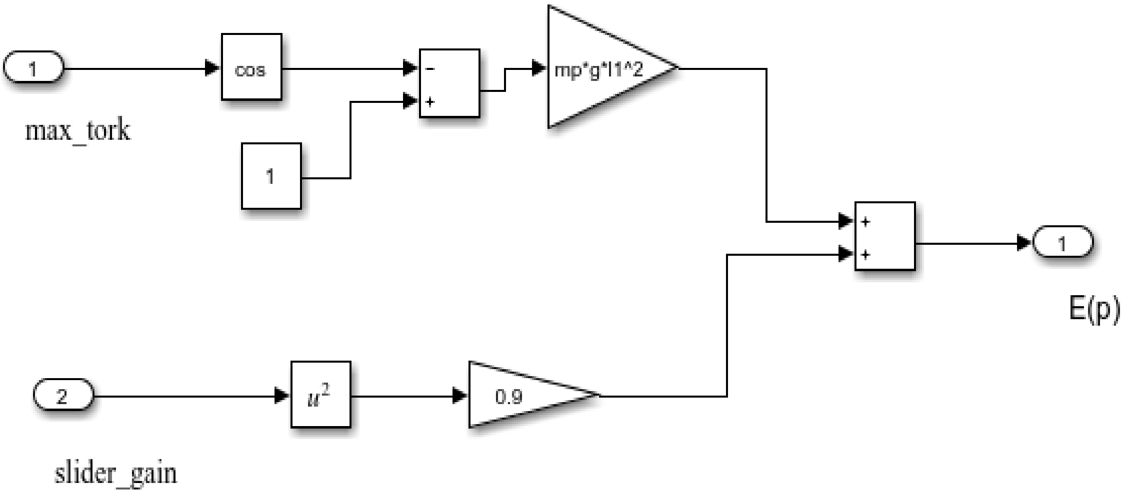

Figure D. 4.Energy of the System

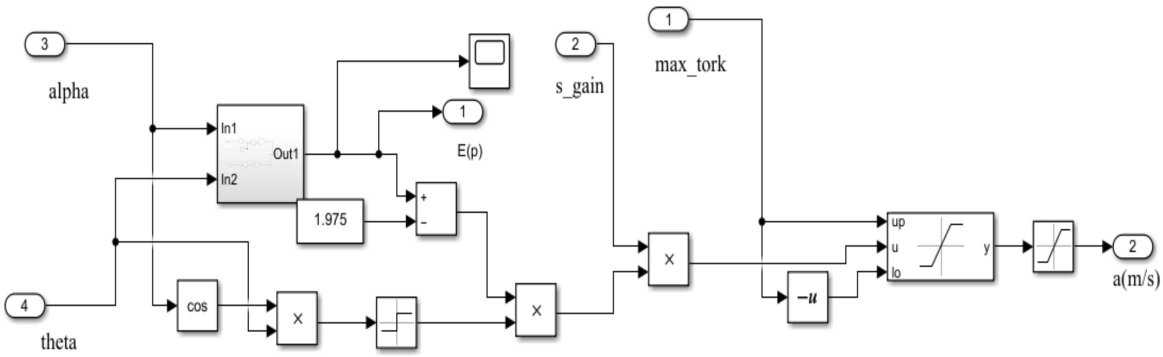

Figure D. 5.Acceleration of the system

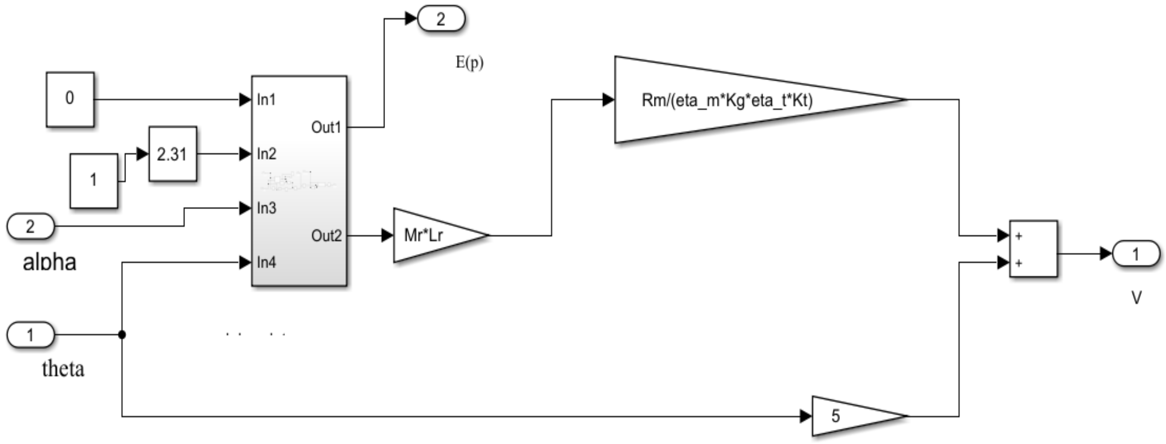

Figure D. 6.Voltage Output for PD input

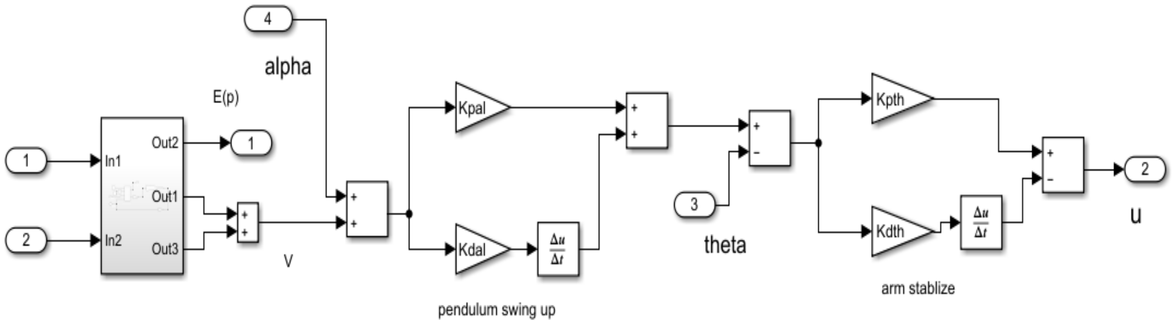

Figure D. 7.Energy Based PD Swing up Controller